THE UNIVERSITY OF ALBERTA

PHOTOCHEMICAL DETERMINATION OF OXALATE BY

OXIDATION WITH IRON(III)

BY

(C)
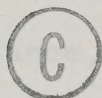
JEAN MARGARET COOLEY

A THESIS

SUBMITTED TO THE FACULTY OF GRADUATE STUDIES AND RESEARCH

IN PARTIAL FULFILMENT OF THE REQUIREMENTS FOR THE DEGREE

OF DOCTOR OF PHILOSOPHY

DEPARTMENT OF CHEMISTRY

EDMONTON, ALBERTA

SPRING, 1977

ABSTRACT

A study of the iron(III) photochemical oxidation of oxalate and several other carboxylic acids has been carried out and applied to the quantitative measurement of these compounds. In initial work the carbon dioxide oxidation product of the photolysis reaction was measured with a pCO_2 electrode in a continuous-flow system using a sampler, proportioning pump, reaction coil and flow-through pCO_2 electrode. In the reaction coil solutions of sample, iron(III), and acid circulated through quartz or borosilicate tubing while being irradiated by an ultraviolet or visible source. Conditions were optimized for the determination of oxalate and several other carboxylic acids, such as citric and tartaric. Computer calculations were used to help in selecting the optimum iron(III) concentration and acidity, and to evaluate the effects of the complexing anions, sulfate and chloride. Several organic compounds, especially some organic acids of low molecular weight and aromatic acids, affect the response of the pCO_2 electrode. This, and the electrode's time response behavior, caused some error in the analysis of real samples.

A gas chromatographic method of measuring the carbon dioxide produced upon oxidation of oxalate with

iron(III) in the presence of light was also used. After
irradiation the volatile components were stripped from
the reaction solution with a stream of helium gas, the
water vapor removed by passage through a column of calcium
sulfate (Drierite), and the carbon dioxide separated from
other gases on a column of silica gel and measured with a
thermal conductivity detector. A 5-minute irradiation
with a small, low pressure mercury lamp in a specially
designed cell gave satisfactory results. Five-ml portions
of solutions containing from 4×10^{-5} $\underline{M}$ to 1×10^{-4} $\underline{M}$ oxalate
could be injected into this system and analyzed with an
accuracy on the order of 2% and a relative standard
deviation of about 0.9%. The method can be applied to
the determination of tartrate or citrate after appropriate
changes in reaction conditions. Overall advantages are
that the procedure is free from many interferences, is
sensitive, and can be used over a wide range of
concentrations. Disadvantages include the time required
per analysis and the special apparatus required.

The applicability of the method to the
determination of urinary oxalate was studied briefly.
The principal interference seemed to be due to high
absorbance by some urinary components of the radiation
needed for the photolysis of the iron(III)-oxalate
complex.

ACKNOWLEDGEMENTS

TABLE OF CONTENTS

LIST OF TABLES

CHAPTER 1

INTRODUCTION

Oxalic acid,

$$\begin{array}{c} COOH \\ | \\ COOH \end{array}$$

the simplest of the dicarboxylic acids, has a K_1 of
5.36×10^{-2} and K_2 of 5.3×10^{-5}. It is present in many plants
and vegetables, e.g., spinach, rhubarb, beets and parsley,
and is a metabolic end product in man, being eliminated in
the urine. Normally, 35-44% of urinary oxalate is derived
from dietary ascorbic acid, while 40% comes from glycine _via_
glyoxylate. The remainder is produced from glycolate, from
other reactions forming glyoxylate and from dietary sources[1].
Increased oxalate excretion can result from oxalate or
ethylene glycol (which is oxidized to oxalic acid) poisoning
and from primary hyperoxaluria[1] (caused apparently by a
problem in glyoxylic acid metabolism which leads to
excessive production of oxalic acid).

The brewing industry is also interested in oxalate
concentrations in beer, as that ion is present in malt and
hops and can combine with calcium in the beer to produce
calcium oxalate crystals. These form an unsightly haze and
can act as nuclei leading to excessive formation of carbon
dioxide bubbles[1].

Methods Used to Measure Oxalate Concentrations

Numerous direct and indirect methods have been proposed for the analysis of oxalic acid. These cover the whole spectrum of analytical methodology. As illustrations, some of the suggested techniques are presented here.

Oxalate can be quantitatively oxidized to carbon dioxide by titration with cerium(IV) or permanganate. In fact, sodium oxalate has been used as a primary standard for both cerium(IV) and permanganate solutions:

$$C_2O_4^{-2} + 2Ce^{+4} \rightarrow 2CO_2 + 2Ce^{+3}$$

$$5C_2O_4^{-2} + 2MnO_4^- + 16H^+ \rightarrow 10CO_2 + 2Mn^{+2} + 8H_2O$$
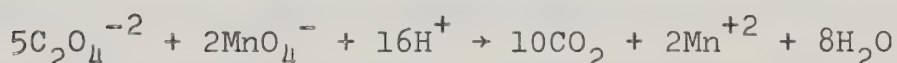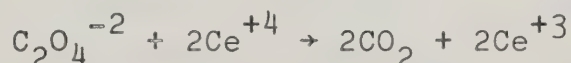
A significant number of methods involve precipitation of oxalate as the relatively insoluble salt, calcium oxalate. This can then be analyzed gravimetrically after conversion to calcium carbonate[2] or the excess calcium in the filtrate can be determined by an EDTA titration[3]. Oxalate can be titrated with calcium chloride using the Orion calcium ion selective electrode[4] or with lead perchlorate in 40% p-dioxane solution using a lead ion selective electrode to determine the end point[5]. After precipitation of the lead oxalate salt, excess lead ions can be titrated with potassium hexacyanoferrate(II) in the presence of potassium hexacyanoferrate(III) and Variamine

Blue[6] or with EDTA in the presence of Pyrocatechol Violet[7].

Dubey and Tandon[8] investigated adsorption indicators for the titration of oxalate with lanthanum, lead and mercury(I). For the first two titrants they suggest Bromopyrogallol red as indicator and for mercury(I), bromocresol green. Bismuth has also been used as a titrant, the oxalate being precipitated as Bi_2Ox_3[9*].

Direct colorimetric methods which have been used include the formation of a red indole complex[10] and a copper-benzidine complex[11]. Indirect colorimetric methods used comprise, among others, measurement of the decrease in absorbance of the iron(III)-salicylate complex[12] or the red uranium(IV)-4-(2-pyridylazo)resorcinol complex[13]. The fact that oxalate quenches the fluorescence of a 1:1 Zr:flavonol chelate also has been used as the basis of a method to determine the acid[14]. Oxalic acid yields glycolic acid when it is reduced by powdered magnesium. The deep red product formed when glycolic acid reacts with 2,7-dihydroxynaphthalene has been used to measure oxalate concentrations indirectly[15].

Many chromatographic methods have been suggested for the separation of oxalic acid from other substances. These include thin-layer chromatography[16], anion-exchange chromatography[17] and gas chromatography of the methylated derivative[18].

---

*Throughout this thesis, $C_2O_4^{-2}$ and Ox will be used interchangeably for the oxalate ion.

The change in absorption caused by the formation, from electrochemically generated lanthanum, of a suspension of lanthanum oxalate[19], or the turbidity of the silver oxalate sol in isopropanol medium[20] have also been used to measure oxalate concentrations.

Amperometry[21], polarography[22,23], coulometry[24] and enzymatic methods[25] have all been employed to analyze oxalic acid. A discussion of a number of methods which have been used to measure urinary oxalate is presented in Chapter 6.

Interferences in the Measurement of Oxalate

While all of these methods and others are applicable to pure oxalic acid or to solutions of oxalate salts, difficulties frequently arise in the presence of various matrices and/or low oxalate concentrations. There is no accurate, fast, reliable, specific method available for measuring oxalate nor is there a method available for measuring the analytically important ionic, as opposed to total, concentration of the ion. Hence, the proliferation of procedures adapted for various matrices.

If oxalate is to be determined gravimetrically, a reprecipitation is often necessary in the presence of interferences. When a calcium or lead ion selective electrode is used to follow the titration of oxalate,

species which complex with calcium or lead will cause
interferences. The pH must be carefully controlled so
that complete precipitation occurs, and so that dissolution
of the precipitate does not take place if back-titration
of excess calcium or lead ions is to be carried out.

A high chloride ion concentration cannot be
tolerated in the direct colorimetric determination with
indole, and the lower limit for this method is only 50 mg/l.
Because absorption spectra of the copper-benzidine complexes
of related acids such as oxalic, tartaric, malonic, citric,
lactic, glycolic, formic and succinic are highly similar,
the copper-benzidine method can only determine, with lowered
accuracy, large amounts of oxalic acid in the presence of
smaller amounts of other acids.

The presence of alkali metals gives curvature
and hence poorly defined end points when oxalate is
determined by turbidimetric titration with lanthanum.

Of the enzymatic methods proposed for the
determination of oxalate, problems owing to nonspecificity
of the enzyme, or, in the case of the specific oxalate
decarboxylase, inhibition by sulfate and phosphate ions[26],
have prevented widespread acceptance.

Purpose of this Research

Possibilities for a better method to determine
oxalate, especially in complicated matrices such as urine,

were investigated in this thesis . After study of the methods available, the iron-oxalate photochemical reaction (discussed in Chapter 2) using a gas sensing electrode or gas chromatography as a detector for the evolved carbon dioxide was chosen for detailed study.

CHAPTER 2

OXALATE ANALYSIS EMPLOYING A $\underline{p}CO_2$ ELECTRODE AS A DETECTOR

INTRODUCTION

Iron-Oxalate Chemistry

The photochemical decomposition of the iron(III)-oxalate complex was selected as the most promising approach for the determination of oxalic acid or oxalate salts in solution. With trivalent metals complexes containing one, two, or three oxalate ligands are known.

The trivalent complex of iron(III) has been the most widely studied because it has replaced the uranyl oxalate actinometer for use in the blue/ultraviolet region of the spectrum. Advantages of trioxalatoferrate(III) as an actinometer reagent include that it is hundreds of times more sensitive than uranyl oxalate. It can be used for polychromatic photometry also, because the quantum efficiency increases gradually from about 0.9 at 480nm to about 1.2 at 254nm. It is stable in the dark for long periods of time and is simple to use. The products of irradiation of potassium trioxalatoferrate(III) include iron(II) and carbon dioxide:

$$2[Fe(C_2O_4)_3]^{-3} \xrightarrow{h\nu} 2[Fe(C_2O_4)_2]^{-2} + C_2O_4^{-2} + 2CO_2$$

7
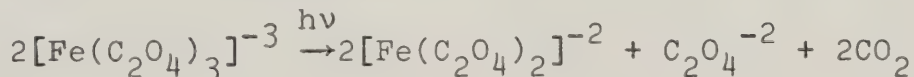
The iron(II) can be measured spectrophotometrically as the tris(1,10-phenanthroline) complex at 510 nm[27].

Industrially, ammonium trioxalatoferrate(III) is used with potassium hexacyanoferrate(III) in the blue-print process[28]. The iron(III) in the oxalate complex is reduced to iron(II) upon exposure to light and then reacts with potassium hexacyanoferrate(III) to produce insoluble Turnbull's blue, $Fe_3[Fe(CN)_6]_2$.

At low pH values and with an excess of iron(III) the monooxalatoferrate(III) complex is formed. This species is of analytical importance. The following sequence has been suggested[29] for its photodecomposition:

$$Fe^{+3}(C_2O_4)^{-2} \underset{\longleftarrow}{\overset{h\nu}{}} Fe^{+2}(C_2O_4)^{-}$$

$$Fe^{+2}(C_2O_4)^{-} \rightarrow Fe^{+2} + C_2O_4^{-}$$

$$C_2O_4^{-} + Fe^{+3}(C_2O_4)^{-2} \rightarrow 2CO_2 + Fe^{+2} + C_2O_4^{-2}$$

$$2(C_2O_4)^{-} \rightarrow 2CO_2 + C_2O_4^{-2}$$
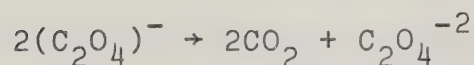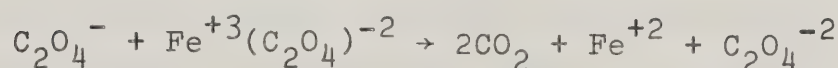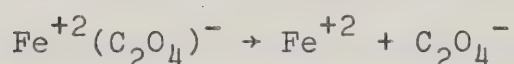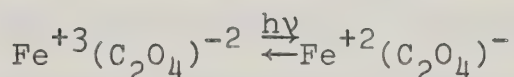
The first step involves an electron transfer and a weakening of the metal-ligand bond, followed by bond breaking in the second step. Various radicals have been postulated as intermediates. However, all schemes yield carbon dioxide and iron(II) as final products.

Early Photochemical Analysis

Rao and Rao[30] estimated iron(III) concentration by employing the photochemical reaction between iron(III) and oxalate. The iron(II) that was formed on exposure to sunlight was titrated with sodium vanadate using diphenyl amine as indicator. In later work[31], they found the sulfuric acid concentration could be varied between 0.1 and 0.8 $\underline{N}$ without appreciably altering the speed of the reaction. When sodium citrate or potassium sodium tartrate was used in place of sodium oxalate the reaction rate was much slower and was influenced by acid concentration, the rate decreasing with increasing acid concentration.

Rao and Aravanudan[32] measured the concentration of oxalic acid in solution by adding an excess (4:1 or greater) of iron(III) alum solution and acidifying with sulfuric acid. The iron(II) that was produced upon exposure to sunlight or artificial light was titrated with sodium vanadate and the oxalate content was calculated from that. When sunlight was used for irradiation the reaction was complete in 15 to 30 minutes; with a 1000-watt tungsten filament lamp an exposure of three hours was required. With a quartz mercury vapor lamp six hours was reported as necessary to complete the oxidation. In further work[33] on determining the iron(III) concentration by reduction with oxalic

acid, it was noted that as the amount of iron(III)
present increased, the time necessary for the reaction
to go to completion also increased. Lactate could be
used in place of oxalate as the reducing agent in neutral
or weakly acidic solutions.

Riggs and Bricker[34] extended the above ideas and
determined oxalate by measuring the photochemically
generated iron(II) by titration with sodium dichromate
(2 ppt accuracy) or, for smaller amounts of oxalate, by
spectrophotometric determination with 1,10-phenanthroline
(3% accuracy). A 15-minute irradiation in a deoxygenated
solution with a 100-watt medium pressure mercury vapor
lamp was used in their analyses. They further investigated
the interferences produced by a number of carboxylic acids.

This chapter discusses an investigation of the
analytical utility of the iron(III)-oxalate reduction
in which a $\underline{p}CO_2$* electrode in a continuous-flow mode is
used to measure the carbon dioxide produced.

$\underline{p}CO_2$ Electrode History

The $\underline{p}CO_2$ electrode evolved primarily as a
clinical tool for analysis of blood gases. Only
recently has it been used for other analytical
applications. Guilbault and Shu[35] used it as an

---

*In this thesis $\underline{p}CO_2$ is used to designate the partial
pressure of carbon dioxide.

enzyme electrode for urea by immobilizing urease on the gas permeable membrane.

The first report of an electrical measurement of pCO_2 in blood was that of Stow and Randall[36]. Further description of the pCO_2 electrode was provided by Stow, Baer, and Randall[37] in 1957. Initially, a glass electrode was separated from the carbon dioxide-permeable rubber membrane (a finger cot) by a thin film of water (the internal filling solution). The carbon dioxide in the test solution diffused across the membrane into the film of water where it hydrated and dissociated, causing a pH change:

$$CO_2 + H_2O \rightleftarrows H_2CO_3$$

$$H_2CO_3 \rightleftarrows H^+ + HCO_3^-$$

$$HCO_3^- \rightleftarrows H^+ + CO_3^{-2}$$
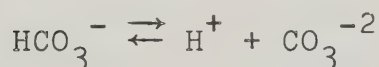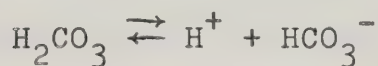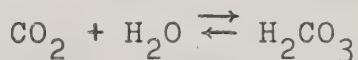
Calibration of the electrode was achieved by placing it in saline solutions which had been equilibrated to a known pCO_2 by bubbling a gas mixture of known CO_2 concentration through it. The slope of a Nernst plot was 30.3 mV and remained constant. For measuring the pCO_2 of blood gases, the electrode was thermostatted at $38 \pm 0.05°C$ (near body temperature). Careful temperature regulation was necessary because the temperature coefficient of solubility of CO_2 is about

5% per degree in this temperature region.

The following year Gertz and Loeschcke[38] reported covering the glass electrode with a polyethylene shell 10 to 20 µm in thickness and using a 1×10^{-3} $\underline{M}$ $NaHCO_3$ solution instead of water as the internal filling solution. Other workers[39] showed that the electrode sensitivity could be doubled by replacement of the water internal filling liquid by a sodium bicarbonate solution. They defined the sensitivity as

$$S = \frac{\Delta\ pH}{\Delta\ \log\ \underline{p}CO_2}$$

With water as the internal liquid S is about 0.5 whereas with a 0.01 $\underline{M}$ $NaHCO_3$ solution it doubled to about 1. A trade off exists, however, in that with water or dilute bicarbonate solutions the response time is faster than with more concentrated bicarbonate solutions. With concentrated solutions more carbon dioxide must be exchanged as increasing amounts of carbonate are produced in the internal filling solution.

The optimum design of Severinghaus and Bradley[39] comprised a Teflon membrane separated from the glass electrode by a thin layer of cellophane whose purpose was to hold a film of liquid between the glass and Teflon. Also, sodium chloride was added to the 0.01 $\underline{M}$ $NaHCO_3$ internal filling solution. This system was more

stable, faster in response and drifted much less than previous designs due to the stabilizing effect of the chloride ion on the silver-silver chloride reference electrode and to the greater conductivity of this solution. They observed a linear response between 1.38 and 11.37% CO_2. For a four-fold rise in CO_2 about 2 minutes was required to reach equilibrium whereas for a similar decrease in CO_2 levels the response time was about 4 minutes. This type of behavior is typical of all gas sensing electrodes. Faster response could be achieved by using thinner films of Teflon but because of lack of mechanical strength these were not satisfactory.

Hertz and Siesjö[40], by utilizing a slightly concave glass electrode membrane surface, were able to omit the cellophane layer. They also reported increased stability through use of a miniature calomel reference electrode instead of the silver-silver chloride one. Most commercial $\underline{p}CO_2$ electrodes, however, incorporate a combination electrode with a silver-silver chloride reference system.

The optimum thickness of the Teflon or polyethylene membrane has been reported to be 20 μm[41]. Decreased thicknesses resulted in faster response, but the results were less reproducible.

Considerable study has been done on the best

method of calibrating gas sensing electrodes. Exposure

to a stream of gas, heated to the electrode temperature

and saturated with water vapor, has been widely used[42].

The possibility that carbon dioxide could diffuse from

the gas mixture and cause errors in calibration led to the

use of acidified sodium bicarbonate[43] or acidified

sodium carbonate[44] solutions. In addition to the obvious

advantage of ease of preparation and hence ease of

obtaining many calibration points, the use of these

solutions as a standard obviates the problems of

incomplete humidification of the gases and electrode

temperature changes due to the flowing gas.

Severinghaus[45], in a later modification,

replaced the cellophane spacer which was believed

responsible for slow electrode response, especially at

low carbon dioxide levels, by a thin piece of

nylon mesh or glass wool. The nylon layer between the

gas permeable membrane and the electrode surface improved

the response of the electrode and its linearity. The

glass wool was thought to catalyze the reaction of carbon

dioxide with water but it was not as reliable as the

nylon layer because the glass wool sometimes cut the

membrane.

A thorough treatment of the theory of

potentiometric gas sensing electrodes has been provided by

Ross, Riseman and Krueger[46]. Among the advantages of
gas electrodes listed by them are that after equilibrium
between the sample and the internal filling solution has
been established there is no further consumption of gas
from the sample. Ionic species do not cross the membrane
and interfere with the measurement. Furthermore,
electrode calibration is independent of the rate of
stirring and membrane thickness, and there is no liquid
junction problem. They derived an equation showing the
response time of the electrode as a function of the
geometry, membrane characteristics, internal electrolyte
composition and experimental conditions. They also
predict that when a series of solutions are measured in
order of increasing concentration, the time response is
independent of the magnitude of the concentration change.
However, for the reverse process, the time response
varies as the ratio of the lower to higher concentration.
The basis of other gas sensing electrodes is also given.

Ruzicka and Hansen[47] recently reported on an
air-gap electrode in which an air gap replaces the gas
permeable membrane. The internal filling solution is
absorbed on the end of a combination glass electrode.
This layer of solution can be renewed between measurements
or can be used in an equilibration mode. The advantages
of this design are its fast response time and the fact
that the electrode does not physically contact the sample.

Other Methods for Oxalate Analysis which Yield Carbon Dioxide

Many substances other than iron(III) oxidize oxalate to carbon dioxide. In these methods either the reduced species is used as a measure of the oxalate concentration or the carbon dioxide is determined by a manometric, volumetric or colorimetric method. The pCO_2 gas electrode could be used for many of these analyses.

The enzyme, oxalate decarboxylase, from the wood-rot fungus, Collybia velutipes, catalyzes the reaction:

$$H_2C_2O_4 \rightarrow HCO_2H + CO_2$$

This enzyme is most active at pH 3.0 and most stable at pH 4.5. Reportedly, it acts specifically on oxalic acid in the presence of small amounts of oxygen[48]. The carbon dioxide evolved through decarboxylation can be measured by the Warburg technique[49]. Work has also been performed on the same enzyme extracted from Aspergillus niger[50].

An enzyme from the obligate plant parasite, Tilletia contraversa, oxidizes oxalate to carbon dioxide and probably hydrogen peroxide.

$$H_2C_2O_4 + O_2 \rightarrow 2CO_2 + H_2O_2$$

Stimulation by riboflavin and flavine mononucleotide (FMN) was shown[51]. Similar findings were reported for an enzyme in barley seedling roots[52,53]. In 1972, however, Halliwell[54] reported that riboflavin and FMN photochemically promoted release of carbon dioxide from oxalate without any added enzyme. He concluded that there was no net stimulation of the enzyme by these substances.

A brief study was made of the use of the pCO_2 electrode to measure carbon dioxide from the oxalate-oxalate decarboxylase and oxalate-riboflavin systems. More extensive work was done on the oxalate-iron(III) system, where those substances which interfered in earlier methods by reducing iron(III) will not be interferences unless they also produce carbon dioxide. Also, after automation this method is less time consuming than earlier ones in which the iron(II) was measured by titration or by spectrophotometry. In those methods of analysis standard titrants or a standard iron(II) orthophenanthroline solution had to be prepared. In addition each oxalate analysis required at least two pipettings. Colored solutions were a problem. For both titrimetric and spectrophotometric methods of analysis oxygen had to be excluded from the reaction vessel[34] or the beaker had to be covered with a quartz lid[33]. If

this were not done, iron(II) was air oxidized to iron(III) and low results were obtained. This precaution was not necessary in the CO_2 method of analysis. A further advantage of the proposed method was that only 10-ml samples were required.

EXPERIMENTAL

Apparatus and Chemicals

Two models of pCO_2 electrodes were used through-
out this research. The first was a Radiometer pCO_2
electrode and the associated blood gas apparatus. This
electrode is a combination glass pH-indicating—silver-
chloride reference electrode with a slightly convex glass
membrane upon which is placed a small piece of Joseph's
paper (a thin chemically resistant kind of tissue paper).
The glass electrode fits inside an outer tube with a
gas permeable Teflon membrane covering one end. In the
tube is placed a small amount of a 0.005 $\underline{M}$ NaHCO$_3$ - 0.5 $\underline{M}$
NaCl solution saturated in silver ions. This is the
internal filling solution.

The second pCO_2 electrode which was used was
manufactured by Instrumentation Laboratory (IL). It
has the same basic Severinghaus design but is different
in that netting is substituted for the Joseph's paper,
Silastic is used in place of the Teflon membrane and
the internal filling solution is reported[35] to be a
0.02 $\underline{M}$ NaHCO$_3$ solution. Throughout the experimental
work different internal filling solutions were
substituted. The glass sensitive tip of the IL
electrode is more pointed than that of the Radiometer
electrode and in the assembled unit pushes against the

19

Silastic, causing only a thin film of liquid to be held between the membrane and the sensing part of the electrode. The Radiometer design appears to retain a greater volume of liquid in this region, and because of this, the response of this electrode was predicted to be slower than that of the IL one.

The plugs on the shielded cables of both electrodes were replaced with Beckman-type plugs so they could be used with an Orion 801 pH meter. A Houston Omni Scribe Model number 5113-5 one-pen recorder or a Hewlett-Packard 7101BM strip chart recorder was connected to the meter to provide a continuous record of electrode response.

Irradiation in the visible region was provided by a General Electric extended service long life tungsten light bulb (200 watts); in the ultraviolet region it was provided by a Hanovia type 30620 utility ultraviolet quartz lamp (140 watts).

All chemicals were reagent grade and were used as received. Distilled water was used throughout.

The automated system employed Sampler II and Pump I units from a Technicon single channel AutoAnalyzer. For the irradiation step two concentric 40-foot Pyrex coils, 1.6 mm i.d. and 1 mm wall thickness, were used. Throughout much of the analysis, the sampling motor in

the Sampler II was replaced by one half as fast . This enabled slower cam speeds to be used. The air that was introduced with the samples and reagents in the pump step was removed by a debubbler prior to the solution's passage beneath the electrode. The purpose of the air bubbles is to segment the liquid stream so as to minimize mixing of one sample with the next by cleaning the tubing circumference after each liquid segment. Without these bubbles laminar flow is more prevalent and cross-contamination from adjacent samples is increased. As shown in Figure 1, after passage through a flow-through compartment of the pCO_2 electrode, the sample solution recirculated through the pump to promote the smooth flow of samples before discharge to waste.

Since a commercial flow-through arrangement is not available for the IL electrode, a compartment was constructed (Figure 2) of Plexiglas in the Department of Chemistry machine shop at the University of Alberta. The electrode was pressure fit into the container and a hand-tightened Nylon set screw near the top insured its immobility. The bottom of the sample well was machined to allow a small volume of solution to flow across the protruding tip of the electrode. A small contact volume kept the rate and sensitivity of response at a high level, while minimizing cross contamination. The inlet
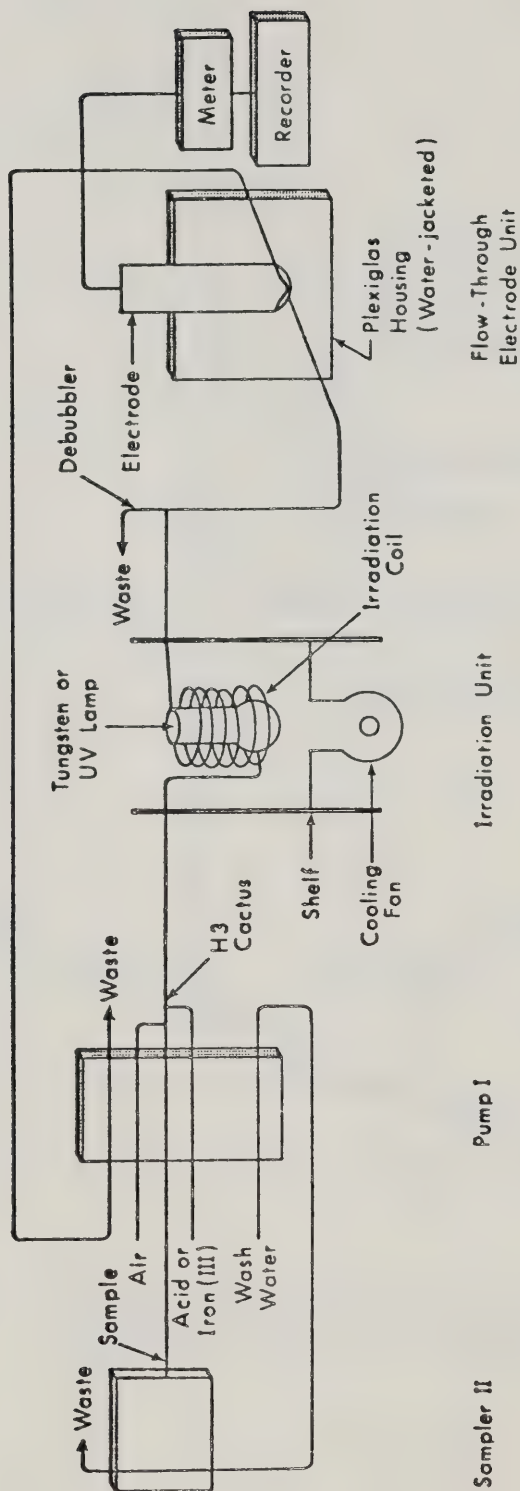
Figure 1 Design of Continuous-Flow Analysis System used to Measure Oxalate Concentrations: Technicon AutoAnalyzer components are used.
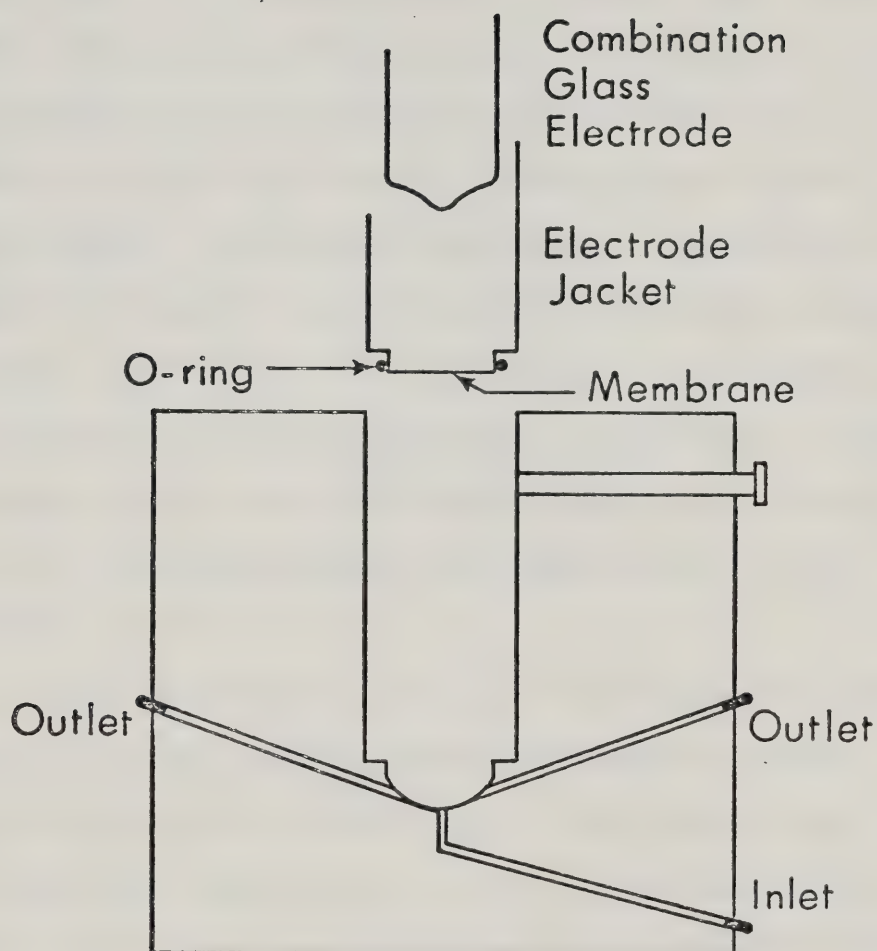
Figure 2 Design of Plexiglas Flow-Through
Compartment for an IL $\underline{p}CO_2$ Electrode.

and outlet were about 1 mm in diameter, and were placed

opposite to each other as shown in Figure 1, or one inlet

and two outlets at about 90° to the inlet were used as

shown in Figure 2. Small metallic nipples were secured

into the openings to provide tubing connections. To

prevent bubbles from becoming entrapped under the

electrode the inlet and outlet channels were angled

slightly upward. The entire electrode flow-through unit

was placed in a 25°C water-jacketed temperature-controlled

container. A Brinkmann Instrument Type K2 circulating

water bath was used to maintain the temperature. Exact

temperature control was not likely maintained, however,

because of the large mass of Plexiglas around the

electrode.

For the oxalate analysis the glass coils were

mounted on a wooden shelf and the irradiation source

placed in the center of the coils. Cool air, blown

upward through a hole in the wooden shelf, prevented

excessive heating of the solutions during irradiation.

The coils were surrounded by aluminum foil to avoid eye

damage when ultraviolet radiation was used, and also

to improve the efficiency by reflecting radiation back

towards the coils. Later a more permanent housing was

designed and built from stainless steel by the

Department of Chemistry machine shop. This consisted of

a large box with a tilted top to allow air circulation, a center shelf upon which the coils rested, and a fan compartment below. Either lamp could be placed inside this box and anchored to a supporting rod.

The sodium bicarbonate solutions used in the automated mode were prepared in 0.5 $\underline{M}$ NaCl while the potassium oxalate solutions were prepared in 0.5 $\underline{M}$ NaCl and 0.1 $\underline{M}$ H_2SO_4 unless otherwise noted. Potassium oxalate was chosen rather than sodium oxalate because it is more soluble. The purpose of the sodium chloride was to increase the ionic strength of the solutions to a level comparable to that of the internal filling solution. Also, it provided a more realistic matrix for the oxalate analysis, since real samples rarely occur in pure water. The $FeNH_4(SO_4)_2 \cdot 12H_2O$ was prepared in 1, 2 or 4 $\underline{M}$ H_2SO_4 or in water. A few drops of a wetting agent, Brij 35, were added to the acid reagent solution for bicarbonate analysis or to the iron(III) solution for oxalate analysis. Use of a wetting agent reduces surface tension of the solutions and thereby improves sample passage through the glass and plastic tubing of the continuous-analysis system.

RESULTS AND DISCUSSION

Preliminary Electrode Studies

Electrode Calibration. Initial checks and calibration of
the Radiometer system were done with calibration gases
(Linde 1.99% and 7.85% CO_2 in O_2) as suggested by the
manual accompanying the instrument. Later these gas
mixtures were replaced with solutions of known
concentrations of sodium bicarbonate in 0.5 M sodium
chloride, acidified with sulfuric acid. Not only was
this less costly, but many different carbon dioxide levels
could be prepared, allowing the response of the electrode
to be more fully determined. Also, since the carbon
dioxide evolved from the oxalate is in aqueous solution
the bicarbonate samples resemble that medium more closely
than do gaseous samples.

Comparison of the Electrodes. A five-point calibration
plot was run with the IL electrode by pipetting solutions
of bicarbonate into a beaker and adding sulfuric acid. A
slope of 56.2 mV was obtained between 5×10^{-4} and 5×10^{-2} M
$NaHCO_3$ (Figure 3). The overall absolute standard
deviation for the linear least square fit was 0.75 mV.
A similar five-point plot with the Radiometer electrode
gave a slope of 49.9 mV between 5×10^{-4} and 1×10^{-2} M $NaHCO_3$
and an overall standard deviation of 1.62 mV after
deletion of the 0.05 M point (Figure 3). During these
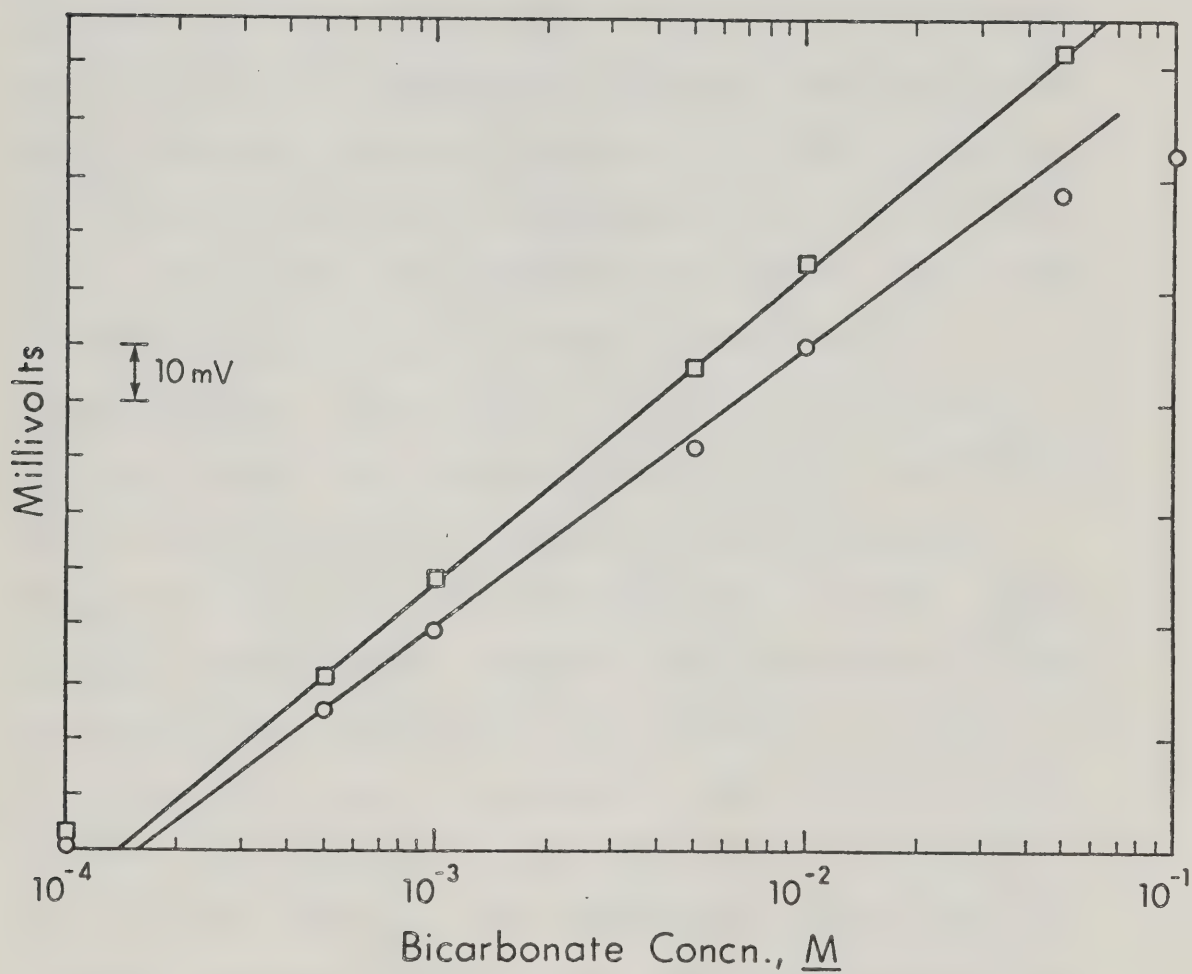
Figure 3   Calibration Plots for Acidified Bicarbonate
Solutions with IL and Radiometer pCO_2
Electrodes: □ IL; ○ Radiometer.

measurements the Radiometer electrode was fitted with a
Silastic membrane. The same internal filling solution,
0.01 $\underline{M}$ NaHCO$_3$, 0.2 $\underline{M}$ KCl and saturated with silver ions,
was used for both electrodes. Because of differences in
the value of E°, experimental millivolt readings differ,
and so absolute voltage values are not given in Figure 3.
The results show that, as predicted, the IL electrode is
more precise than the Radiometer one and is linear over
a larger range of carbon dioxide concentration.

Time Response. At the 5×10^{-4} $\underline{M}$ level 5 minutes were
required before the Radiometer electrode was sufficiently
near equilibrium that a reading could be recorded,
whereas the IL electrode required only 2 minutes. For
0.01 $\underline{M}$ concentrations 3 minutes were required to obtain
an equilibrium reading with the Radiometer, as opposed to
1.5 minutes for the IL electrode. This shows that the
rate of equilibration for the Radiometer electrode is
much slower, and also that Severinghaus electrodes, in
general, respond faster to more concentrated solutions.

Most of the remainder of the studies were
performed with the IL electrode.

Preliminary Iron(III)-Oxalate Experiments

Once the electrode response had been evaluated
with acidified bicarbonate solutions, several qualitative
experiments were done in a manual mode to investigate

the iron(III)-oxalate reaction. When a solution containing iron(III) nitrate and 1×10^{-2} $\underline{M}$ sodium oxalate acidified to pH 1 was irradiated for 15 minutes, with either the Hanovia ultraviolet lamp or with the tungsten light, readings indicating carbon dioxide production were obtained with the $\underline{p}CO_2$ electrode. A solution irradiated with the ultraviolet lamp gave a millivolt reading 29.5 mV higher than one irradiated with the tungsten lamp. From these and other experiments, it became evident that the $\underline{p}CO_2$ electrode could be used to follow the carbon dioxide generation from the iron-oxalate reaction.

Similar experiments showed no qualitative difference between use of iron(III) nitrate or iron(III) ammonium sulfate as the source of iron(III). Also, the slow bubbling of oxygen through the solution did not have any apparent effect on the rate of the reaction, as might be expected if reoxidation of iron(II) were critical. The reaction even proceeded in the presence of moderate concentrations of calcium ions.

Interferences. Mannitol,

$$
\begin{array}{c}
CH_2OH \\
| \\
HO-C-H \\
| \\
HO-C-H \\
| \\
H-C-OH \\
| \\
H-C-OH \\
| \\
CH_2OH
\end{array}
$$
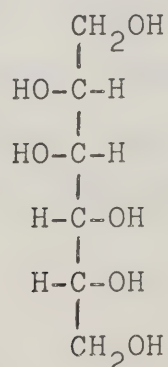
which was an interference in Riggs and Bricker's work[34], was tested as an interference. A 10^{-2} $\underline{M}$ solution was prepared in 0.01 $\underline{M}$ H_2SO_4 and iron(III) was added to it. The resultant solution was irradiated with the ultraviolet lamp. No carbon dioxide was detected. This, then, is an example of a substance which can reduce iron(III) but does not produce carbon dioxide.

Analysis Time. When the pCO_2 electrode is placed in an acidified solution a reading can be obtained in only a few minutes. However, in the iron-oxalate analysis, carbon dioxide is generated slowly and the possibility of loss of carbon dioxide to the atmosphere during the reaction time must be considered. Two solutions of 5×10^{-3} $\underline{M}$ oxalate were irradiated in the presence of iron(III) and acid for 90 minutes, the first in a 10-ml beaker exposed to the atmosphere, and the second in a 20-ml beaker with a rubber stopper fitted around the electrode. In both cases the millivolt readings increased for the first 40 minutes, and then decreased. The increase was likely the result of slow production of carbon dioxide from oxalate, and the decrease was due to the loss of carbon dioxide to the atmosphere. The second system gave readings slightly lower than the first, likely due to a decreased area of solution exposed to the radiation.

<u>Temperature Control</u>. Several modifications were undertaken
to try to improve this crude system. Tungsten bulbs
irradiate in the region beginning at about 330 nm and
extending through the visible region and into the near
infrared. The ultraviolet lamp, a line as opposed to a
continuous source, produces radiation at a large number
of wavelengths in the visible and ultraviolet region.
Considerable heat is emitted by both lamps, especially
the tungsten bulb, and results in a temperature rise in
the solution under study. Carbon dioxide is less soluble
at higher temperatures. For optimum results, therefore,
all samples and standards should be kept at the same
temperature. To try to accomplish this, the beaker
containing the iron-oxalate solution was placed in a
water-jacketed temperature-controlled container and
irradiated through the water. This was of some help
but with the extra glass and water to absorb the light
the irradiation reaching the solution was diminished.
Further reduction took place if any iron(III) salt
spilled and coated the walls of the water jacket.
Although the rate of carbon dioxide production was slow,
if care was exercised, good Nernstian calibrations could
be obtained (Figure 4) with a 20 minute irradiation time.
The millivolt readings are lower than those obtained for
a set of similar bicarbonate measurements, because of the
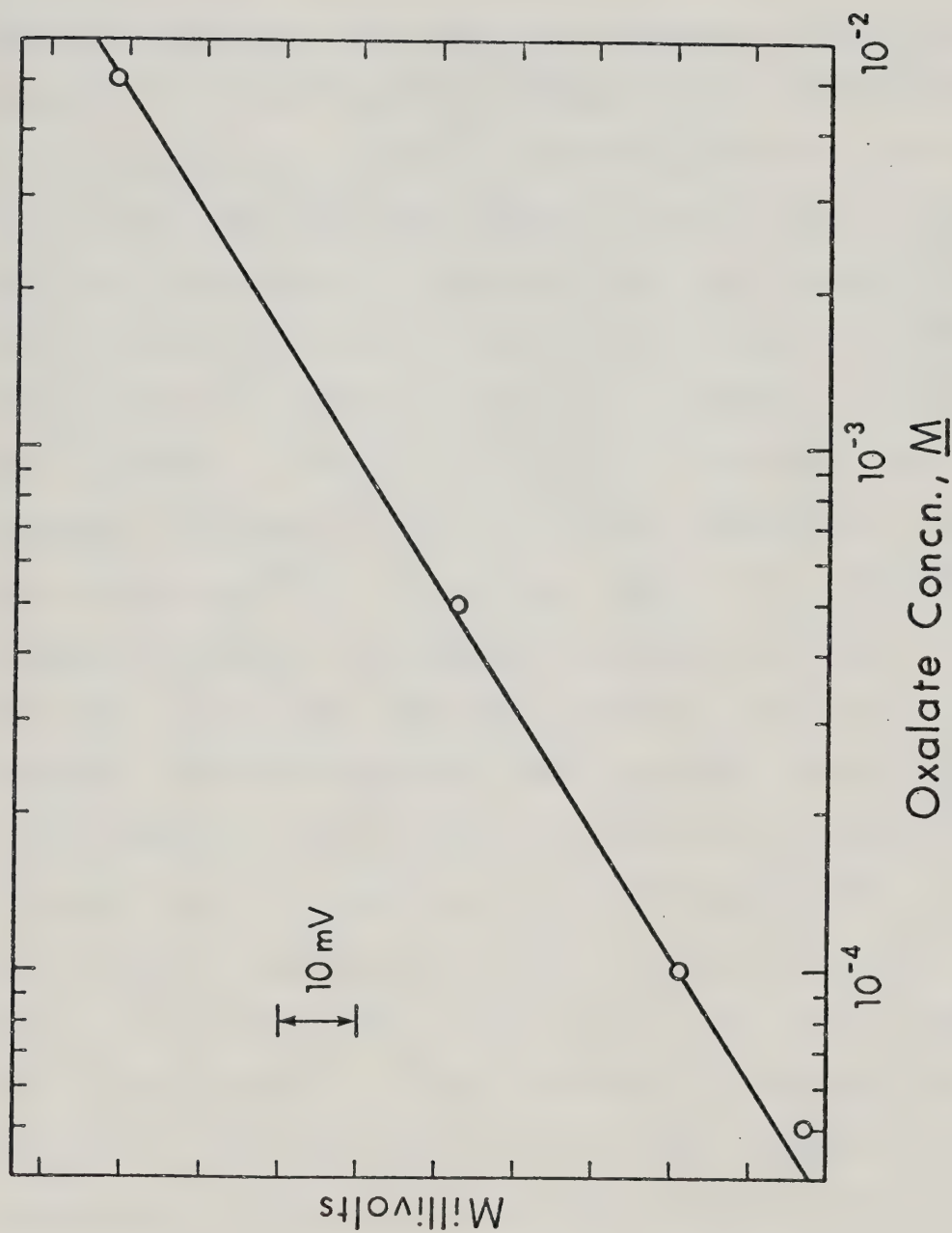
Figure 4   Calibration Plot for Oxalate Samples on a Batch Basis. IL Electrode used, with a 20-minute exposure to ultraviolet radiation.

large amount of iron(III) present. This point will be
discussed more fully in the section on automated oxalate
analysis.

Multiple Analysis. To speed the analysis a shaker was
employed so that a number of samples could be irradiated
at the same time. Acidified potassium oxalate solutions
containing iron(III) were placed in small glass stoppered
jars and irradiated for varying times, with gentle shaking.
After irradiation each solution was stirred in a 25°C
water bath for 4 minutes and then a reading was taken with
the electrode. For $5x10^{-3}$ $\underline{M}$ oxalate solutions, the
readings increased by 12.5 mV as the irradiation time
increased from 38 to 67 minutes, while for a $5x10^{-4}$ $\underline{M}$
oxalate solution, the readings increased by only 5.8 mV
when the irradiation time was increased from 40 to 69
minutes. Thus it was shown that solutions of different
concentrations should either be irradiated so that the
reaction goes to completion or be irradiated for a constant
time period. The easier of these two choices would
appear to be the latter, although this was not as simple
as it would appear. It was difficult to arrange the
samples so that each received the same intensity of
irradiation. The solutions should all be read at the
same time after irradiation to minimize variations in
carbon dioxide equilibrium with the atmosphere. This is

difficult to accomplish with the Severinghaus electrode, since the time necessary to read a sample depends on its concentration.

Use of $\underline{p}CO_2$ Electrode with Other Reagents
for Oxalate Analysis

Cerium(IV) as Oxidizing Agent. Iron(III) is one of several oxidizing agents capable of oxidizing oxalate to carbon dioxide. Cerium(IV), added as $(NH_4)_2Ce(NO_3)_6$, generated carbon dioxide quickly from oxalate without any irradiation. Nernstian results could be obtained over the same range as with the iron(III). However, because of its lower reduction potential iron(III) was chosen as the oxidizing agent for the majority of the studies (0.77 V versus 1.61 V for Ce(IV) – Ce(III)).

Oxalate Decarboxylase Experiments. Several different types of enzyme electrodes were prepared and investigated in a qualitative manner. The first was made by immobilizing oxalate decarboxylase No. 0-3500 Grade II (Sigma Chemical Company) on nylon mesh in a polymer matrix. The polymer sheet was then placed over the Teflon membrane of the Radiometer $\underline{p}CO_2$ electrode so that carbon dioxide produced from the oxalate by the enzyme could be measured directly. Less than milligram amounts of the enzyme were added to acrylamide and methylene acrylamide in the presence of catalytic amounts of

riboflavin and potassium persulfate in pH 3.5 citrate buffer. The polymer was then cured by irradiation with a 200-watt tungsten bulb in a nitrogen atmosphere for about an hour. After placement of the polymer sheet over the Teflon gas permeable membrane a potential could be obtained in oxalate-containing solutions.

A similar method involved placing dissolved enzyme on Joseph's paper and placing it against the Teflon membrane, being held in place with a piece of cellulose. Oxalate could pass through the cellulose to react with the enzyme but the enzyme could not escape into the bulk solution.

The third method for utilizing the enzyme involved adding it to a vial containing pH 3.5 buffer and then adding the oxalate sample to this solution. After reaction, the pCO_2 electrode was immersed in the solution and the potential recorded.

In all of these cases readings could be obtained in solutions that contained at least 1×10^{-3} $\underline{M}$ oxalate. However, there were many drawbacks to the procedure, an important one being the high cost of the enzyme. The reaction was relatively slow, especially if low enzyme concentrations were used. Since formic acid, a product of the reaction, was later shown to interfere with carbon dioxide measurement using the pCO_2

electrode, complexing of the electrode with oxalate decarboxylase does not appear promising at the present time as a method for oxalate determination.

Riboflavin Experiments. Experiments were conducted in which carbon dioxide evolved from the reaction of oxalate with riboflavin was sensed by a $\underline{p}CO_2$ electrode. The acidity had to be kept in the range of pH 3 to 6, but concentrations of oxalate as low as $1x10^{-4}$ $\underline{M}$ could be detected by irradiation of a solution of oxalate containing riboflavin. Nevertheless, because of the insolubility of the riboflavin further experimentation in this area was discontinued. Automation of a system such as this, using a Technicon system, would be impossible as the riboflavin would plug the small diameter tubing used.

Automated Carbon Dioxide Analysis

One way to eliminate variability in sample treatment and to minimize carbon dioxide loss to the atmosphere is to convert the system to a continuous-flow mode. In this pseudoclosed system, irradiation time and temperature would be standardized and the time between irradiation and measurement could be made more reproducible. The method could be adapted to routine use on a large number of samples.

Carbon Dioxide Calibration. A typical calibration plot for acidified solutions of sodium bicarbonate utilizing

the set-up described in the experimental section and optimized as outlined below is shown in Figure 5.

Samples were introduced through 0.065 in. i.d. tubing and mixed with air, also introduced through 0.065 in. i.d. tubing and sulfuric acid, introduced through 0.020 in. i.d. tubing.

A series of runs using $5x10^{-3}$ $\underline{M}$ $NaHCO_3$ and 2 $\underline{M}$ H_2SO_4 were made to study the effects of sampling speed, sample arrangement and presence of wetting agent. The bicarbonate and acid solutions, mixed in the pump, flowed through a 40-foot Pyrex coil before being measured by the IL $\underline{p}CO_2$ electrode. Five runs were made for each condition that was tested.

Effect of Sampling Time. A cam on the sampler controlled the rate of analysis by controlling the time the sample probe spent in a sample cup and in wash liquid. For these measurements, a cam equivalent to the Technicon 10 2/1 unit was used. This designation means that the sampling rate is 10 samples/hour and the ratio of time the probe spends in the test solution compared to the wash liquid is 2 to 1. When the sampling speed was increased from 10 samples per hour to 20 and then 30 (with samples directly following each other) the standard deviation for a set of 5 runs increased from 0.32 to 0.44 to 1.80 mV, clearly showing the slower rate of sampling
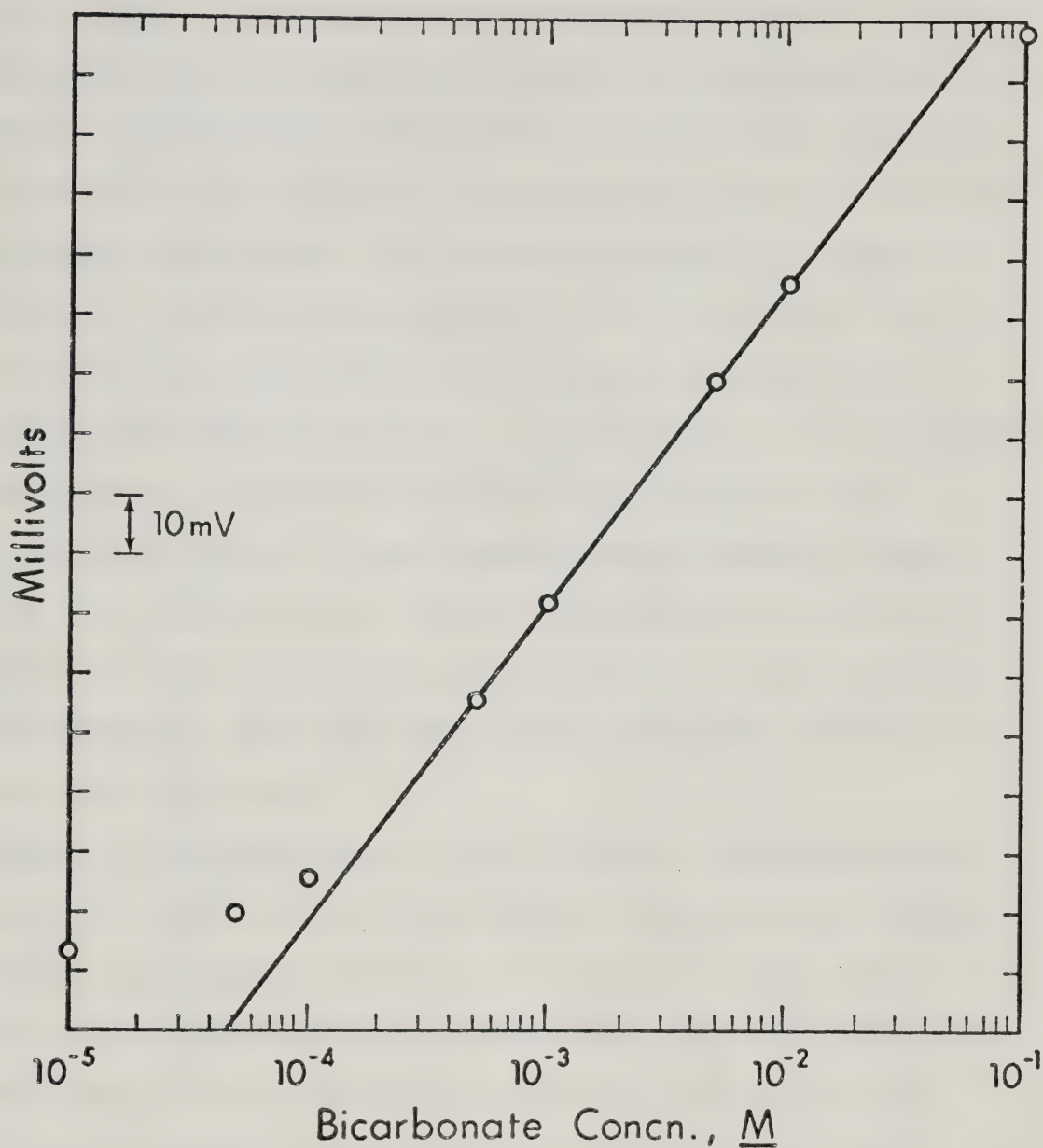
Figure 5 Calibration Plot for Acidified Solutions of
Sodium Bicarbonate using an IL pCO_2 Electrode
in a Continuous-Flow Mode.

to be optimum.   At faster rates successive readings
on a sample of the same concentration increased,
indicating that equilibrium was not being attained in the
earlier measurements.   Two further samples were analyzed
to estimate the length of time necessary for the electrode
to reach equilibrium.   The results obtained are shown in
Table 1.   At sampling times of 1.3 or 2.0 minutes, the
electrode had only 0.67 or 1.0 minutes in which wash
liquid separated the samples.   Consequently, the electrode
never came to equilibrium with either sample or wash
liquid, resulting in each reading being slightly higher
than the previous one.   Since 4 minutes was the longest
sampling time conveniently obtainable with the Technicon
AutoAnalyzer, this time was adopted throughout most of
the succeeding work.

Effect of Sampling Rate.   The effect of sampling rate on
electrode response was investigated by inserting a empty
sample cup between samples in the sampler tray.   While
the sampler probe was in an empty cup, only air and acid
were being pumped through the system.   The extra time
between samples allowed the carbon dioxide which had
diffused across the membrane and into the filling
solution of the electrode to diffuse out again.   The
absolute standard deviation for a set of five samples,
separated by one empty cup between each sample, was 0.08,

TABLE 1

Effect of Sampling Time on Bicarbonate Analysis

Sampling Time, min.	Sampling Conditions[a] samples/hour-sample:wash ratio		Average of 5 Runs mV	First Sample Reading mV
1.3	30	2:1	28.10	27.33
2	20	2:1	28.80	28.62
4	10	2:1	29.04	28.91
10	—		—	29.30
20.8	—		—	29.50

[a]The actual cams used were 60, 40 and 20 per hour with sample:wash ratios of 2:1, but because the speed of the sampling motor was reduced to half, the effective cam speeds were as listed in the table.

compared with 0.32 mV for a set in which the samples were
run in consecutive cups. The condition selected for
routine analysis, was to include two empty cups following
each sample. Empty cups were found more effective than
water-filled ones in minimizing sample memory by the
electrode.

Effect of Wetting Agent. Addition of a wetting agent,
Brij 35, to the acid improved the precision, mainly by
decreasing the noise appearing at the sample plateau.

E_∞ Calculation. Müller[55] suggested that one should
always report E_∞ as opposed to E values at some fraction
of the equilibrium value. Recognizing that the time
required to reach equilibrium is long for many electrodes,
he suggested that E_∞ values be computed. A plot of t/E
versus t, where t is time, gives a straight line with a
slope of b and intercept of a. The value of E_∞ is 1/b.
Several of these plots were attempted for the pCO_2
electrode and, as predicted, a straight line was obtained
if the initial points, where experimental conditions were
ill-defined, were omitted. To perform this calculation
accurately, the 4-minute sampling time did not yield
enough data, however, and this approach was abandoned.

Inclusion of a Debubbler. Another parameter that was
investigated in the use of the pCO_2 electrode in the
continuous-flow mode was the need of a debubbler prior

to the electrode. For example, in AutoAnalyzer methods employing a colorimeter, it is important that no bubbles enter the flowcell because they cause a sharp off-scale movement in the recorder pen. In other automated methods generating carbon dioxide for analysis, it is the gas in the air bubbles that is analyzed and hence must be separated from the liquid. The pCO_2 electrode is different from these colorimetric systems. Therefore, five samples of 1×10^{-3} $\underline{M}$ $NaHCO_3$ were run, each separated by two empty sample cups in the sampler tray. With no debubbler, the absolute deviation was 1.7 mV. It improved to 1.1 mV with the insertion of the debubbler. Similarly, with four samples each of 1×10^{-4} and 1×10^{-3} $\underline{M}$ $NaHCO_3$ run alternately the standard deviation was 5.8 and 1.7 mV resp. for the samples without the debubbler, and 2.4 and 0.9 mV resp. with it. In further work, the debubbler was routinely used. Even with its use, some air passed through the electrode flow-through compartment during those times when air replaced the sample, but this did not seem to affect the results adversely.

Effect of Membrane Thickness. The Silastic material supplied by IL for the electrode gave better results than Teflon did. The individual membranes, supplied with pieces of cardboard backing for convenience in assembly, are 0.003 in. thick. Dow Corning

manufactures Silastic sheeting, with and without Dacron reinforcement, for the medical profession. After a thorough washing with soap and water to remove the bicarbonate dusting, pieces of 0.005 in. and Dacron-reinforced 0.007 in. Silastic sheeting were cut to fit the electrode jacket. As can be seen from Figure 6, there is little difference between these membranes and the 0.003 in. thick size supplied by IL. Substitution of membranes was made throughout the course of these studies. The Dow Corning membranes were much less expensive than the IL-supplied ones, and were more sturdy. Medical Adhesive Silicone Type A cream could be used satisfactorily to repair small holes in the membrane.

Composition of Internal Filling Solution. The effect of variation in internal filling solutions on electrode response was also investigated. Bicarbonate concentrations of 1×10^{-2}, 1×10^{-3} and 1×10^{-4} $\underline{M}$ for the internal solution were studied. The slope of a calibration plot varied from 57 to 54 to 49 mV with decreasing $NaHCO_3$ concentration; and the overall standard deviation for a least squares plot varied from 0.99 to 0.17 to 0.39 mV. The 1×10^{-3} $\underline{M}$ concentration of $NaHCO_3$ appeared to give the best compromise between sensitivity, speed of response, and precision in this automated system.
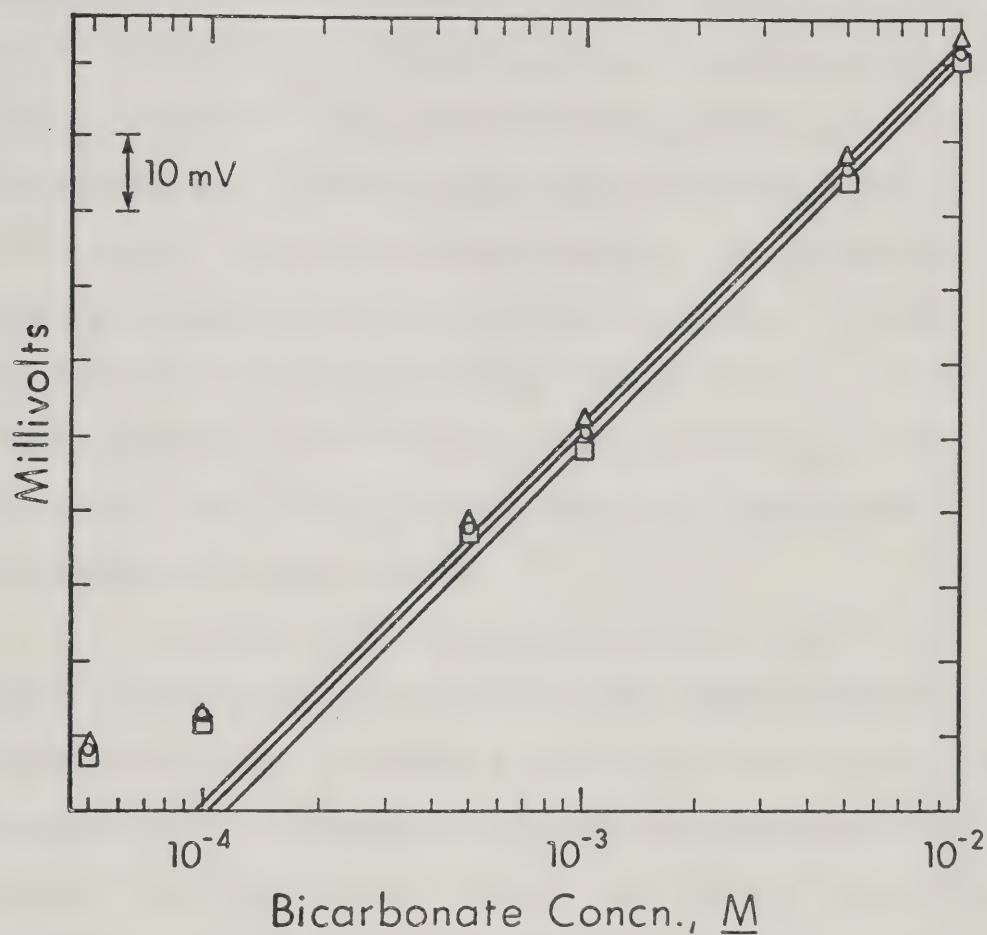
Figure 6   Effect of Membrane Thickness on the IL
$\underline{p}CO_2$ Electrode Response to Acidified
Bicarbonate Solutions: o 0.003 in. Silastic;
Δ 0.005 in. Silastic; □ 0.007 in.
Dacron-reinforced Silastic.

Automated Oxalate Analysis

Oxalate samples in 10-ml sample cups were pumped through a 0.020 in. i.d. tube; mixed in an H3 cactus with air which was introduced through 0.065 in. i.d. tubing and 0.5 $\underline{M}$ iron(III) in sulfuric acid containing Brij 35 which was pumped through 0.090 in. i.d. tubing. In initial experiments, the ultraviolet lamp was placed on the bench near the coil or the tungsten lamp was suspended inside the coils. In later modifications, the UV lamp was placed initially above the coils, and finally inside the coils after removal of the commercial lamp shield.

Oxalate samples ranging between 5×10^{-3} and 1 $\underline{M}$ could be analyzed in this sytem using 0.5 $\underline{M}$ iron(III) ammonium sulfate in either 1 or 2 $\underline{M}$ sulfuric acid with irradiation or acidified cerium(IV) ammonium sulfate without any irradiation. Using the sizes of pump tubing described above, the AutoAnalyzer diluted the samples with iron by approximately 18:1. When Fe:Ox ratios are very high, the automated method is unable to detemine the low concentration samples that could be analyzed manually. Consistent with the Severinghaus electrode behavior, better and faster plateaus could be obtained with the 0.01 $\underline{M}$ oxalate solution compared to lower concentration samples. A hysteresis effect is evident

with this system. The overall standard deviation obtained by running samples in decreasing concentration order increased by about 50% compared to results obtained by running samples in the reverse order.

Effect of Temperature. A significant amount of heat is produced by the tungsten lamp during the irradiation step. If the fan is turned off while the lamp is on, the coils become very hot and the tubing carrying solution from the pump to the coils tends to blow off, even when anchored with wire. In one run using a 200-watt tungsten lamp in conjunction with the fan, the temperature at the tubing outlet of the Pyrex coil was measured with a chromel-alumel thermocouple and a value of about 33°C was obtained. To lower this temperature prior to passage beneath the $\underline{p}CO_2$ electrode, the last foot of tubing carrying the sample from the irradiation unit was placed in the water bath surrounding the electrode so that the solution could be brought nearer the electrode temperature before measurement.

Effect of Pump and Sampler Speed. At the pump speeds employed, samples were exposed to radiation for about 5 minutes per coil. Since this was less than in the manual mode, the reaction was likely far from complete. When the ratio of the pump gears was changed to reduce the pumping speed to about 1/3, the resulting increase

in the irradiation time of the samples did not improve
the detection limit or the precision of the method. The
overall standard deviation for a linear least squares fit
of the data increased from 1.4 to 1.8 mV with the
decreased pump speed. Millivolt readings were slightly
increased and the slope increased from 49 to 54 mV.

The electrode readings began to increase
rapidly when exposed to a carbon dioxide solution. If
possible, it is desirable and more precise to read
plateau potentials rather than electrode potentials prior
to this. For oxalate analysis a cam rate of 10 samples
per hour was used to give the longest sampling time easily
obtainable.

Sample:Reagent Ratio. A new inlet system was designed to
increase the ratio of sample to reagent in the mixed
solution. This consisted of a three-pronged cactus
(junction), each prong being equal in diameter, as
opposed to the H3 cactus. By using 0.065 in. i.d.
tubing in the pump, the rate of flow of the samples
was increased from 0.16 ml/min to 1.60 ml/min - a 10-
fold increase. This permitted a corresponding 10-fold
improvement in the detection limit to $5x10^{-4}$ $\underline{M}$ oxalate.
When the i.d. of the pump line introducing the iron(III)
was reduced from 0.065 in. i.d. to 0.030 in. i.d., the
linear range of the electrode was extended to $1x10^{-4}$ $\underline{M}$.

The i.d. of the air line could also be reduced. This decrease in the lower response limit of the electrode was accompanied occasionally by a deviation from linearity for the higher concentrations. However, samples of higher concentration could be accommodated by dilution before analysis or, if desired, by increasing the amount of iron(III) used; in this way linearity of the calibration curve could be provided in the region of interest.

Hysteresis Effect. Most of this initial work was performed at a cam speed of 10 samples/hour (sampling time – 4 minutes) with the samples generally arranged in order of increasing concentration. If the samples were run in the reverse order much higher corresponding readings were obtained. Thus, as for the bicarbonate analysis, empty sample cups were placed between oxalate samples to give the electrode more time to reach the baseline between samples. It can be seen from Figure 7 that the extra time allowed for the electrode to return to baseline with this arrangement was still not sufficient. The oxalate samples in Figure 7 were run with a 0.5 $\underline{M}$ iron(III) ammonium sulfate solution in 2 $\underline{M}$ sulfuric acid in increasing, decreasing and then in increasing concentration order. The reproducibility is poorest at lower concentrations. From this it is
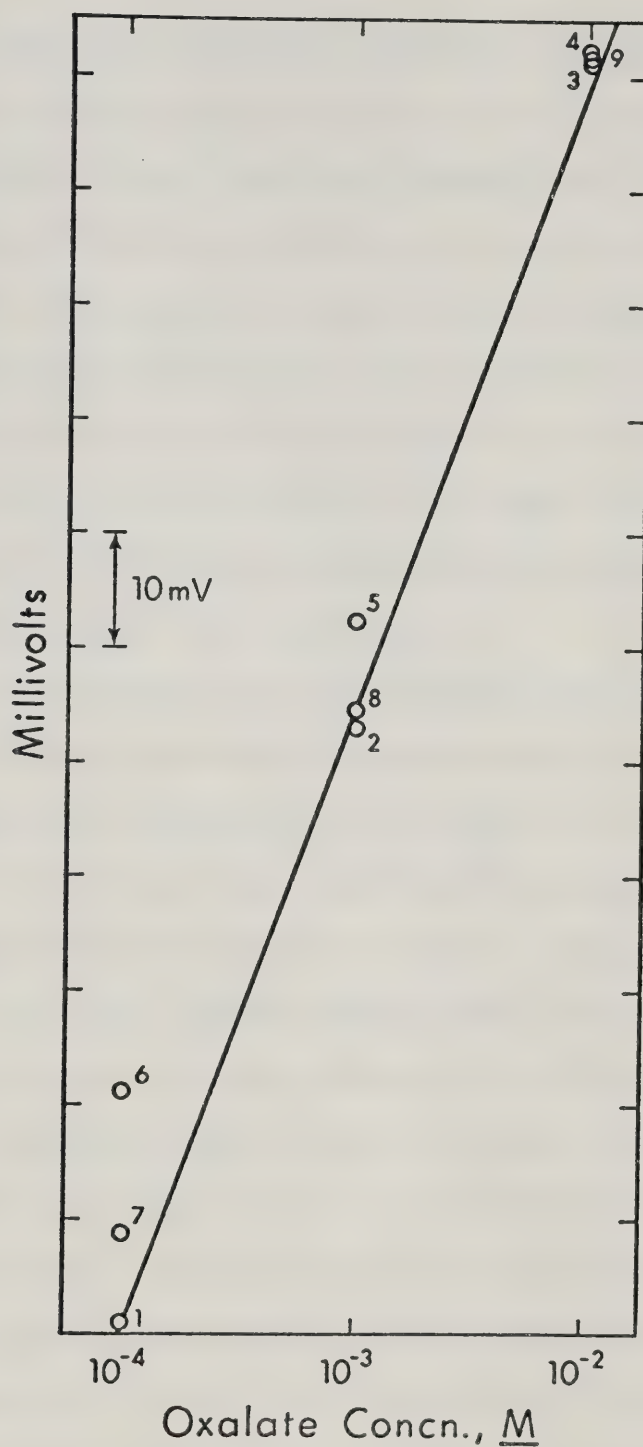
Figure 7 Hysteresis Effect with Three
Oxalate Samples Analyzed in a
Continuous-Flow Mode: numbered
according to the order of
analysis.

evident that the electrode reading for a given oxalate concentration is significantly affected by the concentration of the previous samples, as predicted in the response time analysis for a theoretical gas electrode. The rate of carbon dioxide diffusion out of the internal filling solution around the glass electrode is not sufficiently rapid under these conditions to allow the system to reach equilibrium after a sample of higher carbon dioxide concentration has passed beneath the electrode.

The possibility of flushing the internal filling solution of the electrode between samples was investigated as a means of increasing the precision and rate of analysis. The electrode jacket was enlarged and eight holes were drilled along its length. These entered the internal solution chamber just above the gas permeable membrane. Half of these channels were connected to a syringe containing $NaHCO_3$-NaCl internal filling solution while the other half served as outlets for the spent liquid. The protruding tip of the electrode and the presence of the nylon netting as a spacer between the glass electrode tip and the gas permeable membrane made it difficult to fully replace the filling solution and avoid introducing air bubbles in this important area. The outlet tube had to be raised and pinched during

analysis to prevent the solution from siphoning out.
Furthermore, on injecting large volumes of solution into
the electrode the Silastic membrane bulged and disrupted
the established AutoAnalyzer flow pattern. After no
major improvement could be observed the idea was abandoned.
Effect of Coil Length. The effect of using two 40-foot
Pyrex coils in series in the irradiation unit was compared
with the use of only one 40-foot length. Five samples
varying from $5x10^{-5}$ to $1x10^{-3}$ $\underline{M}$ in oxalate were run first
in increasing order and then randomly. In every case
the percentage error for the random run was less with
only one coil than that for a similar run with two coils.
For example, at the $1x10^{-4}$ $\underline{M}$ oxalate level and with one
coil the errors for two random samples were 3 and 6%,
whereas with the two coils it was 10 and 15%. The
higher errors may be attributed to the greater time the
samples have to interact in the extra coil.

Since there was considerable shielding of the
outer coil by the inner coil, the readings obtained with
two coils were only slightly greater than with only one.
This shielding was evidenced by the fact that the last
sample run in the two-coil system was often significantly
higher than expected. The reason for this phenomenon
was that after this sample was in the irradiation unit
the pump lines were all placed in water to begin the

cleaning process. Normally, a sample in the outer coil is shielded owing to absorption of radiation by the sample in the inner coil. When the inner coil contained only water, the last sample received more radiation while in the outer coil than corresponding earlier shielded samples. This situation was remedied in later analyses when two coils were used. However, generally only one coil was employed.

Substitution of the H3 Cactus. There appeared to be a concentration gradient at the exit of the three-pronged junction. Following each air bubble the colorless oxalate solution became more and more yellow through mixing with the yellow iron(III) solution. Since proper mixing of the solutions was essential the inlet system was modified. The H3 cactus which had originally been used was substituted for the modified cactus, and a 0.020 in. i.d. tubing was used to introduce the iron(III) and a 0.065 in. i.d. tubing was used for the oxalate, i.e., a large volume of oxalate sample was being diluted by and reacting with a small amount of concentrated iron(III) solution. This appeared to solve the gradient problem and did not adversely affect the detection limit.

Effect of Pump Speed. All of the above results were obtained with the pump operating at 1/3 normal speed. When it was returned to its original speed the detection

limit became somewhat poorer. (The sampling-motor speed was not changed.)

The earlier result using the slow pump speed and three-pronged inlet indicated that a single coil gave better precision than two coils. This was confirmed with the faster pump speed and the H3 cactus with its modified pump tubing. As was found experimentally with the bicarbonate work, inclusion of a debubbler before the electrode improved the precision of the oxalate analysis.

The straight baseline which was obtained when six oxalate solutions ranging between 1×10^{-4} and 5×10^{-2} $\underline{M}$ were mixed with water showed that oxalate, by itself, did not diffuse through the membrane and cause a pH change.

Hysteresis Effect. Many experiments were done over one decade in concentration in which seven oxalate solutions were run in increasing order, in decreasing order and, after a three-point increasing order calibration, in random order. Usually, when the seven solutions were run in decreasing order, higher millivolt readings were obtained, especially at the lower concentration, e.g., see Figure 7. Sometimes, in the random analysis, all the solutions read higher than the initial calibration; more often, only those solutions which were preceded by a higher concentration sample were high whereas those

preceded by a lower concentration sample were closer to the initial calibration line. Because these electrode reading errors were due to electrode "memory" characteristics and not primarily to drift or interaction between the samples, the normal methods of correcting for errors in continuous-flow analysis were of no benefit. In one experiment, after obtaining a three point calibration curve between 1×10^{-4} and 1×10^{-3} $\underline{M}$ oxalate, errors in values for random samples ranged to 8%. Two characteristics of this system are that the major factor controlling the rate of analysis is the response time of the electrode and that when a lower concentration sample follows one of higher concentration, the response time of the electrode varies as the ratio of the lower to higher concentration.

Oxalate Calibration. A typical Nernstian calibration for oxalate is shown in Figure 8. The potassium oxalate was prepared, as for most of the work, in 0.5 $\underline{M}$ NaCl and 0.1 $\underline{M}$ H_2SO_4 and the iron(III) ammonium sulfate (0.5 $\underline{M}$) in 4 $\underline{M}$ H_2SO_4. The upper limit could be extended either by diluting the samples prior to analysis or by increasing the iron(III) concentration. Methods for extending the lower limit of detection will be discussed later. Of the 10-ml sample volume, 7 to 8 ml were used in each analysis.
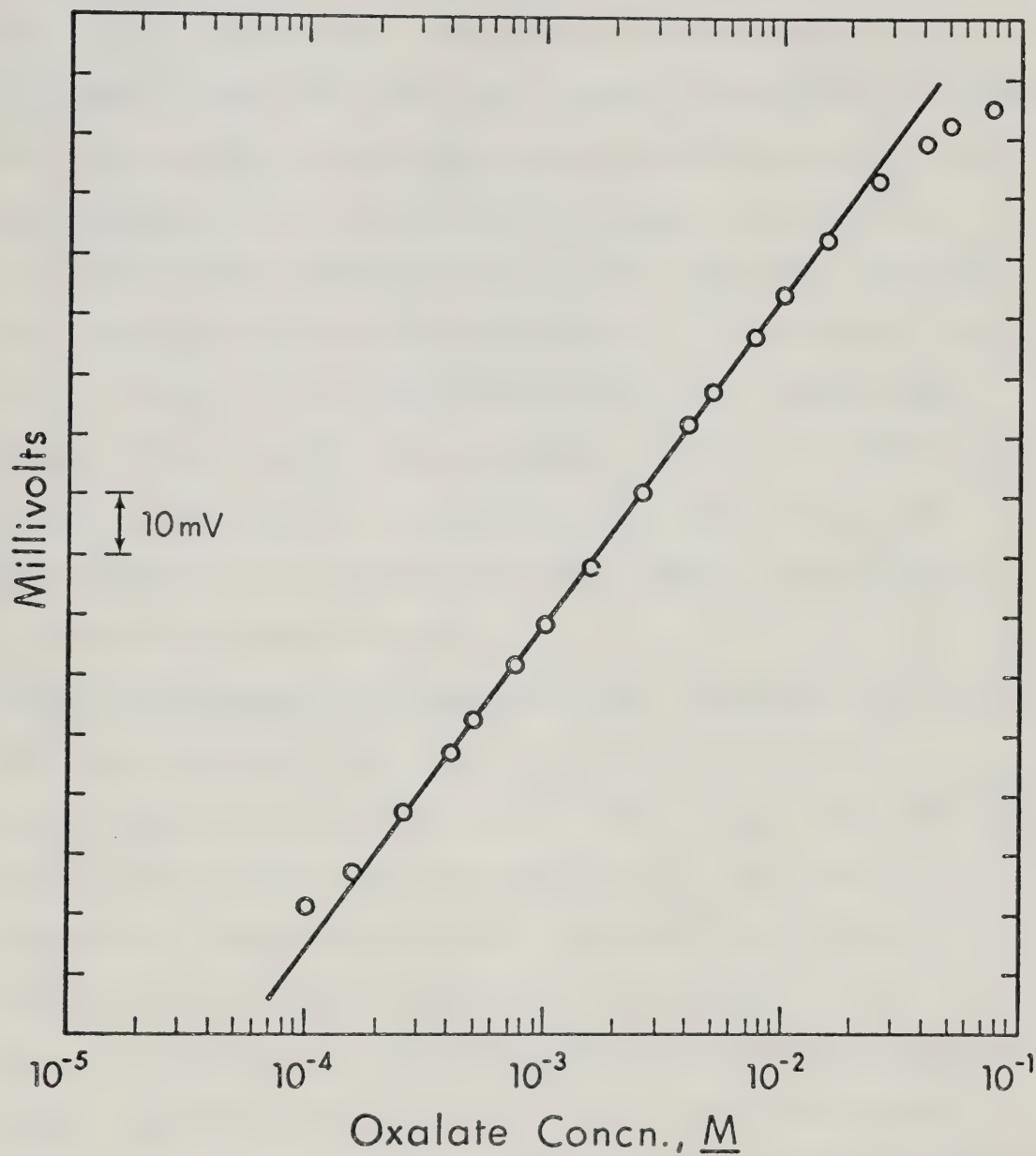
Figure 8 Calibration Plot for Irradiated Iron(III)-Oxalate
Solutions using an IL pCO_2 Electrode in a
Continuous-Flow Mode.

Electrode Response. Figure 9 is a reproduction of the
chart paper from the measurement of $1x10^{-3}$ $\underline{M}$ oxalate.
The central four peaks were analyzed at a cam rate of
10 samples/hour with two blank spaces between each sample.
On either side is an example of the results obtained when
the samples follow each other directly. This figure
illustrates the speed with which the electrode responds
to increasing carbon dioxide levels. It also shows that
the E_∞ value is not attained during the 4 minutes the
sample flows beneath the electrode. The slower rate of
return to baseline is evident as are those times when
the sampling probe was in an empty sample cup and when
it was in the wash liquid.

Effect of Internal Filling Solution. Different internal
filling solutions were used in analyzing oxalate
solutions ranging between $1x10^{-4}$ and 0.1 $\underline{M}$. The $1x10^{-3}$ $\underline{M}$
$NaHCO_3$-0.5 $\underline{M}$ NaCl solution seemed to be the best
compromise compared to either the $1x10^{-4}$ or 0.01 $\underline{M}$
$NaHCO_3$ in 0.5 $\underline{M}$ NaCl solutions. As expected, the
lowest concentration filling solution performed best for
lower concentration oxalate solutions and the 0.01 $\underline{M}$
$NaHCO_3$ solution was best for higher oxalate concentrations.
Since the electrode seemed to require some time to
equilibrate when different filling solutions were used,
the $1x10^{-3}$ $\underline{M}$ $NaHCO_3$-0.5 $\underline{M}$ NaCl solution was used unless
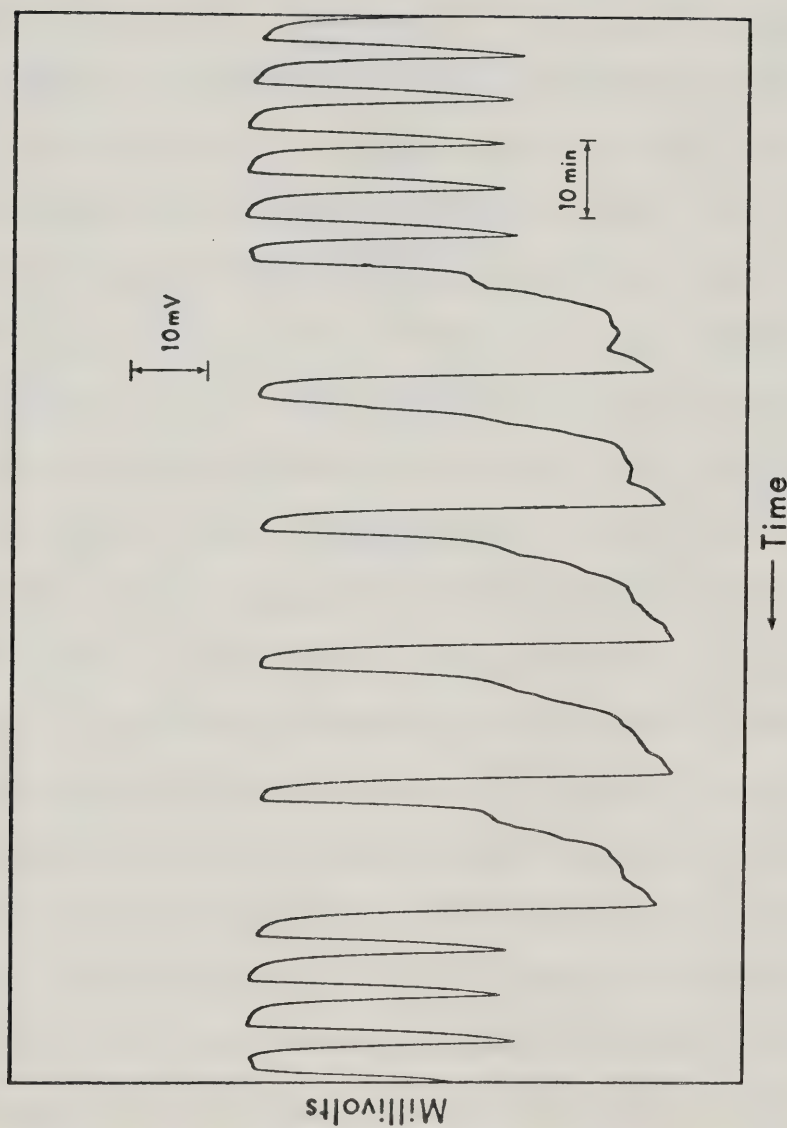
Figure 9   Reproduction of Chart Output showing IL pCO_2
Electrode Response Characteristics and
Reproducibility when used in a Continuous-Flow
Mode.

all analyzed solutions were known to be at one end of the
concentration scale.

Irradiation Conditions. Seven potassium oxalate solutions
ranging from 1×10^{-3} to 0.01 $\underline{M}$ were used to optimize
irradiation conditions. Comparisons were made between the
tungsten and the ultraviolet lamps and between the 40-foot
circular Pyrex coil and a 40-foot square quartz coil in
the irradiation compartment. The quartz coil was prepared
in the University of Alberta chemistry glass shop and
consisted of about 19 turns of 1.65 mm i.d., 3.5 mm o.d.
tubing. The height of this finished coil was about 7 cm
compared to 10.5 cm for the Pyrex coil. The iron(III)
was introduced as a 0.5 $\underline{M}$ $FeNH_4(SO_4)_2$ solution in 2 $\underline{M}$
H_2SO_4 and the oxalate solutions were prepared as in
earlier analysis. Each sample was followed by two empty
sample cups. As shown in Figure 10, the Pyrex coil-
ultraviolet lamp combination gave the lowest yield of
carbon dioxide, while the quartz coil-tungsten light
combination gave the highest. The necessity of using
more than a 10-foot coil was demonstrated by using a
10-foot quartz coil and finding carbon dioxide levels
that were below those obtained with the longer coil.

Using the above optimum conditions, the
relative error, expressed in per cent, for six solutions
of 1×10^{-3} $\underline{M}$ K_2Ox was 1.2% which was identical to the
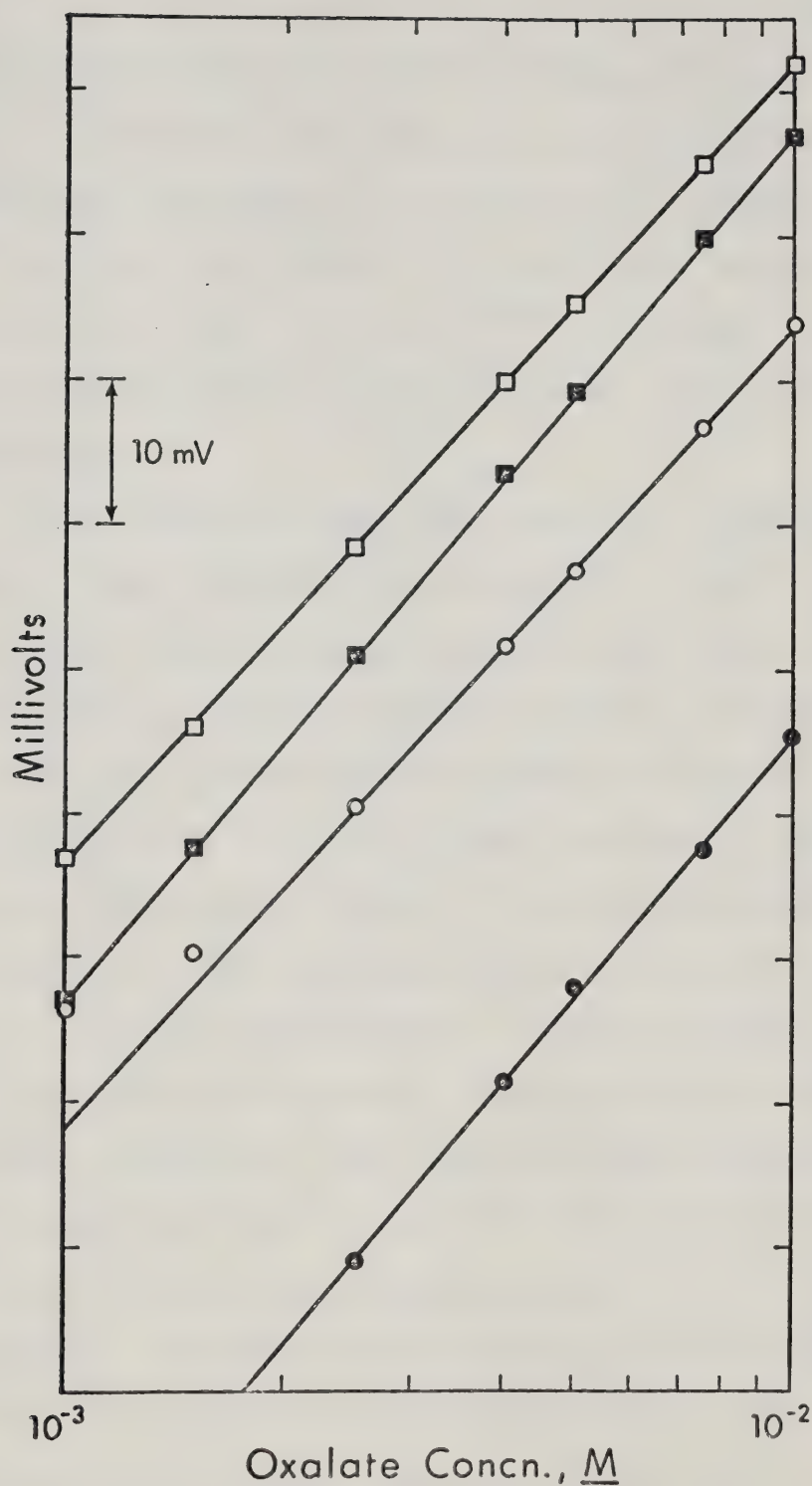
Figure 10   Effect of Irradiation Conditions
on Oxalate Analysis in a Continuous-
Flow Mode: □ quartz coil, tungsten
lamp; ○ quartz coil, ultraviolet
lamp; ■ Pyrex coil, tungsten lamp;
● Pyrex coil, ultraviolet lamp.

value obtained for four acidified solutions of 1×10^{-3} M

$NaHCO_3$. A 0.1 mV error in reading an electrode potential

of an electrode responding to a univalent ion leads to a

relative error of 0.39%, while a 1.0 mV error leads to a

relative error of 3.9%, i.e., $(10^{\Delta E/59} - 1)(100\%)$. Thus,

small millivolt errors in reading can mean large errors

in concentration.

Other tungsten lamps were tested to investigate

the effect of lamp wattage on the reaction. Four

different bulbs, 200W, 100W, 60W and 25W were used to

analyze the seven oxalate solutions. Figure 11 shows

that the amount of carbon dioxide generated from the

oxalate increases as the lamp wattage increases. This

is because of the greater amount of irradiation being

radiated from the higher wattage bulbs, especially in

the region of shorter wavelengths. A 4-watt General

Electric F4T5-CWX 6-inch hanging fluorescent bulb and a

high pressure ultraviolet lamp equipped with a transformer

and water jacket were also tested but both were less

efficient than the 200-watt tungsten bulb.

Acidity Effect. To ascertain the effect of the acidity

of the iron(III) solution on the system, three different

solutions of 0.5 M iron(III) ammonium sulfate were

prepared, one in distilled water, another in 2 M H_2SO_4

and a third in 4 M H_2SO_4. By keeping the acidity high,
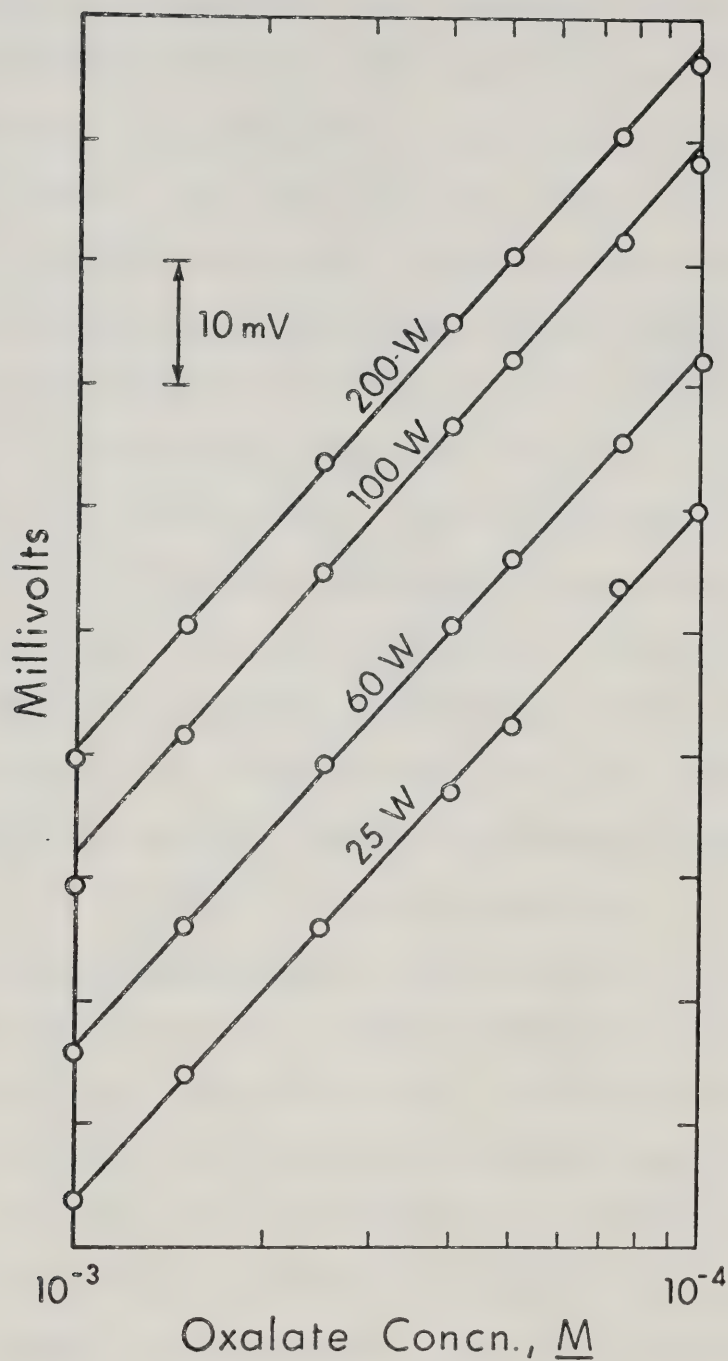
Figure 11   Effect of Tungsten Lamp Wattage
            on the Yield of Carbon Dioxide
            from the Iron(III)-Oxalate
            Reaction.

the hydrolysis of iron(III) was minimized. Seven oxalate solutions ranging between $1x10^{-3}$ and 0.01 $\underline{M}$ in oxalate, and containing 0.5 $\underline{M}$ NaCl and 0.1 $\underline{M}$ H_2SO_4, as all the analyzed oxalates did, were run with each of the different iron(III) solutions. After mixing in the H3 cactus, the acidities of the three sample-reagent solutions were about 0.1, 0.3 and 0.5 $\underline{M}$ in H_2SO_4. From Figure 12 it can be seen that there is little difference among the three calibrations. Thus adjustment of the pH of the iron(III) ammonium sulfate solution is not a critical variable for oxalate analysis. When the analysis with the 2 $\underline{M}$ H_2SO_4 solution of Fe(III) was repeated without any wetting agent, Brij 35, added to the solution the overall standard deviation increased from 0.36 to 0.98 mV for the seven samples.

Effect of Iron Concentration. For practical utility, after initial calibration, unknown samples of varying concentration must be determinable. Although only two moles of iron(III) are required to oxidize each mole of oxalate, the iron(III) was prepared as a 0.5 $\underline{M}$ solution so that there would be sufficient iron(III) for a wide range of oxalate concentrations. With the hysteresis effect it became apparent that solutions of several orders of magnitude could not be analyzed consecutively, especially if a low concentration sample followed one of

Figure 12   Effect of Sulfuric Acid Concentration
            of Iron(III) Solution on the
            Iron(III)-Oxalate Reaction: oxalate
            solutions prepared in 0.1 $\underline{M}$ H_2SO_4-

            0.5 $\underline{M}$ NaCl:iron(III) solutions prepared
            in water, $\triangle$; 2 $\underline{M}$ H_2SO_4, o and 4 $\underline{M}$ H_2SO_4, □

            to give final iron(III)-oxalate solution
            acidities of 0.1 $\underline{M}$, $\triangle$; 0.3 $\underline{M}$, o and
            0.5 $\underline{M}$, □ .

higher concentration. Since the samples would have to be
analyzed in narrower concentration ranges the iron:oxalate
ratio became a variable that could be optimized, although
Riggs and Bricker[34] state that their results are
independent of the iron(III) concentration as long as at
least two iron ions are present for each oxalate. Rao and
Aravamudan[32] maintained a 4:1 or greater iron:oxalate
ratio. To ascertain the effect on the present system
three solutions of $1x10^{-3}$ $\underline{M}$ potassium oxalate, each
separated in the sampler tray by two blank cups, were
analyzed with progressively decreasing concentrations of
$FeNH_4(SO_4)_2$ in 2 $\underline{M}$ H_2SO_4. For one set of data the
tungsten lamp and Pyrex coil were used while for the
second set the experiment was repeated using the medium
pressure Hanovia lamp and quartz coil. The results,
shown in Figure 13, indicate that the tungsten lamp gave
higher readings than the ultraviolet lamp at high
iron(III) concentrations, as were used to obtain the
data in Figure 10. However, when the Fe:Ox ratio was
lowered to 5:1 or less the ultraviolet lamp yielded
higher readings. The optimum ratio for irradiation with
a tungsten lamp was 50:1 to 1:1 while for the ultraviolet
lamp, it was 5:1 to 0.5:1. Much higher yields of carbon
dioxide could be obtained from the ultraviolet system
under its optimum conditions. A similar trend was
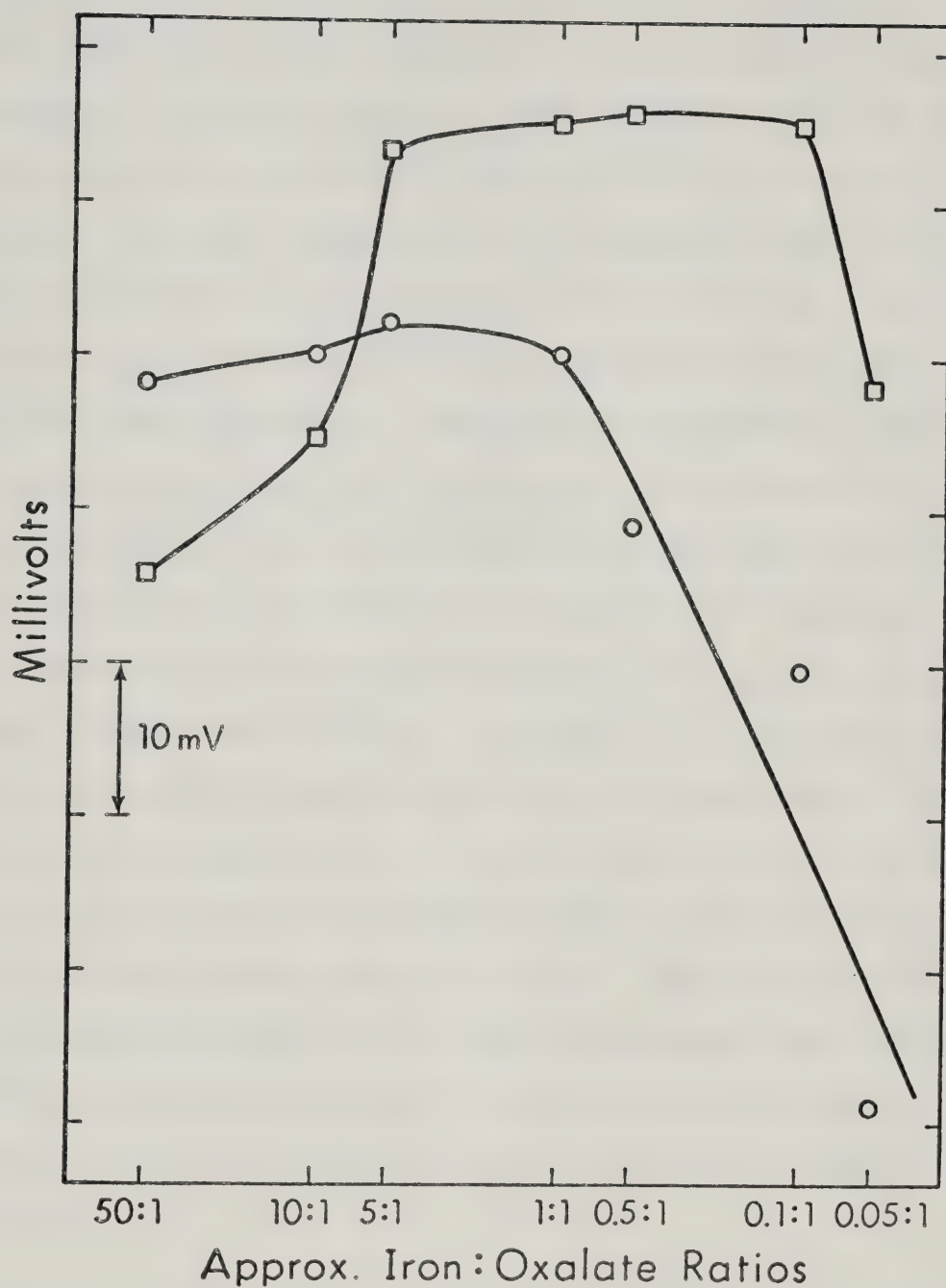
Figure 13   Effect of Iron(III) Concentration on the
Iron(III)-Oxalate Reaction using
1×10^{-3} M Oxalate and Two Different
Irradiation Systems: □ ultraviolet
irradiation and quartz coil; ○ visible
irradiation and Pyrex coil.

evident when the oxalate concentration was lowered to
1×10^{-4} M except optimum ratios for the ultraviolet system
increased to include ratios as high as 50:1 while for the
visible system, up to 500:1 Fe:Ox ratios were satis-
factory. The iron:oxalate ratios, therefore, did not
seem as critical at lower oxalate concentrations. In
contrast, with 0.01 M oxalate the optimum iron:oxalate
ratio for the ultraviolet irradiation system was 0.5:1.
At ratios higher and lower than this, the readings were
markedly lower. At high oxalate concentrations, a corres-
pondingly high concentration of iron(III) is required.
All iron(III) species absorb significantly in the ultra-
violet region, and so cause the amount of radiation reach-
ing the iron(III)-oxalate complex to be diminished. For
this reason a high ratio of iron to oxalate gives a lower
yield of carbon dioxide at high oxalate concentrations
than at lower oxalate concentrations. Because the time
available for irradiation in this continuous-flow system
is fixed, the optimum lower iron:oxalate ratios should
be used to extend the lower limit of electrode response to
oxalate.

Nernstian Calculations. The photochemical decomposition
of iron(III) oxalate yields two moles of carbon dioxide
for each mole of oxalate, yet a slope close to 59 mV was

obtained. This can be explained by considering the Nernst equation for the $\underline{p}CO_2$ electrode:

$$E = E° + 0.059 \log \underline{p}CO_2$$

But if two carbon dioxides are evolved from each oxalate:

$$2[Ox] = \underline{p}CO_2$$

Substituting this in the Nernst equation and expanding:

$$E = E° + 0.059 \log 2[Ox]$$

$$E = E° + 0.059 \log 2 + 0.059 \log [Ox]$$

$$E = E° + 0.0178 + 0.059 \log [Ox]$$

Thus a 59 mV slope is predicted but the absolute value of the readings for the same concentration of acidified bicarbonate and irradiated iron(III) oxalate should differ by 17.8 mV. Under the above-determined optimum conditions, this is found to be true. Nernstian results were obtained (Figure 8) under non optimum conditions but the electrode potentials were not displaced from the bicarbonate plot by 17.8 mV.

Effect of Oxygen. Since each oxalate required two iron(III) ions to fully react, the low optimum ratios observed with the ultraviolet lamp must mean the iron(II) in the solution is reoxidized to iron(III). Oxygen from

the air, introduced into the pump air line, served as the oxidizing agent, because when this line was connected to a nitrogen stream, the lower iron:oxalate ratios became less favorable. Purging the oxalate solutions with nitrogen prior so their analysis further reduced the size of the carbon dioxide peak when less than a 2:1 iron:oxalate ratio was used.

Effect of Chloride Ions. Figure 12 showed that the acidity of the iron(III) solution was not critical. Riggs and Bricker[34] suggested that sulfuric acid should be used rather than hydrochloric acid since the latter prevented the reaction from going to completion in a reasonable period of time. The formation of iron(III)-chloride complexes in solution was suggested by them to result in absorbtion of a significant portion of the incident radiation. However, Rao and Rao[30,31], when using oxalate in a photochemical method to estimate iron(III) concentration, found that hydrochloric acid could be substituted for sulfuric acid without any ill effects. In this work, the acid that was used was sulfuric but the salt content of the solutions was adjusted with sodium chloride and hence the final iron-oxalate solutions contained iron-chloride complexes. To test the effect of chloride ion concentration upon the reaction, a 1×10^{-3} $\underline{M}$ solution of potassium oxalate was prepared in 0.167 $\underline{M}$ sodium sulfate and a 0.012 $\underline{M}$

solution of iron(III) ammonium sulfate was prepared in 2 and 4 $\underline{M}$ HCl and 4 and 8 $\underline{M}$ H_2SO_4. After passage through the H3 cactus the final iron(III) concentration was about 1.2×10^{-3} $\underline{M}$ and the acid concentration 0.2 or 0.4 $\underline{M}$ in HCl or 0.4 or 0.8 $\underline{M}$ in H_2SO_4. Almost identical readings were obtained for the first three solutions and slightly lower results were obtained with the more concentrated sulfuric acid solution. This was attributed to its high acid content. Clearly under the conditions used here, chloride concentrations as high as 0.4 $\underline{M}$ do not interfere either with the formation of the iron(III)-oxalate complex, or with the absorption of radiation by that complex. Since chloride is a common component of many samples, especially biological ones, it is important to know that it does not interfere to any significant extent. Furthermore, no trends were evident in earlier experiments in which the ionic strength was varied through addition of sodium chloride or sodium sulfate. This suggests that changes in ionic strength of a few tenths were negligible in the presence of the high concentrations of iron(III) ammonium sulfate and sulfuric acid that were used.

Effect of Membrane Thickness. The effect of replacing the 0.003 in. Silastic membrane supplied with the IL electrode by Dow Corning's 0.005 in. and Dacron reinforced 0.007 in. ones was tested with the iron-oxalate

system. The very similar Nernstian calibration graphs
displayed in Figure 14 show the independence of membrane
thickness on the electrode response. This corroborates
the earlier results obtained on the bicarbonate system
(Figure 6).

Effect of Other Substances. Glycine and L-histidine were
tested as potential interferences. Solutions of these
substances (1 $\underline{M}$) in 0.1 $\underline{M}$ H_2SO_4 gave no response when
mixed with iron(III) and irradiated. Similarly, 0.1 $\underline{M}$
creatinine solutions in 0.1 $\underline{M}$ H_2SO_4 and 0.5 $\underline{M}$ NaCl and
0.01 $\underline{M}$ β-alanine solutions gave no response. Many urea
solutions over a wide concentration range did not interfere.

Other Carboxylic Acids

The advantage of determining the oxalate
concentration by analyzing the evolved carbon dioxide
instead of the iron(III) generated in the iron-oxalate
reaction is that those substances which are oxidized by
iron(III) but which do not produce carbon dioxide are
not interferences in the former method. As an example,
Riggs and Bricker[34] found mannitol to be an interference.
In the $\underline{p}CO_2$ electrode determination of oxalate it did
not interfere.

Iron(III)-Citrate and Iron(III)-Tartrate Analysis. Other
carboxylic acids are capable of being oxidized by iron(III)
to carbon dioxide. The principal carboxylic acids
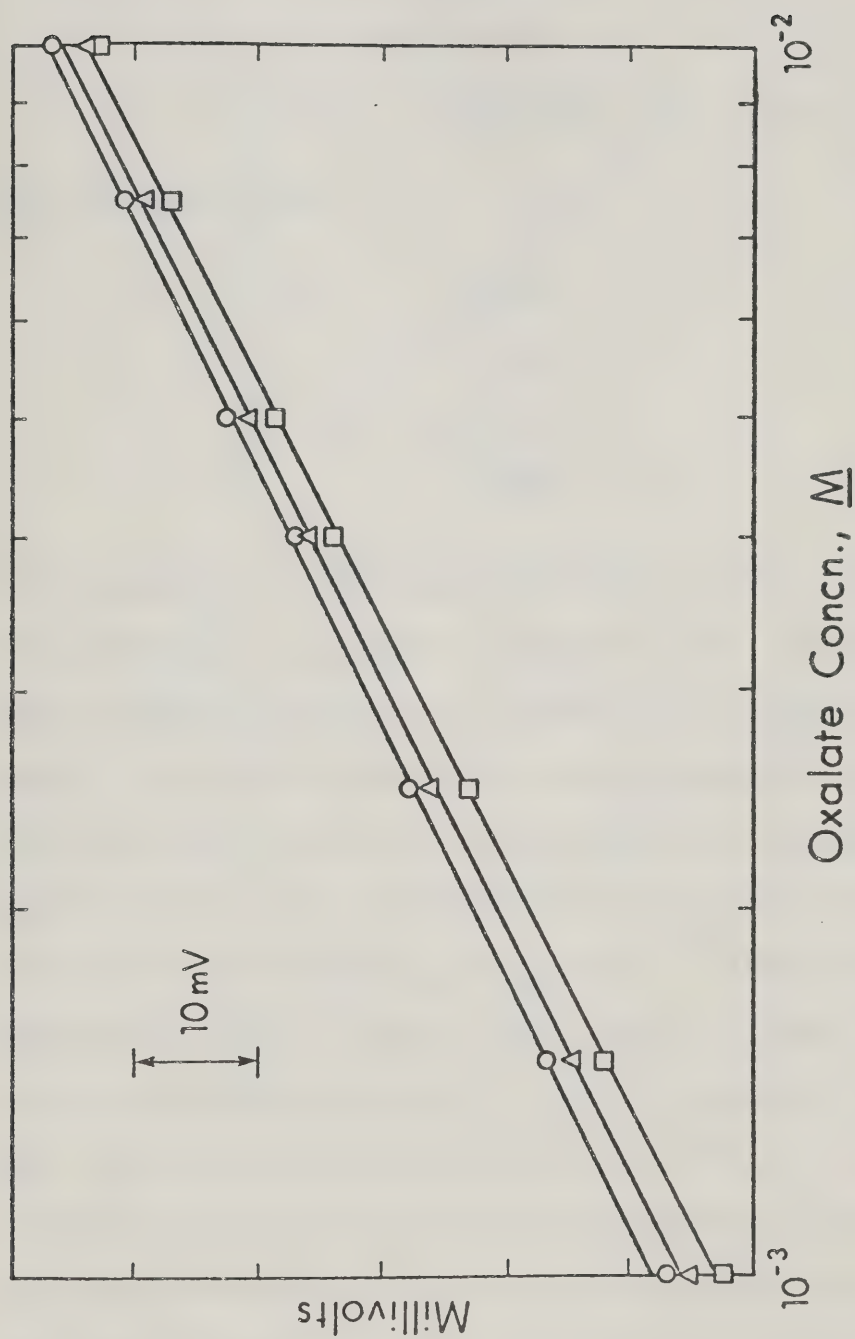
Figure 14 Effect of Membrane Thickness on the IL pCO_2 Electrode
Response to Irradiated Iron(III)-Oxalate Solutions:
□ 0.003 in. Silastic; ▲ 0.005 in. Silastic;
○ 0.007 in. Dacron-reinforced Silastic.

investigated were citric acid,

$$CH_2-COOH$$
$$|$$
$$HO-C-COOH$$
$$|$$
$$CH_2-COOH$$

and tartaric acid,

$$COOH$$
$$|$$
$$H-C-OH$$
$$|$$
$$HO-C-H$$
$$|$$
$$COOH$$
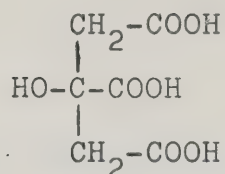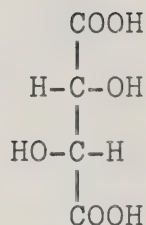
In a manual or continuous-flow mode these two acids could be analyzed in a similar manner to that for oxalic acid using either iron(III) or cerium(IV) as the oxidizing agent. The one notable difference from the oxalate analysis was the effect of the acid concentration. With oxalate there was little influence on the extent of the reaction due to acidity (Figure 12). When similar experiments were repeated with sodium citrate and potassium sodium tartrate solutions prepared in a 0.5 $\underline{M}$ NaCl and 0.1 $\underline{M}$ H_2SO_4 medium, a low pH in the irradiated solution was found to inhibit the reaction while with less acid results closer to Nernstian ones could be obtained (Figures 15 and 16). This indicates that proper acidity is the key to reducing the interference in the
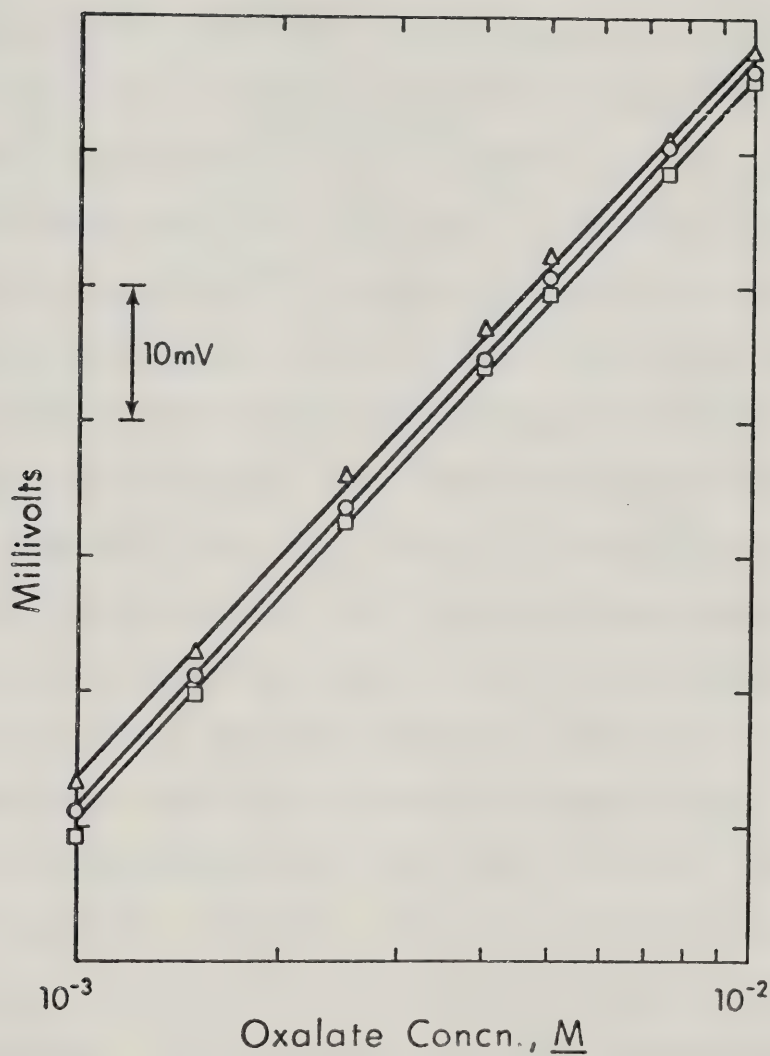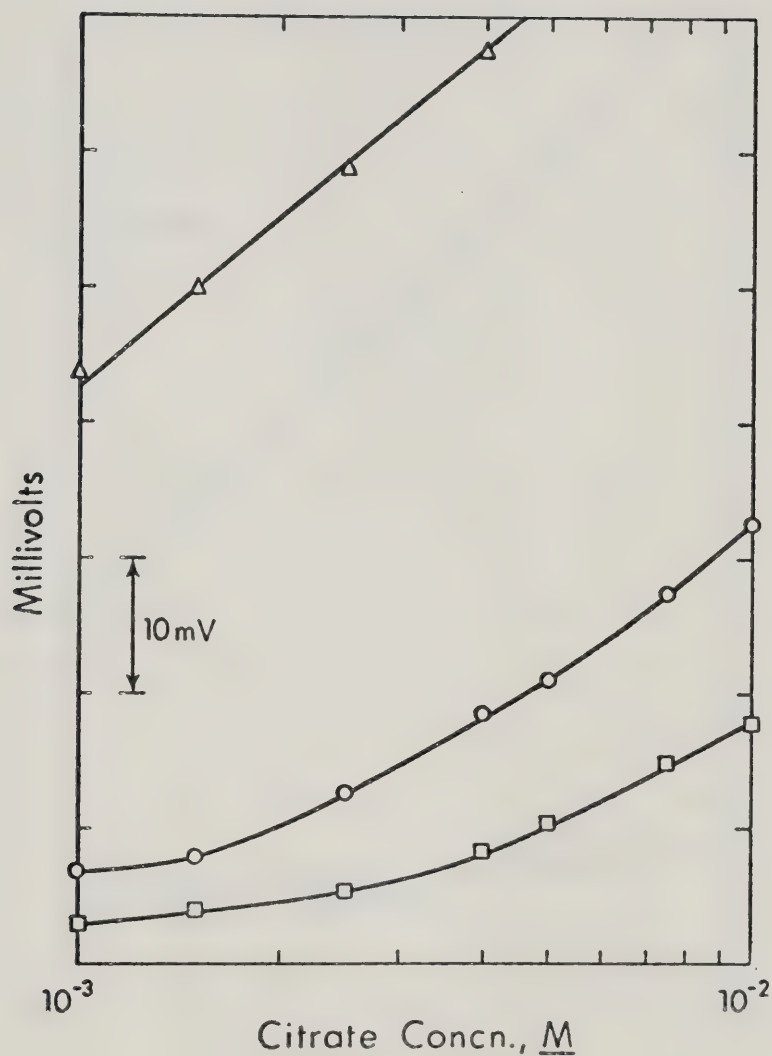
Figure 15   Effect of Sulfuric Acid Concentration
of Iron(III) Solution on the
Iron(III)-Citrate Reaction: citrate
solutions prepared in 0.1 $\underline{M}$ H_2SO_4-

0.5 $\underline{M}$ NaCl:iron(III) solutions prepared
in water, Δ ; 2 $\underline{M}$ H_2SO_4, o and 4 $\underline{M}$ H_2SO_4, □

to give final iron(III)-citrate solution
acidities of 0.1 $\underline{M}$, Δ ; 0.3 $\underline{M}$, o and
0.5 $\underline{M}$, □   .
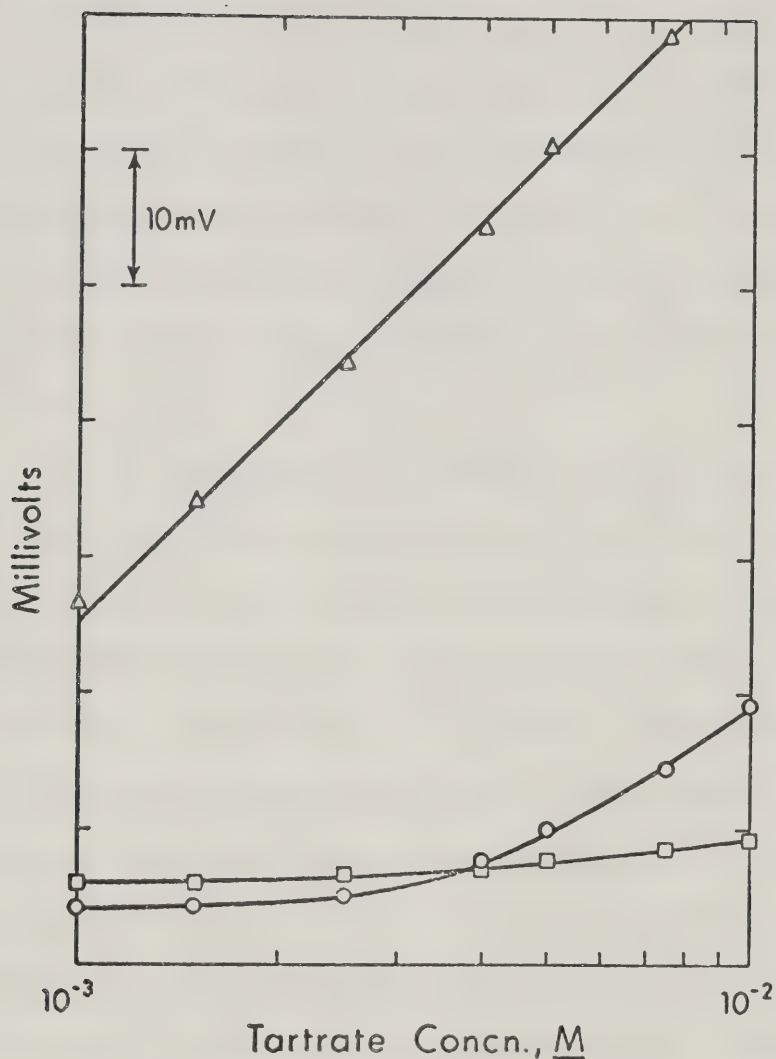
Figure 16   Effect of Sulfuric Acid Concentration
of Iron(III) Solution on the
Iron(III)-Tartrate Reaction: tartrate
solutions prepared in 0.1 $\underline{M}$ H_2SO_4-

0.5 $\underline{M}$ NaCl:iron(III) solutions prepared
in water, $\triangle$, 2 $\underline{M}$ H_2SO_4, o and 4 $\underline{M}$ H_2SO_4. $\square$

to give final iron(III)-tartrate solution
acidities of 0.1 $\underline{M}$, $\triangle$; 0.3 $\underline{M}$, o; and
0.5 $\underline{M}$, $\square$.

oxalate analysis by these carboxylic acids. However, an
iron(III) solution prepared in distilled water forms
hydroxide species on standing. These absorb a larger
amount of irradiation than iron(III) ions. For an analysis
between $1x10^{-3}$ and 0.01 $\underline{M}$ sodium citrate in 0.5 $\underline{M}$ NaCl-
0.1 $\underline{M}$ H_2SO_4 the slope increased from 45.8 to 54.6 mV when
a freshly prepared aqueous iron(III) ammonium sulfate
was substituted for one several months old. The slope
improved to 59.3 mV when the sodium citrate solutions
were prepared in 0.5 $\underline{M}$ NaCl medium and freshly prepared
iron(III) was used.

It is possible to determine citric and tartaric
acids by utilizing the photochemical iron(III) redox
method if the reaction is run at low acidity. Figure 17
shows calibration plots for sodium citrate and potassium
sodium tartrate analyzed in 0.5 $\underline{M}$ NaCl. Aqueous 0.5 $\underline{M}$
iron(III) ammonium sulfate was used. The linear range of
these graphs could be extended by utilizing a longer
irradiation time and/or a more optimum iron(III)
concentration. The iron(III) concentration to be used in
the analysis of citrate was optimized using a $1x10^{-3}$ $\underline{M}$
solution of sodium citrate in 0.5 $\underline{M}$ NaCl while varying
the concentration of aqueous iron(III) ammonium sulfate.
These results are shown in Figure 18 and are similar to
the oxalate results seen in Figure 13. The highest yields
of carbon dioxide were obtained by using the ultraviolet
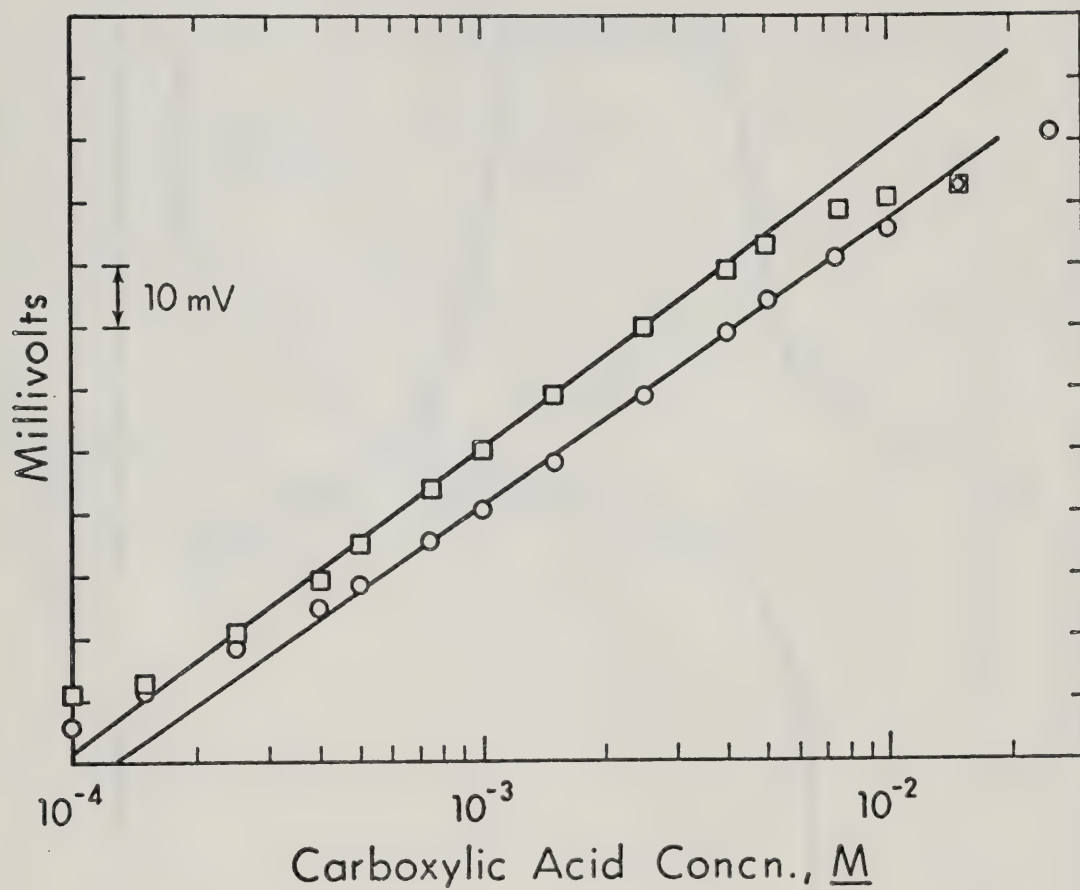
Figure 17   Calibration Plots for Irradiated Iron(III)-
Citrate and Iron(III)-Tartrate Solutions using
an IL pCO_2 Electrode in a Continuous-Flow Mode:
○ citrate; □ tartrate.
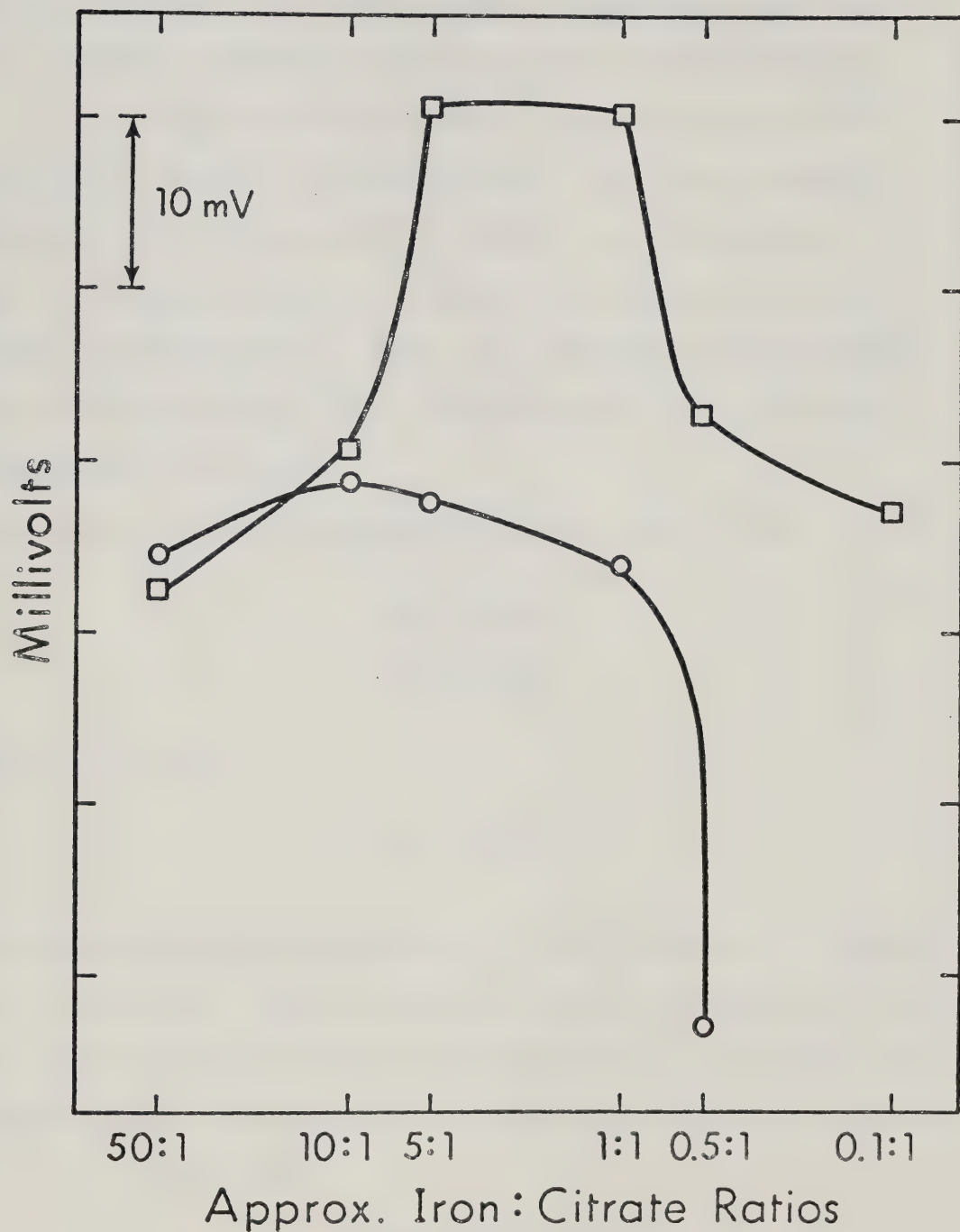
Figure 18 Effect of Iron(III) Concentration on the
Iron(III)-Citrate Reaction using 1×10^{-3} $\underline{M}$
Citrate and Two Different Irradiation
Systems: □ ultraviolet irradiation and quartz
coil; ○ visible irradiation and Pyrex coil.

lamp and quartz coil and keeping the iron:citrate ratio between 5:1 and 1:1. The visible irradiation unit was not optimum, except as high iron(III) concentrations.

If each mole of sodium citrate decomposed to yield three moles of carbon dioxide, one would expect a Nernstian slope displaced by 28 mV, i.e., 59 log(3), when readings are plotted versus the logarithm of the citrate concentration. This was confirmed experimentally when an optimum iron(III) concentration and ultraviolet irradiation were used.

Other Iron(III)-Carboxylate Analyses. Malic acid

$$HO-CH-COOH$$
$$|$$
$$H_2-C-COOH$$

and pyruvic acid

$$\overset{\overset{\displaystyle O}{\parallel}}{CH_3-C-COOH}$$
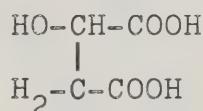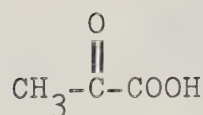
are both highly acid dependent in their extent of reaction with iron(III). Figure 19 shows typical calibration curves for these acids when they are prepared in 0.5 $\underline{M}$ NaCl and analyzed with an aqueous 0.5 $\underline{M}$ iron(III) ammonium sulfate.

Lactic acid

$$COOH-CHOH-CH_3$$

also seemed to be acid-sensitive in its extent of
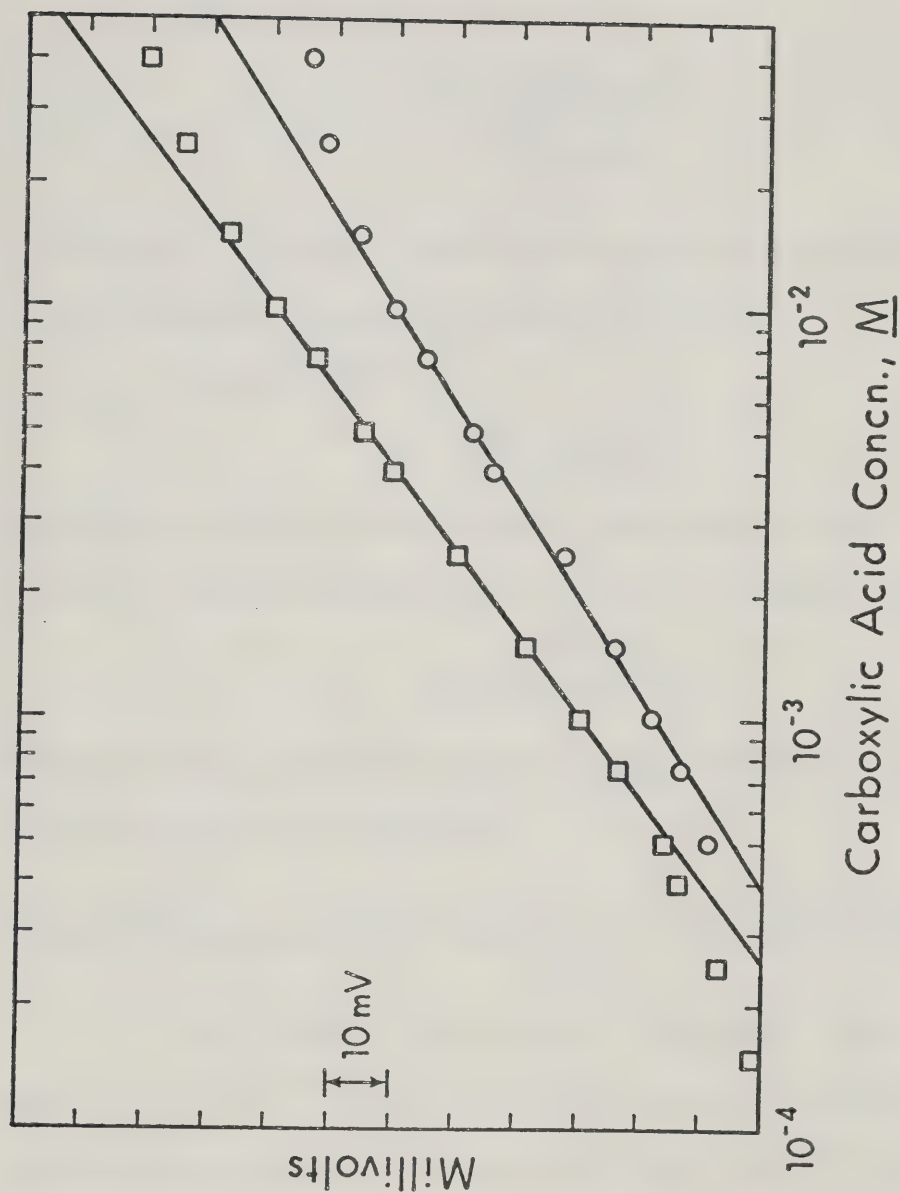
Figure 19 Calibration Plots for Irradiated Iron(III)-Malate and Iron(III)-Pyruvate Solutions using an IL pCO_2 Electrode in a Continuous-Flow Mode; o malate; □ pyruvate.

reaction. However, extensive measurements were not made as the acid was only available as a 60% syrup solution and the purity and concentration were uncertain.

Maleic acid,

$$H-C-COOH$$
$$\|$$
$$H-C-COOH$$
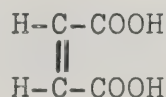
in contrast, did not seem to be nearly so acid dependent in its extent of reaction with iron(III).

Malonic acid

$$COOH-CH_2-COOH$$
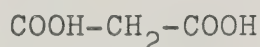
reacted to only a small extent with any of the 0.5 $\underline{M}$ iron(III) solutions, while a 0.1 $\underline{M}$ cysteine solution

$$HS-CH_2-\overset{\overset{\displaystyle NH_2}{|}}{C}H-COOH$$
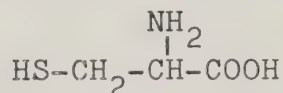
yielded carbon dioxide when irradiated with a 4 $\underline{M}$ H_2SO_4 solution of iron(III).

Interference in Oxalate Analysis Due to Other Carboxylic Acids

To confirm the acidity influence on the reaction, a 5×10^{-3} $\underline{M}$ oxalate solution and a solution containing both 5×10^{-3} $\underline{M}$ oxalate and 5×10^{-3} $\underline{M}$ citrate were analyzed with iron(III) solutions of differing pH. The medium for both carboxylic acid solutions was 0.1 $\underline{M}$ H_2SO_4, 0.5 $\underline{M}$ NaCl. Table 2 shows the difference in

TABLE 2

Citrate Interference in Oxalate Analysis as a
Function of Acidity

Iron(III) Medium	Millivolt Difference due to Presence of Citrate[a]	% error $(10^{\Delta E/59}-1)(100\%)$[b]
H_2O	4.1	17.4
1 $\underline{M}$ H_2SO_4	1.2	4.8
2 $\underline{M}$ H_2SO_4	0.4	1.6
4 $\underline{M}$ H_2SO_4	0.5	2.0

---

[a]The difference between a 5×10^{-3} $\underline{M}$ oxalate and 5×10^{-3} $\underline{M}$
citrate solution and one that was 5×10^{-3} $\underline{M}$ in oxalate
only. Both solutions prepared in 0.1 $\underline{M}$ H_2SO_4 and
0.5 $\underline{M}$ NaCl.

[b]This assumes a Nernstian electrode response of 59 mV.

readings between the two solutions and confirms that the error due to citrate interference decreases as the pH is lowered. The observation that the most concentrated acid solution apparently gave more error in oxalate analysis than the 2 $\underline{M}$ H_2SO_4 solution of $FeNH_4(SO_4)_2$ can be explained as due to the hysteresis effect.

In a similar type of experiment groups of aqueous solutions 2.5×10^{-3} $\underline{M}$ in oxalate, 2.5×10^{-3} $\underline{M}$ in both oxalate and citrate, and 2.5×10^{-3} $\underline{M}$ in both oxalate and tartrate were tested for interference due to citrate and tartrate. A 4 $\underline{M}$ H_2SO_4 solution of 0.5 $\underline{M}$ Fe(III) was used. The concentration of the interfering carboxylate salt was raised by factors of ten. When the interference became significant more sulfuric acid was added to the solution being analyzed. The results are summarized in Table 3. These data assume that the electrode responded in a similar Nernstian manner throughout the several days it took to obtain all the readings. Errors in individual readings were minimized in that averages of four analyses were used.

Another method to determine interference levels is to establish an oxalate calibration and then to measure mixtures containing oxalate and the interferences. This approach involves an addition error - if the oxalate calibration were run in increasing concentration order

TABLE 3

Interference in Oxalate Analysis due to Citrate and Tartrate

Oxalate Concentration	Citrate Concentration	Tartrate Concentration	Ratio, Oxalate:Interfering Carboxylate	% Error $(10^{\Delta E/59}-1)(100\%)$ [a]
2.5×10^{-3} $\underline{M}$	2.5×10^{-3} $\underline{M}$	–	1:1	2[b]
2.5×10^{-3} M	–	2.5×10^{-3} $\underline{M}$	1:1	2[b]
2.5×10^{-3} $\underline{M}$	2.5×10^{-2} $\underline{M}$	–	1:10	8[b]
2.5×10^{-3} M	–	2.5×10^{-2} $\underline{M}$	1:10	15[b]
2.5×10^{-3} $\underline{M}$	2.5×10^{-1} $\underline{M}$	–	1:100	30[c]
2.5×10^{-3} $\underline{M}$	–	2.5×10^{-1} $\underline{M}$	1:100	47[c]
2.5×10^{-4} $\underline{M}$	2.5×10^{-1} $\underline{M}$	–	1:1000	496[c]
2.5×10^{-4} $\underline{M}$	–	2.5×10^{-1} $\underline{M}$	1:1000	679[c]
2.5×10^{-4} $\underline{M}$	2.5×10^{-1} $\underline{M}$	–	1:1000	50[d]
2.5×10^{-4} $\underline{M}$	–	2.5×10^{-1} $\underline{M}$	1:1000	185[d]

[a] Actual millivolt difference between 2.5×10^{-3} and 2.5×10^{-4} $\underline{M}$ oxalate solutions was 59.52 mV.

[b] Acidity of these oxalate and oxalate-carboxylate solutions was 0.1 $\underline{M}$ H_2SO_4.

[c] Acidity of these oxalate and oxalate-carboxylate solutions increased to 0.45 $\underline{M}$ H_2SO_4.

[d] Acidity of these oxalate and oxalate-carboxylate solutions increased to 1.35 $\underline{M}$ H_2SO_4.

and then the interference was analyzed in one of the lower concentration solutions an error due to the hysteresis effect would be added to any error due to the interference. To eliminate this possibility, after the seven-point calibration was obtained, the initial solution was measured several times and a line drawn parallel to the calibration line through the reading obtained for the initial solution. Then, using this plot to calculate interference levels, single solutions of various interference ratios were measured (Table 4) in increasing concentration order. The carboxylate salt solutions were prepared in 0.1 $\underline{M}$ H_2SO_4 and 0.5 NaCl and the iron(III) ammonium sulfate was prepared in 4 $\underline{M}$ H_2SO_4. The interference level due to malic and pyruvic acids could, presumably, be lowered if more acid was used, similar to the citrate system.

Interference with the pCO_2 Electrode

While it is apparent that the reaction of some acids with iron(III) can be minimized by adjusting the pH, other acids interfere in a different manner, i.e., by diffusing across the gas permeable membrane into the internal filling solution of the electrode, dissociating there, and causing a pH change. These acids cannot be easily removed from the internal filling solution. In the literature acetic acid is the only molecular species reported[35] to interfere in this manner.

TABLE 4
Interferences in Oxalate Analysis due to Tartrate, Malate, Pyruvate and Malonate.

Oxalate Concentration, M	Interfering Carboxylate Salt	Ratio, Oxalate:Carboxylate Salt	Absolute % Error (Calculated from Calibration Plot)
5×10^{-4}	tartrate	1:1	0.4
5×10^{-4}	tartrate	1:3	3
1×10^{-3}	tartrate	1:4	0
1.5×10^{-3}	tartrate	1:0.3	0.2
1.5×10^{-3}	tartrate	1:1	0.7
2×10^{-3}	tartrate	1:1.5	0
3×10^{-3}	tartrate	1:0.67	0
4×10^{-3}	tartrate	1:0.25	4
5×10^{-4}	tartrate	1:5	0
5×10^{-4}	tartrate	1:8	3
5×10^{-4}	tartrate	1:10	10
5×10^{-4}	malate	1:0.5	7
5×10^{-4}	malate	1:1	8
5×10^{-4}	malate	1:2	10
5×10^{-4}	malate	1:4	13
5×10^{-4}	malate	1:6	20
5×10^{-4}	malate	1:10	21
5×10^{-4}	malate	1:20	26
5×10^{-4}	pyruvate	1:0.5	4
5×10^{-4}	pyruvate	1:1	10
5×10^{-4}	pyruvate	1:2	34
5×10^{-4}	pyruvate	1:4	55
5×10^{-4}	pyruvate	1:6	74
5×10^{-4}	malonate	1:0.5	3
5×10^{-4}	malonate	1:1	0
5×10^{-4}	malonate	1:2	2
5×10^{-4}	malonate	1:4	2
5×10^{-4}	malonate	1:6	6

Formic acid,

$$HCOOH$$

propionic acid,

$$CH_3-CH_2-COOH$$

and other small carboxylic acids also appeared to diffuse
slowly across the membrane. Pivalic acid

$$CH_3-\overset{\overset{\displaystyle CH_3}{|}}{\underset{\underset{\displaystyle CH_3}{|}}{C}}-COOH$$
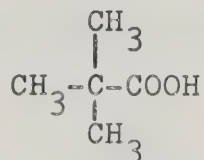
entered the internal filling solution and caused a
large change in the reading, too. Quantitative measurement
of this rate of diffusion was difficult to obtain. A
more serious problem was provided, however, by ringed
compounds such as benzoic acid
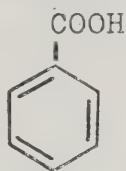
or cinnamic acid
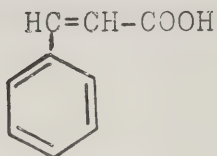
In both cases the millivolt reading of the electrode
dramatically increased upon addition of these compounds,
often reaching much higher millivolt readings than were
possible with carbon dioxide solutions. After exposure
to these acids, soaking for several hours in an aqueous
solution failed to achieve baseline readings. The

internal filling solution had to be changed many times
and the electrode thoroughly cleaned before it became
serviceable again. Phenol

OH
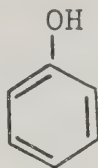
was another species that was found to diffuse through
the membrane. However, it did not cause the pH of the
internal filling solution to change as dramatically as
the above two acids (K_a for benzoic acid is 6.4×10^{-5},
K_a for cinnamic acid is 3.5×10^{-5} and K_a for phenol is
1.0×10^{-10})[56].

Another substance which seemed capable of
diffusing into the internal filling solution was ICl,
apparently because of its hydrolysis in water.

Other gases capable of hydrolysis and causing
a pH change, such as ammonia, were not interferences
because of the acid conditions under which the
electrode was used.

SUMMARY

After a review of the chemistry of the iron(III)-oxalate system, a method was developed to determine oxalate photochemically using excess iron(III) in an acidic medium. The oxalate was oxidized to carbon dioxide, which was measured with a pCO_2 electrode. A history of the development of this electrode was presented. The determination could be carried out either batch-wise or in a continuous-flow mode. A sampler, proportioning pump and reaction coil from a Technicon single-channel AutoAnalyzer were used in combination with a visible or ultraviolet radiation source and an Instrumentation Laboratory pCO_2 electrode in the flow-through system. This experimental design provided a relatively fast and accurate method of analysis for oxalate concentration. An advantage over previous methods for oxalate determination using the iron(III)-oxalate reaction is that the determination of carbon dioxide is more specific than the measurement of the iron(II) produced upon irradiation.

A rate of analysis of three or four samples per hour was chosen, primarily because of the slow time response of the electrode. The acidity, ionic strength and the presence of other anions were not found to be critical variables for the iron(III)-oxalate analysis.

The optimization of the iron(III) concentrations was discussed. Investigation into the interference produced by other carboxylic acids led to the conclusion that at high acid concentrations the extent of their reaction was usually greatly reduced. At low acidities, on the other hand, the concentration of iron(III)-carboxylate formed by many of the carboxylate salts was sufficiently great that the photochemical reaction could be used to measure their concentration.

The pCO_2 electrode has had only limited use by analytical chemists and so a brief study was undertaken of potential interferences. Organic acids of low molecular weight and aromatic compounds appeared to diffuse through the membrane rendering false readings for the pCO_2 of a test solution.

Because of the slow speed of analysis necessary with the pCO_2 electrode measurement of the carbon dioxide evolved from the carboxylate analysis and also because of the inherent errors in the use of the gas electrode, further investigations of the iron(III)-oxalate and iron(III)-carboxylate systems were carried out via computer calculations. The concentrations of ionic species present in various solutions as a function of the iron(III) concentration, acidity and anion were evaluated and are presented in the following chapter.

CHAPTER 3

COMPUTER STUDIES OF IRON(III) EQUILIBRIA
WITH CARBOXYLIC ACIDS

INTRODUCTION

For maximum effectiveness of conversion of
oxalate to carbon dioxide by irradiation of the iron(III)
complex, the fraction of oxalate in the form of the
iron(III) complex must be maximized. The optimization of
conditions to achieve this is not simple. Thus, the
concentration of iron(III), of acid, and the concentration
and nature of the counterions that are present must be
taken into account. Chloride and sulfate, added with the
iron(III) or acid, or present in the sample, form complexes
that decrease the amount of free iron(III) available to
complex with the oxalate. Also, when the carboxylic acids
are present as interferences, it is necessary to adjust
conditions so as to minimize their effects. Or, when other
carboxylic acids are measured by irradiation of their
iron(III)-carboxylate complex, the conditions must be such
as to form the maximum amount of complex. Iron(III)
formation and acid dissociation constants for many of the
carboxylic acids are available, but in systems containing
a large number of components, many reactions are
interdependent. Because manual calculation of the

concentration of each species in such systems is difficult and time consuming, a computer was used to aid in the work.

Previous Work

Swinnerton and Miller [57] used a digital computer in 1959 to determine equilibrium ion concentrations in solutions of iron(III) ammonium sulfate, ammonium trioxalatoferrate(III), oxalic acid, potassium oxalate and sulfuric acid. Hydrolysis of iron(III) and ammonium ions was neglected in their system. Figures showing the effect of sulfuric acid concentration (10^{-3}-10^{0} $\underline{N}$) on the distribution of chemical species in 0.01 $\underline{M}$ ammonium trioxalatoferrate(III) and the change in concentration of the various species in 0.03 $\underline{M}$ potassium oxalate and 0.1 $\underline{N}$ sulfuric acid over an iron(III) ammonium sulfate concentration range of 10^{-4} to 10^{-1} $\underline{M}$ were included. The species in their calculations were H^+, HSO_4^-, SO_4^{-2}, H_2Ox, HOx^-, Ox^{-2}, Fe^{+3}, $FeOx^+$, $Fe(Ox)_2^-$ and $Fe(Ox)_3^{-3}$.

Extension of this Work

For this study, Swinnerton and Miller's work was extended to include the hydrolysis of iron(III) and formation of sulfate and chloride complexes of iron(III) under a variety of conditions.

EXPERIMENTAL

The Newton-Raphson method of successive approximations used by Swinnerton and Miller was employed here, but with several modifications. In their study, the appropriate mass balance and equilibrium constant equations were first listed and then the initial set of equations (4 mass balance and 6 formation and acidity equations were necessary for their system) in 10 unknowns were combined algebraically to yield 3 equations in 3 unknowns. Initial guesses were tabulated for these 3 unknowns and successively corrected until the desired precision was obtained. From these data concentrations for all 10 species then could be calculated.

To apply this method, computer programs were written for the University of Alberta IBM 360/67 computer by D. Webster of the University of Alberta Chemistry Department. Appendix 1 contains an example of one program that was used. Since a versatile program was necessary to allow calculations to be performed with a variety of species at different concentrations, the system was reduced to _n_ equations in _n_ unknowns, where _n_ is the number of mass balance equations used. Initially, four mass-balance equations, in iron, sulfate, hydrogen and oxalate, were employed.

Equilibria involving dissociation of ammonium ions or formation of ammine complexes were ignored

throughout this work. Formation constant data were included for HSO_4^-, $FeSO_4^+$, $Fe(SO_4)_2^-$, $FeOx^+$, $Fe(Ox)_2^-$, $Fe(Ox)_3^{-3}$, HOx^-, H_2Ox and $FeOH^{+2}$. Values of the constants that were used for these species, along with others later added to the program, are tabulated in Table 5. Stability constants were chosen, where available, at an ionic strength of one and a temperature of $25^{\circ}C$ as this represented the experimental conditions more closely than standard conditions of zero ionic strength and $0^{\circ}C$. Later the program was extended to include chloride and citrate species, which increased the number of mass balance equations and hence the number of initial guesses required. Table 5 contains the formation constants for the added $FeCl^{+2}$, $FeCl_2^+$, $FeCl_3$, $FeCl_4^-$, $FeCit^*$, $HCit^{-2}$, H_2Cit^- and H_3Cit.

In all calculations the contribution to the hydrogen mass balance from the hydrolysis of iron(III) was assumed to be small; this amount, for simplicity, was omitted in the value given to the hydrogen mass balance equation. The validity of this assumption was confirmed for most of the calculations. Further corrections were not added for those cases where the assumption was invalid. (Below pH 3 a negligible error was introduced.) Activity coefficient corrections were omitted.

---

* Cit is used as the symbol for citrate anion throughout this thesis.

TABLE 5

Equilibrium Constant Values Used in Computer Calculations
of Species Concentrations

Ligand	Species[a]	Formation[b] Constant	Temperature $^\circ$C	Medium[c]	Reference[d]
Oxalate	FeX	3.89×10^7	25	0.5 LiClO$_4$	58
	FeX$_2$	4.39×10^{13}	25	0.5 LiClO$_4$	58
	FeX$_3$	3.09×10^{18}	25	0.5 LiClO$_4$	58
	H$_2$X	4.37×10^4	25	1 NaClO$_4$	59
	HX	3.72×10^3	25	1 NaClO$_4$	59
Sulfate	FeX	1.07×10^2	28	1 H(ClO$_4$)	60
	FeX$_2$	1.01×10^3	28	1 H(ClO$_4$)	60
	HX	1.29×10^1	20	1 (NaClO$_4$)	61
Hydroxide	FeX	1.00×10^{-3}	25	3 (NaClO$_4$)	62
Chloride	FeX	4.20	26.7	1 (H, NaClO$_4$)	63
	FeX$_2$	5.46	26.7	1 (H, NaClO$_4$)	63
	FeX$_3$	2.18×10^{-1}	26.7	1 (H, NaClO$_4$)	63
	FeX$_4$	2.29×10^{-3}	20	0 corr	64
Citrate	FeX	7.08×10^{11}	25	1 NaClO$_4$	65
	H$_3$X	1.21×10^{12}	25	1 (KNO$_3$)	66
	H$_2$X	2.83×10^9	25	1 (KNO$_3$)	66
	HX	2.19×10^{11}	25	1 (KNO$_3$)	66

[a]X is the ligand; charges on species omitted for simplicity.

[b]Overall formation constant.

[c]0.5 LiClO$_4$ means a constant concentration (0.5 $\underline{M}$) of LiClO$_4$ has been
used.

1 H(ClO$_4$) means the concentration of H was held constant at 1 mole/liter
with ClO$_4$ as the inert anion.

1 (NaClO$_4$) means the ionic strength was held constant at 1 mole/liter
by the addition of NaClO$_4$.

0 corr means constants corrected to zero ionic strength.

[d]All references from The Chemical Society's "Stability Constants of
Metal-Ion Complexes"[67].

In the Newton-Raphson method, values of the derivatives of the $\underline{n}$ equations are evaluated with respect to each of the $\underline{n}$ unknowns. For each set of conditions, values of the $\underline{n}$ x $\underline{n}$ matrix coefficients, the right hand side of the matrix, the corrections to be added to the original estimates and the corrected estimates were printed. In this way, the number of times the iteration had to be repeated and hence the speed of convergence could be ascertained easily.

Uncertainties in some of the results may be moderately large. Double precision was used throughout, but because concentrations and constants often varied widely in magnitude, some truncation errors were introduced. Further, since the equilibrium constants were measured under a wide range of conditions and by different workers, the results may not be completely uniform and constant. However, they were useful to indicate trends and aid in selecting experimental conditions.

In the second part of these computer calculations, data for the formation constants of other iron(III)-carboxylate species and acidity data for these acids were substituted into the program in place of the iron(III)-oxalate formation and acidity constants. The carboxylic acids which were chosen for study, and their formulas, are listed in Table 6, while Table 7 gives their formation and

TABLE 6

Carboxylic Acids Chosen for
Equilibrium Study

Acid	Formula
Formic acid	$H-COOH$
Acetic acid	CH_3-COOH
Propionic acid	CH_3-CH_2-COOH
Succinic acid	$COOH-CH_2-CH_2-COOH$
Lactic acid	$CH_3-CHOH-COOH$
Malonic acid	$COOH-CH_2-COOH$
Malic acid	$COOH-CHOH-CH_2-COOH$
Tartaric acid	$COOH-CHOH-CHOH-COOH$
Mandelic acid	$C_6H_5-CHOH-COOH$

TABLE 7

Equilibrium Constant Values Used in Computer Calculations of Species
Concentrations for Different Carboxylic Acids

Ligand	Species[a]	Formation[b] Constant	Temperature °C	Medium[c]	Reference[d]
Formate	FeX	7.08×10^1	25	1	68
	FeX$_2$	4.07×10^3	25	1	68
	FeX$_3$	8.91×10^3	25	1	68
	HX	1.26×10^3	20	1 NaClO$_4$	69
Acetate	FeX	2.40×10^3	18-22	0.1	70
	FeX$_2$	1.26×10^6	18-22	0.1	70
	FeX$_3$	5.01×10^8	18-22	0.1	70
	HX	2.00×10^4	30	1 NaClO$_4$	71
Propionate	FeX	2.82×10^3	20	1 NaClO$_4$	72
	HX	4.57×10^4	20	1 NaClO$_4$	72
Succinate	FeX	7.59×10^6	25	0.5 LiClO$_4$	58
	H$_2$X	1.51×10^9	25	1 (KNO$_3$)	73
	HX	1.58×10^5	25	1 (KNO$_3$)	73
Lactate	FeX	2.51×10^6	–	→ 0	74
	HX	5.48×10^3	20	0.2 (KCl)	75
Malonate	FeX	2.88×10^7	25	0.5 LiClO$_4$	58
	H$_2$X	7.10×10^7	25	1.00 (KNO$_3$)	73
	HX	1.29×10^5	25	1.00 (KNO$_3$)	73
Malate	FeX	1.26×10^7	20	0.1 (NaClO$_4$)	76
	H$_2$X	8.52×10^7	20	0.1 (NaClO$_4$)	77
	HX	5.13×10^4	20	0.1 (NaClO$_4$)	77
Tartrate	FeX	3.09×10^6	20	0.1 (NaClO$_4$)	78
	FeX$_2$	7.24×10^{11}	20	0.1 (KClO$_4$)	79
	H$_2$X	1.48×10^6	18	1 NaCl	80
	HX	4.90×10^3	18	1 NaCl	80
Mandelate	FeX	5.13×10^3	25	–	81
	HX	1.38×10^3	25	1 (KNO$_3$)	82

[a]X is the ligand; charges on species omitted for
simplicity.

[b]Overall formation constant.

[c]1 means an ionic strength of 1 mole/liter.

1 NaClO$_4$ means a constant concentration (1.0 $\underline{M}$) of

NaClO$_4$ has been used.

1 (KNO$_3$) means the ionic strength was held constant

at 1 mole/liter by the addition of KNO$_3$.

→ 0 means extrapolated to zero ionic strength.

[d]All references from The Chemical Society's "Stability
Constants of Metal-Ion Complexes"[67].

acidity constants. Only those acids which had both H^+ and Fe^{+3} stability constants listed in The Chemical Society's "Stability Constants of Metal-Ion Complexes"[67] were chosen for analysis. Thus, some interesting carboxylic acids were not studied. Of those carboxylic acids chosen for study, only those iron(III)-carboxylate species which formed without the displacement of hydrogen ions were included. Only the simplest iron(III)-hydroxide species was included, primarily because inclusion of polynuclear hydroxides markedly increases the complexity of the system. Some data regarding these species are included in Chapter 4.

RESULTS AND DISCUSSION

Effect of Variation in Iron(III) Concentration on Equilibria

The effect of the iron(III) concentration on the amount of iron(III) oxalate complex in solution was investigated by varying the iron(III) ammonium sulfate concentration between $5x10^{-5}$ and $1x10^{-1}$ $\underline{M}$ in a theoretical solution containing 1 $\underline{M}$ sulfuric acid and $1x10^{-4}$ $\underline{M}$ oxalate. The calculation was repeated with the sulfuric acid replaced by hydrochloric acid and the iron(III) added as the chloride species. A third calculation was performed in which the interfering counterions, sulfate and chloride, were deleted. The data obtained are presented in log-log plots in Figures 20, 21 and 22. The calculated concentration of the species $Fe(Ox)_3^{-3}$ was below the range covered in all of these diagrams.

In all three cases the $FeOx^+$ concentration increases with increasing iron(III) concentration, as expected. Concentrations of the di- and tri-oxalate complexes and the free oxalate are several orders of magnitude below that of the monooxalatoferrate(III) species. At moderate to high concentrations of sulfate or chloride, the fraction of iron(III) tied up as sulfate or chloride complexes is more than the amount bound as the iron-oxalate complex.
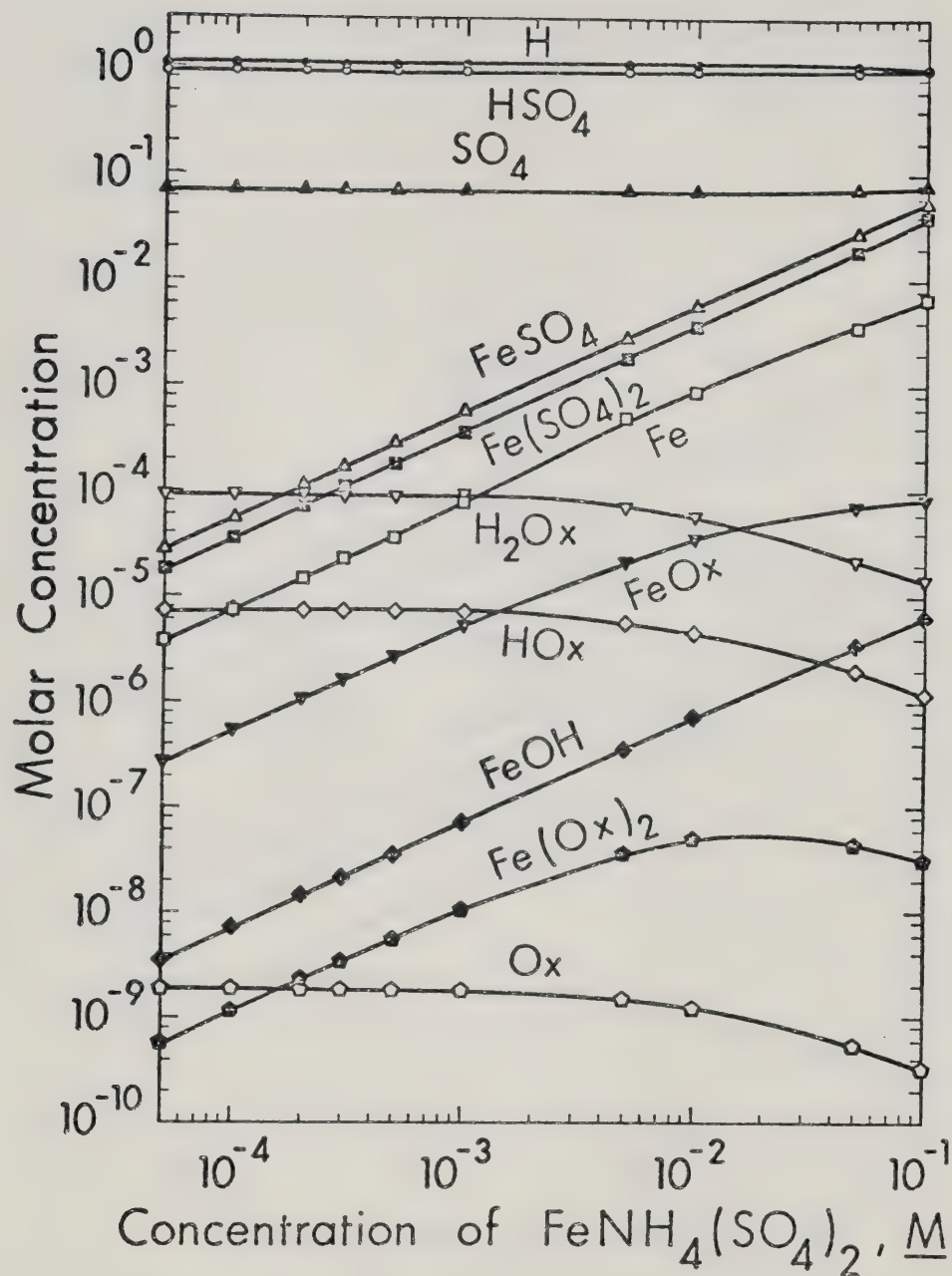
Figure 20   Effect of Iron(III) Ammonium Sulfate
            Concentration on the Distribution of
            Chemical Species in 1x10^{-4} $\underline{M}$ Oxalate
            and 1 $\underline{M}$ Sulfuric Acid. Ionic charges
            omitted for simplicity.
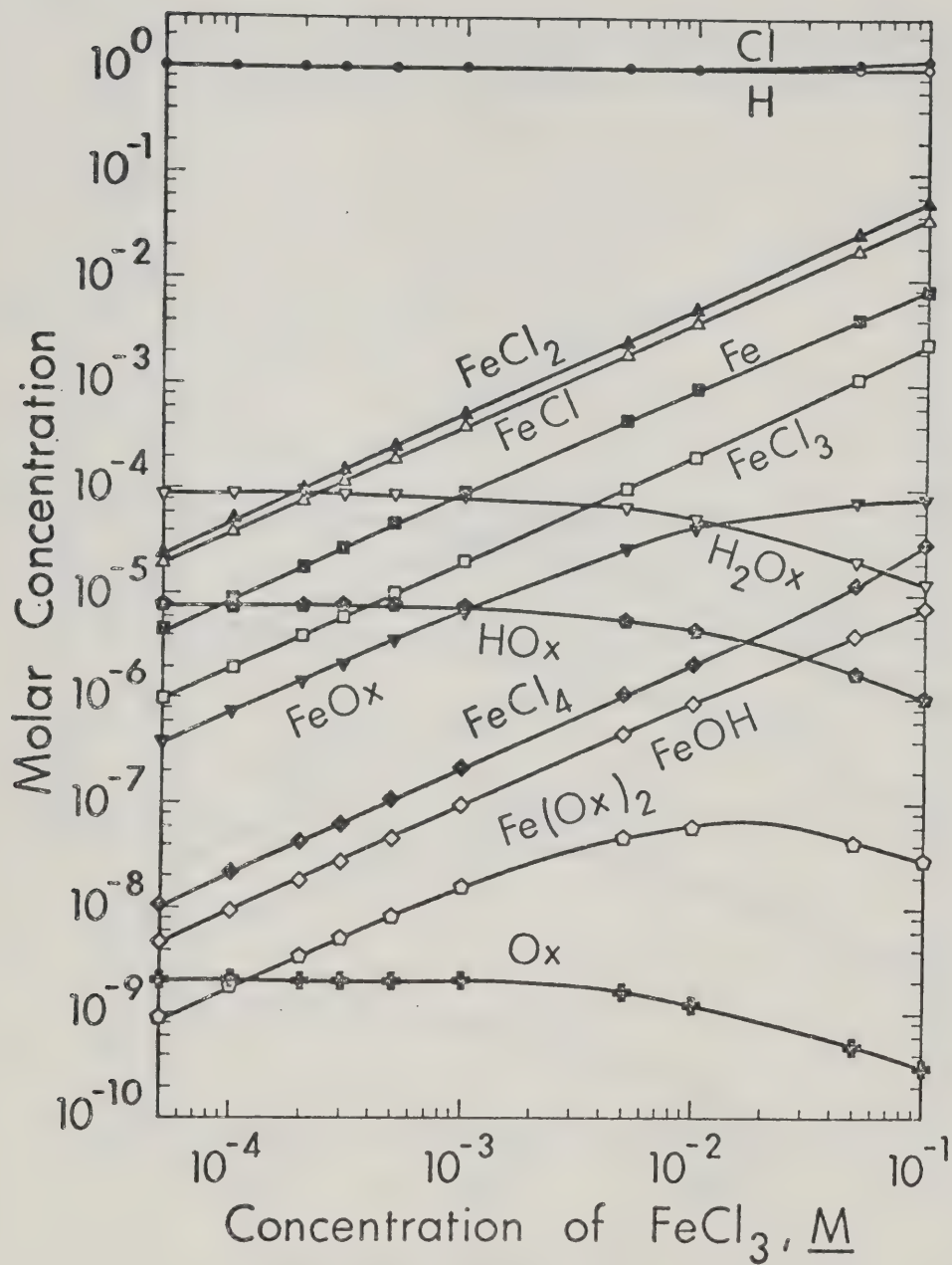
Figure 21 Effect of Iron(III) Chloride Concentration on the Distribution of Chemical Species in 1×10^{-4} M Oxalate and 1 M Hydrochloric Acid. Ionic charges omitted for simplicity.
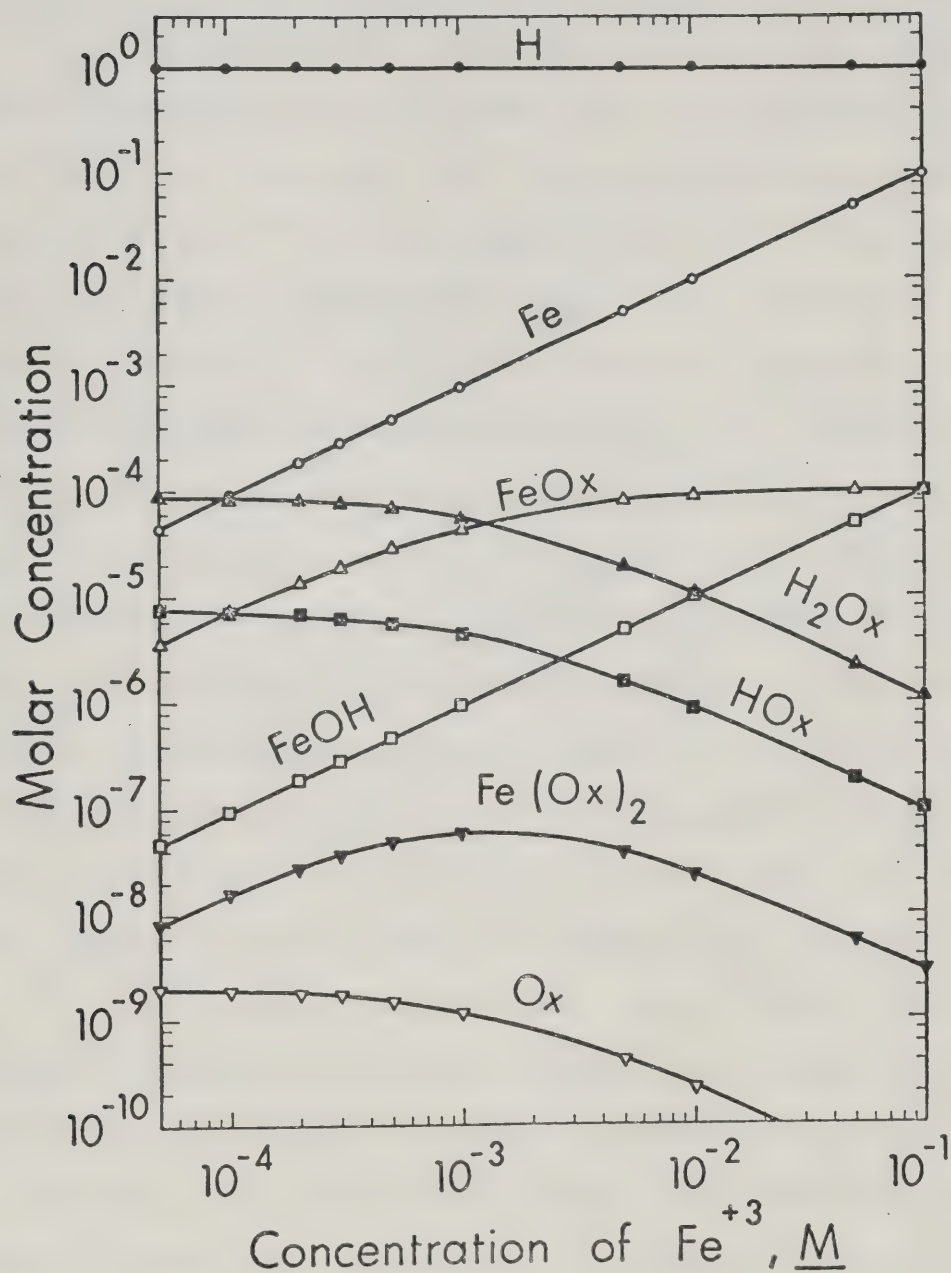
Figure 22 Effect of Iron(III) Concentration on the
Distribution of Chemical Species in
1×10^{-4} M Oxalate and 1 M Hydrogen Ion.
Ionic charges omitted for simplicity.

Effect of Variation in Acid Concentration on Equilibria

A second set of calculations was done in which the concentration of acid added was varied between 1×10^{-4} $\underline{M}$ and 10 $\underline{M}$. In each case, the total concentration of oxalate was held at 1×10^{-4} $\underline{M}$, and iron(III) at 3×10^{-4} $\underline{M}$. This iron(III) concentration was chosen so as to provide an excess of iron(III) relative to oxalate (each mole of oxalate requires two moles of iron(III) for complete oxidation) and yet to minimize screening of radiation in the photolysis step due to the absorption by iron(III) or its sulfate and chloride complexes. The first experiment used sulfuric acid with iron(III) ammonium sulfate; the second, hydrochloric acid with iron(III) chloride; and the third, perchloric acid with iron(III) perchlorate, i.e., with no interfering counterions present. The data obtained are shown on log-log plots in Figures 23, 24 and 25.

From these calculations, it is evident that the optimum concentration of acid required to produce the maximum concentration of $FeOx^+$ is generally below 0.1 $\underline{M}$. As expected, with increasing acidity the protonated oxalate species become more predominant. Concentrations of the di- and tri-oxalatoferrate(III) species are a factor of ten or more below that of the monooxalatoferrate(III) complex. The concentration of the iron(III)-hydroxide species in 1×10^{-4} $\underline{M}$ acid is significant; in general, at pH values above
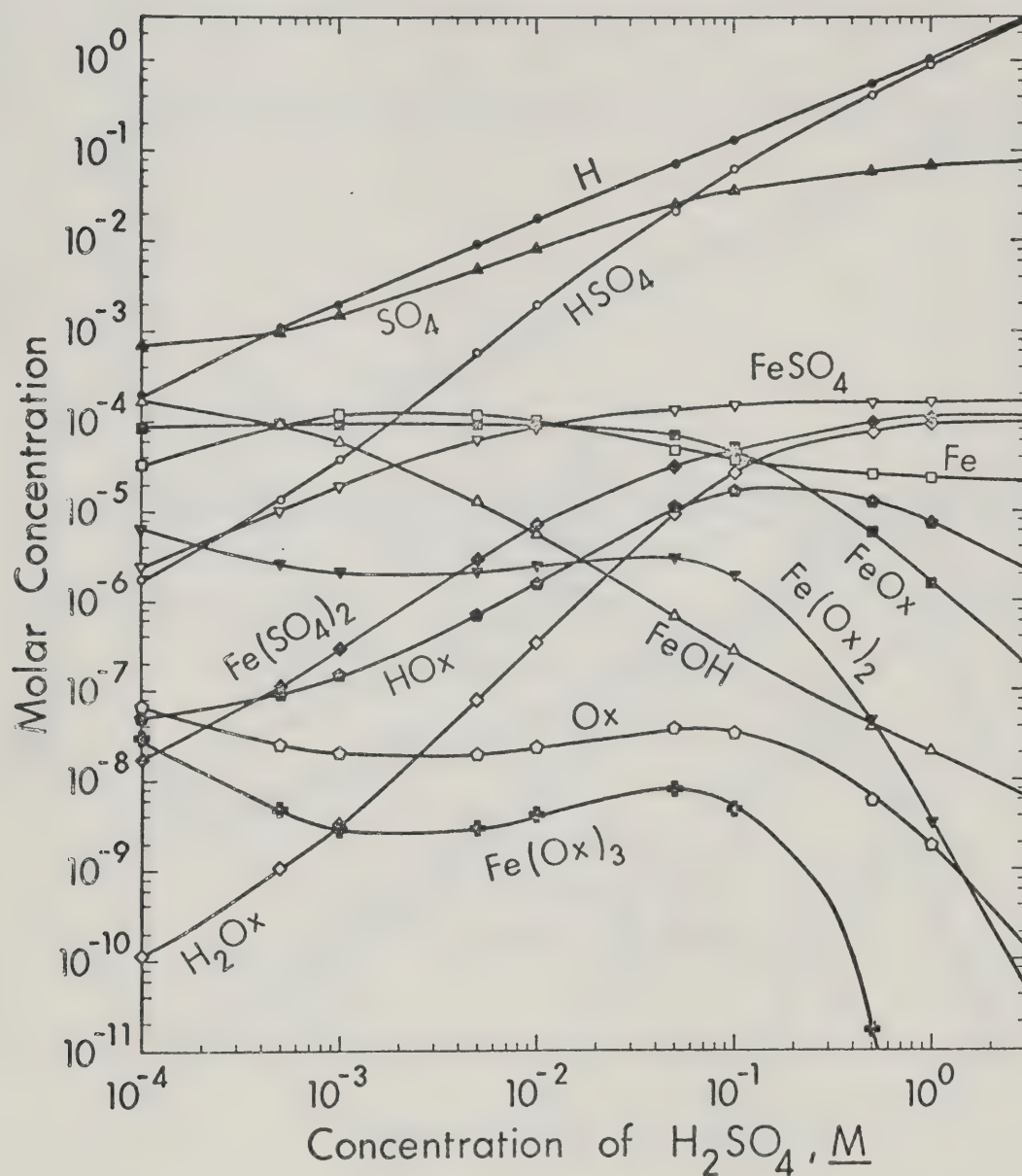
Figure 23   Effect of Sulfuric Acid Concentration on the
            Distribution of Chemical Species in 1×10^{-4} $\underline{M}$
            Oxalate and 3×10^{-4} $\underline{M}$ Iron(III) Ammonium
            Sulfate. Ionic charges omitted for simplicity.
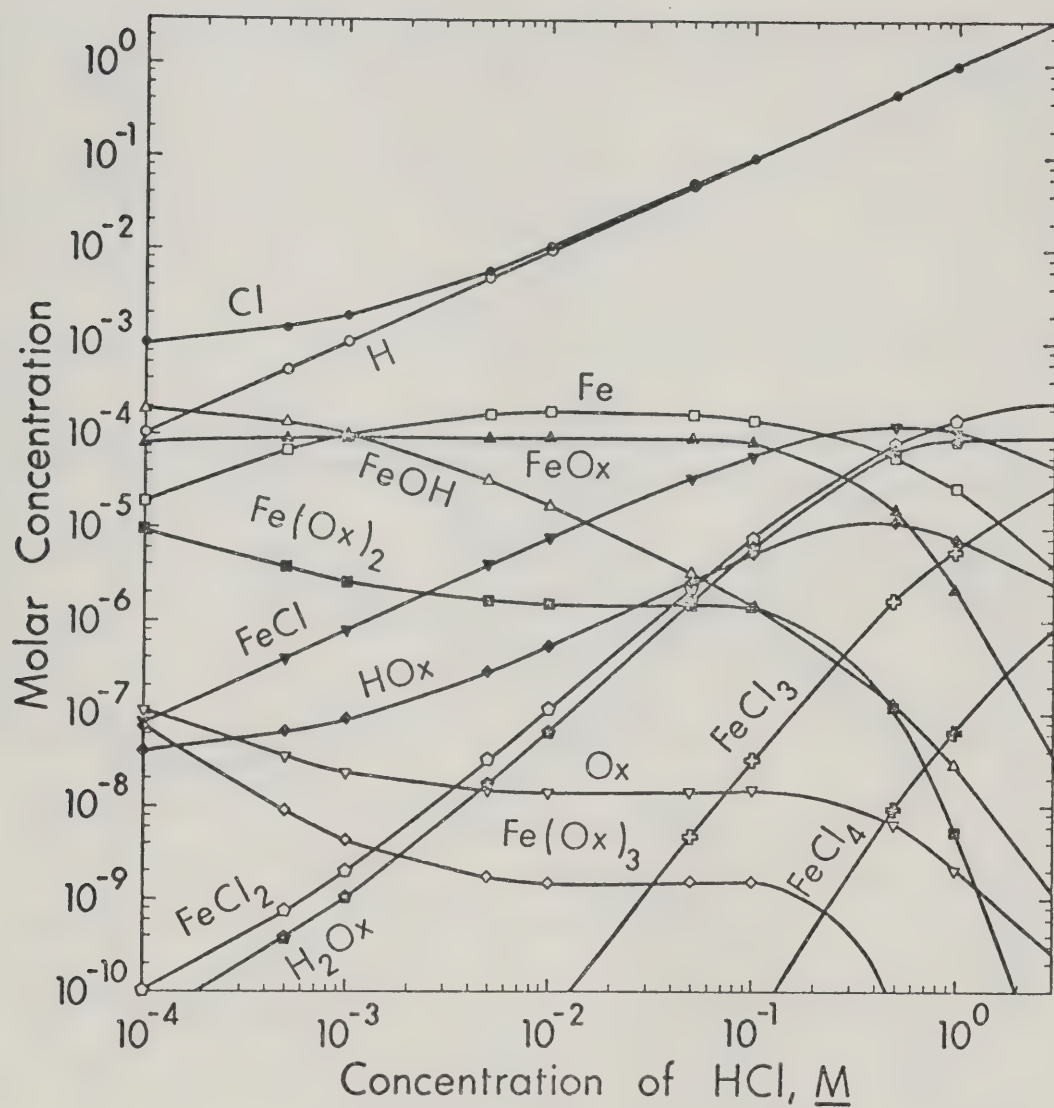
Figure 24   Effect of Hydrochloric Acid Concentration on
the Distribution of Chemical Species in 1×10^{-4}
$\underline{M}$ Oxalate and 3×10^{-4} $\underline{M}$ Iron(III) Chloride.
Ionic charges omitted for simplicity.
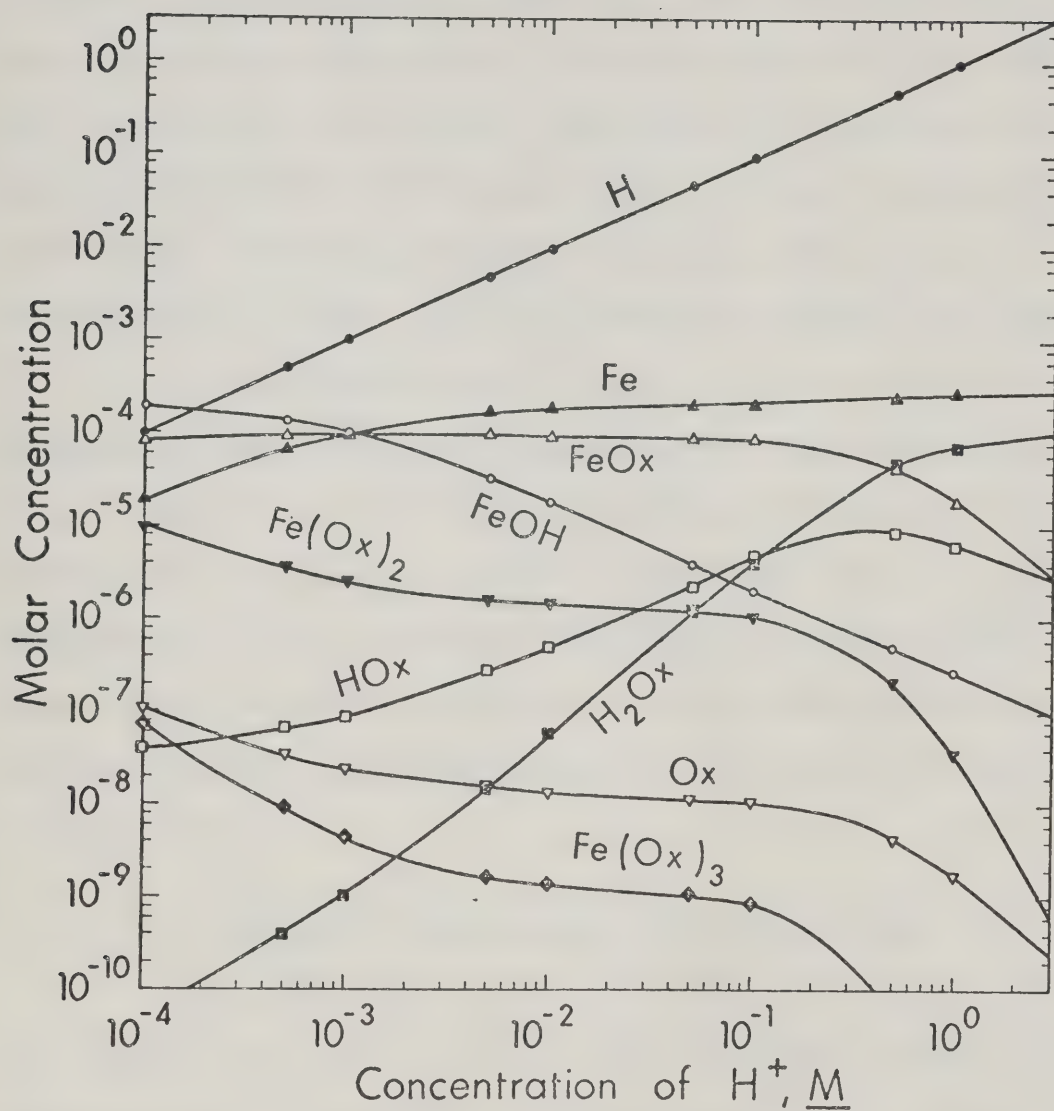
Figure 25 Effect of Hydrogen Ion Concentration on the
Distribution of Chemical Species in 1×10^{-4} $\underline{M}$
Oxalate and 3×10^{-4} $\underline{M}$ Iron(III). Ionic
charges omitted for simplicity.

3, the error due to the initial assumption that the hydroxide species can be neglected in the hydrogen mass balance equation is appreciable. However, above pH 3 the system is not of practical importance for the purpose of this work. As the acidity is raised by the addition of sulfuric or hydrochloric acid, the concentration of the counterions, sulfate or chloride, increases and thus, also, the concentration of the iron(III) complexes formed from them.

Comparing Figures 20 and 21, and 23 and 24, a slightly greater amount of monooxalatoferrate(III) is formed in the presence of chloride counterions compared to that formed when sulfate is present. This confirms the experimental data presented in Chapter 2 which showed no decrease in the amount of carbon dioxide generated from oxalate analysis when hydrochloric acid was substituted for sulfuric acid.

Iron(III) Equilibria with Citric Acid

Calculations similar to those for oxalate were also carried out with $1x10^{-4}$ $\underline{M}$ total citrate in which the concentration of iron(III) ammonium sulfate was varied from $5x10^{-5}$ to 0.1 $\underline{M}$ in 1 $\underline{M}$ sulfuric acid. An additional set of calculations was done in which the sulfuric acid concentration was varied between $1x10^{-4}$ and 10 $\underline{M}$ at an iron(III) ammonium sulfate concentration of $3x10^{-4}$ $\underline{M}$ and

citrate concentration of 1×10^{-4} $\underline{M}$. From the results presented in Figure 26 it can be seen that in 1 $\underline{M}$ sulfuric acid, the predominant citrate species is the molecular acid at all iron(III) concentrations although the iron(III)-citrate complex increases in importance as the iron(III) concentration is raised. In Figures 26, 27 and 28, the calculated concentration of Cit^{-3} was below the ranges plotted. Figure 27 shows that above 1×10^{-2} $\underline{M}$ sulfuric acid the amount of iron(III)-citrate complex formed rapidly decreases and the protonated forms become more important. The influence of acid concentration on the iron(III)-citrate reaction observed in Chapter 2 can now be understood. The behavior of other species such as the iron(III)-sulfate complexes is similar to that observed in the oxalate calculations.

A further calculation was done of the effect of acid concentration (1×10^{-4} to 1 $\underline{M}$ H_2SO_4) on equilibria in a solution containing 1×10^{-4} $\underline{M}$ total oxalate and 1×10^{-4} $\underline{M}$ total citrate. The analytical concentration of iron(III) ammonium sulfate was held at 3×10^{-4} $\underline{M}$ for these calculations. This iron(III) concentration is insufficient to provide the stoichiometric amount needed to oxidize the oxalate and citrate to carbon dioxide. The effect of acid over the range 5×10^{-2} to 1 $\underline{M}$ H_2SO_4 was similarly computed in a solution containing analytical concentrations of 1×10^{-4} $\underline{M}$
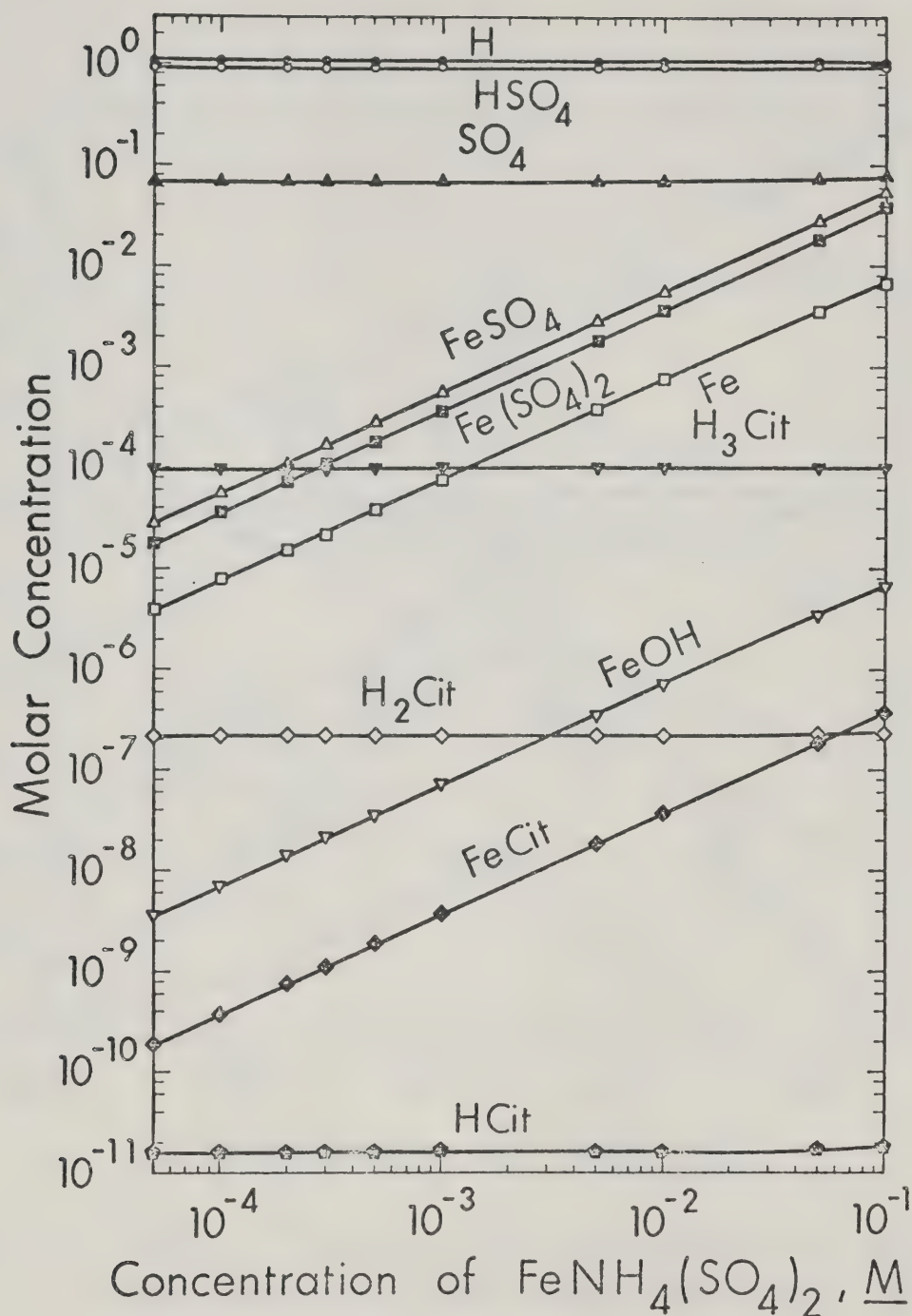
Figure 26 Effect of Iron(III) Ammonium Sulfate
Concentration on the Distribution of
Chemical Species in 1×10^{-4} $\underline{M}$ Citrate
and 1 $\underline{M}$ Sulfuric Acid. Ionic charges
omitted for simplicity.
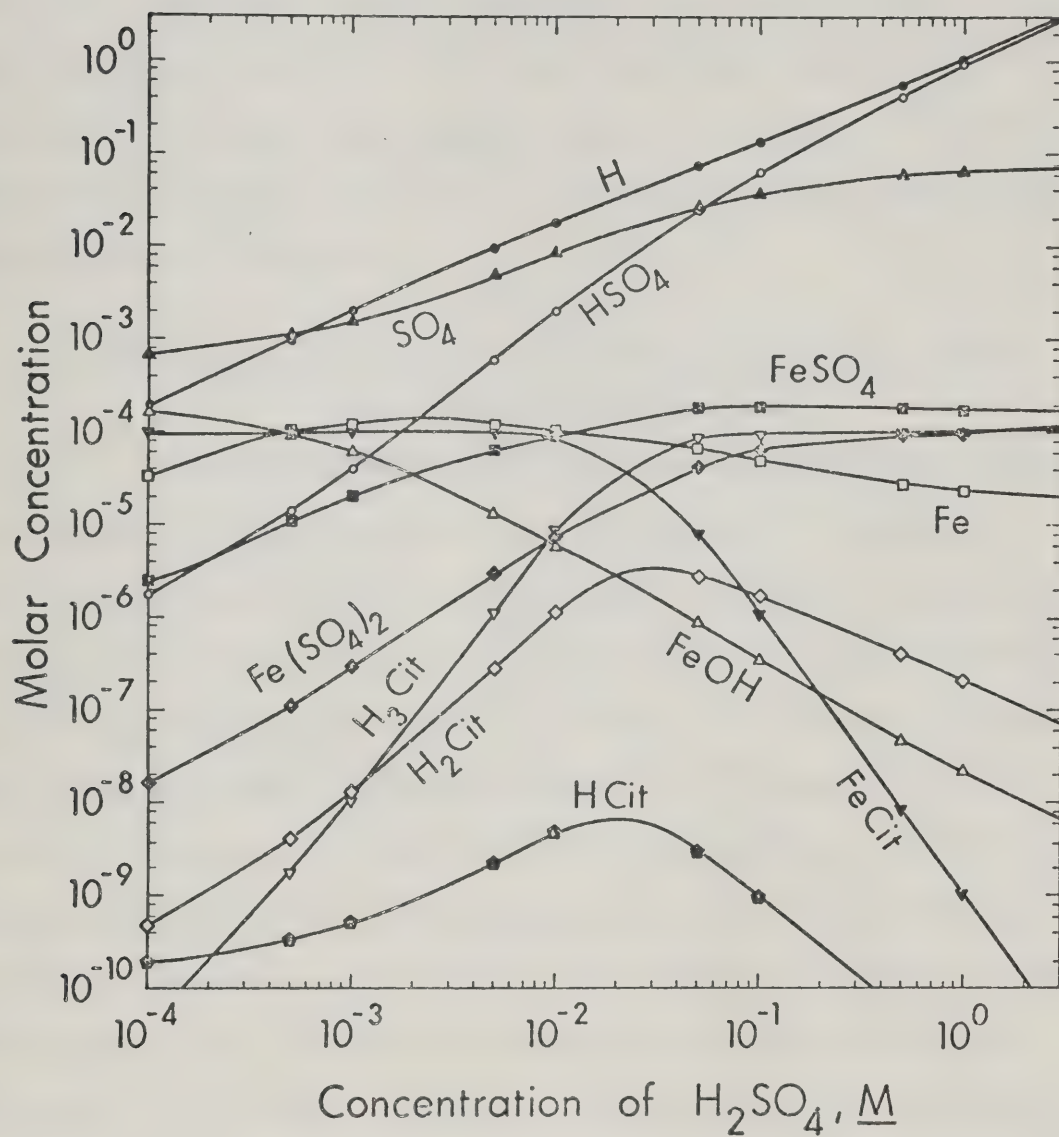
Figure 27 Effect of Sulfuric Acid Concentration on the
Distribution of Chemical Species in 1×10^{-4} $\underline{M}$
Citrate and 3×10^{-4} $\underline{M}$ Iron(III) Ammonium
Sulfate. Ionic charges omitted for simplicity.

oxalate and 1×10^{-3} $\underline{M}$ citrate. The analysis of mixtures of
the two carboxylic acids resembles the combination of the
two separate analyses with the exception that the two
carboxylic acids must compete for the available iron(III).
The data obtained for the 1:1 oxalate:citrate calculation
are shown in Figure 28.

Iron(III) Equilibria with Other Carboxylic Acids as a Function of Acidity

The acidity was found to be an important variable
for many of the carboxylic acids studied in Chapter 2. To
ascertain the effect of acidity on a variety of carboxylate
salts, individual calculations were done on solutions of
1×10^{-4} $\underline{M}$ carboxylate, 3×10^{-4} $\underline{M}$ iron(III) ammonium sulfate
and sulfuric acid varying between 1×10^{-4} and 1 $\underline{M}$. The
effect of acidity on the iron(III)-carboxylate species is
shown in Figure 29. For comparison, the corresponding
results obtained with oxalate and citrate are also included.
The importance of pH on the degree of formation of the
complex is evident. Because oxalate forms the strongest
iron(III) complex of all the carboxylic acids studied, the
pH of the solutions to be analyzed can be lowered to
decrease the extent of formation of other iron-carboxylate
complexes while still maintaining a high concentration of
iron(III)-oxalate complex.
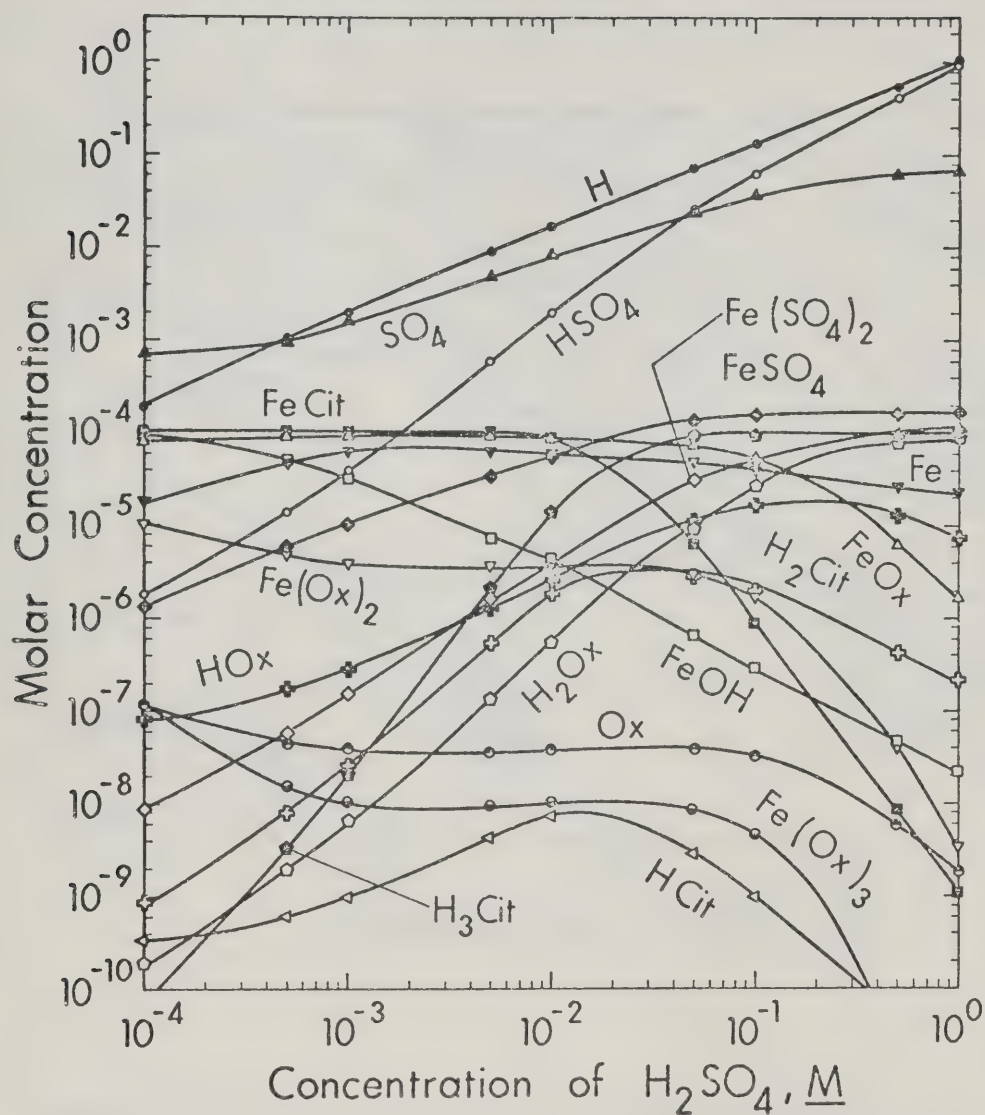
Figure 28   Effect of Sulfuric Acid Concentration on
            the Distribution of Chemical Species in
            1×10^{-4} $\underline{M}$ Oxalate, 1×10^{-4} $\underline{M}$ Citrate and
            3×10^{-4} $\underline{M}$ Iron(III) Ammonium Sulfate. Ionic
            charges omitted for simplicity.
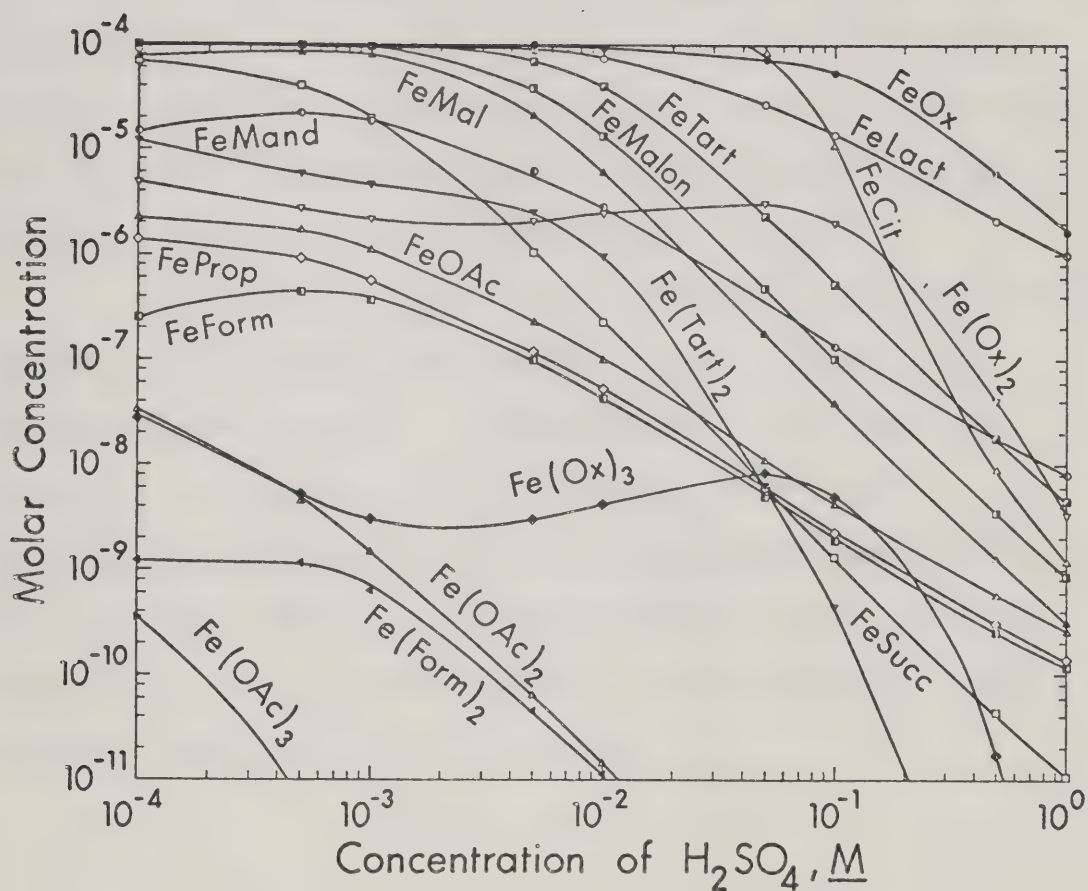
Figure 29   Effect of Sulfuric Acid Concentration on the
            Concentration of Iron(III)-Carboxylate Species
            for a Variety of Carboxylate Salts (1×10^{-4} $\underline{M}$)
            in 3×10^{-4} $\underline{M}$ Iron(III) Ammonium Sulfate. Ox is
            oxalate, Cit is citrate, Form is formate,
            OAc is acetate, Prop is propionate, Succ is
            succinate, Lact is lactate, Malon is malonate,
            Mal is malate, Tart is tartrate and Mand is
            mandelate. Ionic charges omitted for
            simplicity.

The data were of limited usefulness in interpreting the ion selective electrode data. Because of the availability of oxygen in the AutoAnalyzer system, less than stoichiometric amounts of iron(III) could be used under optimum conditions. Furthermore, the calculated data are only valid for an initial non-irradiated solution. As oxalate is removed, new equilibria are reached.

These data are useful for the gas chromatographic method of determining the evolved carbon dioxide as described in Chapter 5. In that method, no oxygen is present. If the quantum efficiencies of both the iron(III)-oxalate and iron(III)-interfering carboxylate are identical, then useful information could be obtained about the amount of interference to be expected. This, however, does not seem to be true.

SUMMARY

A Newton-Raphson type of calculation was done
to estimate concentrations of the species present in
solutions of: (a) iron(III) ammonium sulfate, sulfuric
acid and potassium oxalate; (b) iron(III) chloride,
hydrochloric acid and potassium oxalate; and (c) iron(III)
ammonium sulfate, sulfuric acid and a variety of
carboxylate salts. Graphs are shown to illustrate the
effect of variation in iron(III) concentration, acid
concentration and anion on the degree of formation of the
monooxalatoferrate(III) complex. Studies of the effect
of acidity on the extent of iron(III)-carboxylate
formation were undertaken for the formate, acetate,
propionate, succinate, lactate, malonate, malate, citric,
tartrate and mandelate systems. The data obtained
confirmed that of the acids studied, oxalate forms the
strongest iron(III) mono-complex, and also that in all
systems, as the acidity is raised, the extent of
formation of the iron(III)-carboxylate complexes is
decreased. This confirmed experimental results which
showed the interference from other carboxylic acids on
the iron(III)-oxalate reaction to decrease with
decreasing pH. To aid in further optimizing the
experimental parameters the following chapter will

present spectra for some of the systems studied in this chapter. The differences in the spectra as a function of acidity, anion, and carboxylate added will be evident.

CHAPTER 4

SPECTROSCOPIC STUDIES OF IRON(III)-CARBOXYLATE
COMPLEXES

INTRODUCTION

Nozaki and Kurihara[83], in a spectroscopic study, found that 1:1, 1:2 and 1:3 oxalate complexes of iron(III) formed in aqueous solutions. They estimated the molar absorptivities at 290 nm to be 1.6×10^3, 3.2×10^3 and 4.4×10^3, respectively. The ultraviolet absorption of these complexes was used as the basis for a method to determine iron(III)[83], oxalic acid and calcium(II)[84].

To determine oxalic acid, iron(III) was added to the oxalate solution to form the monooxalatoferrate(III) complex and the absorbance of the complex measured in perchloric acid solution at 290 nm. Calcium(II) was determined by precipitation as calcium oxalate, the precipitate then dissolved in perchloric acid and the oxalate measured as above.

The iron(III) complexes of sulfate, chloride, and hydroxide also absorb in the ultraviolet region. The radiation emitted by medium and low pressure mercury lamps, unlike that produced by tungsten lamps, is not continuous, but consists predominantly of mercury emission lines of varying intensities. Both of these

factors must be considered to obtain the most effective radiation for decomposition of the iron(III)-oxalate complex. Since the presence of other absorbing iron(III) species not only decreases the amount of iron(III) available for complex formation with oxalate, as seen in Chapter 3, but also diminishes the radiation reaching the oxalate complex, theoretical and experimental studies were undertaken to optimize conditions so as to be able to minimize their filtering effects.

EXPERIMENTAL

Spectra were run on a Cary 118 recording spectrophotometer in the Auto Slit mode, using 1-cm rectangular silica cells. A chart speed of 10 nm/in and scanning speed of 1 nm/sec were employed, along with automatic baseline correction.

RESULTS AND DISCUSSION

Background Absorbance in Iron(III)-Oxalate Solutions

Molar absorptivities over limited wavelength regions are available for each of the sulfate, chloride and hydroxide complexes of iron(III) discussed in Chapter 3. Using the data listed in Table 8, together with concentrations of all complexes present in solutions containing 1×10^{-4} $\underline{M}$ total oxalate, 1 $\underline{M}$ H_2SO_4 or HCl, and iron(III) concentrations ranging between 1×10^{-4} and 0.1 $\underline{M}$ as $FeNH_4(SO_4)_2$ or $FeCl_3$ (data from Figures 20 and 21), estimates were made of the total contribution to the absorbance of these solutions from species other than the iron-oxalate complexes. Table 9 summarizes the results at two wavelengths, 300 and 280 nm. In all cases, the total absorption increases markedly with increasing iron(III) concentration, as expected. However, at these wavelengths the contribution from the chloride species is less than that from the sulfate species. When the concentration of iron(III) to be used for the oxalate or citrate analysis by ion selective electrode was optimized (Chapter 2, Figures 13 and 18), low ratios of iron(III) to oxalate or citrate were preferred because other complexes screened the radiation from the iron(III)-oxalate complex at high iron(III) concentrations. A related reason could be the presence of absorbing

TABLE 8

Molar Absorptivities of Iron(III) Complexes used to Calculate Total Absorbance

Species[a]	Molar Absorptivities		Reference
	300 nm	280 nm	
Fe	300	800	64
FeOH	2490	2050	60
$FeSO_4$	2160	1760	60
$Fe(SO_4)_2$	2910	2450	60
FeCl	650	800	64
$FeCl_2$	1150	1200	64
$FeCl_3$	900	1900	64
$FeCl_4$	6000	6100	64

[a]Charges omitted for simplicity.

TABLE 9

Calculated Total Absorbance of Solutions Containing
Complexes of Iron(III)[a] as a Function of Iron(III)
Concentration and Anion

Total Fe(III) Concentration, $\underline{M}$	Total Absorbance for $FeNH_4(SO_4)_2-H_2SO_4$ System[b]	Total Absorbance for $FeCl_3-HCl$ System[c]
	At 300 nm	
10^{-4}	0.23	0.087
10^{-3}	2.27	0.87
10^{-2}	22.8	8.7
10^{-1}	233.	90.
	At 280 nm	
10^{-4}	0.19	0.10
10^{-3}	1.92	1.02
10^{-2}	19.3	10.2
10^{-1}	196.	104.

[a]Excluding the iron(III)-oxalate complexes.

[b]Contains $1 \times 10^{-4} \underline{M}$ C_2O_4, 1 $\underline{M}$ H_2SO_4 and $FeNH_4(SO_4)_2$.

[c]Contains 1×10^{-4} $\underline{M}$ C_2O_4, 1 $\underline{M}$ HCl and $FeCl_3$.

iron(III)-hydroxide species at high iron(III) concentrations. In the computer calculations only one hydroxide species, $FeOH^{+2}$, was included. This complex becomes significant whenever the acidity drops to 0.1 $\underline{M}$ or lower. However, other species, such as $Fe(OH)_2^{+}$, $Fe_2(OH)_2^{+4}$ and $Fe_3(OH)_4^{+5}$, can also form. Thus, at a pH of 1, ionic strength of 1 $\underline{m}$, and total iron(III) concentration of 0.1 $\underline{m}$, the distribution of species is 35% Fe^{+3}, 5% $FeOH^{+2}$, 45% $Fe_2(OH)_2^{+4}$ and 15% $Fe_3(OH)_4^{+5}$ [85]. Under the same conditions, but with a total iron(III) concentration of 1×10^{-5} $\underline{m}$, the distribution is 85% Fe^{+3} and 15% $FeOH^{+2}$. Since at lower iron(III) concentrations there are fewer hydroxide species (which absorb more strongly than hydrated Fe(III) at 300 nm) and no $Fe_2(OH)_2^{+4}$ (which absorbs more strongly than $FeOH^{+2}$ at 300 nm) this could also have contributed to the better performance seen in Chapter 2 at lower ratios of iron(III) to oxalate or citrate.

A similar study was made of the effect on total absorbance of varying the H_2SO_4 or HCl concentrations in a solution containing 1×10^{-4} $\underline{M}$ total oxalate and 3×10^{-4} $\underline{M}$ $FeNH_4(SO_4)_2$ or $FeCl_3$. Data on the concentration of species present were obtained from Figures 23 and 24. The total absorbances at 300 and 280 nm for all species but the iron(III)-oxalate species are presented in

Table 10. From the values shown in this table, it again is seen that at the high acidities at which the analysis is carried out absorption by chloride complexes of iron(III) is less than by sulfate complexes at these two wavelengths.

Spectra of Iron(III) Salts

Only selected wavelengths could be studied as above because of lack of absorptivity data. To obtain more information, spectra were obtained for iron(III) ammonium sulfate, iron(III) chloride and iron(III) perchlorate in 1 $\underline{M}$ solutions of their respective acids (Figure 30). The concentrations of these solutions were calculated to within 1 to 2% from the weight of salt taken. The sulfate salt has absorbance maxima at 304 and 226 nm, the chloride at 336 and 222 nm and the perchlorate at 240 nm. Since, as discussed previously, oxalate analysis would rarely be performed in the absence of complexing anions, the sulfate and chloride spectra were used to calculate molar absorptivities at selected wavelengths. The principal wavelengths emanating from low and medium pressure mercury lamps have been tabulated by Calvert and Pitts[86]. Molar absorptivities of the iron(III) solutions at wavelengths corresponding to those at which the lamps emit more than 15% of the energy of the most intense line in the 350 to 220 nm region are listed in Table 11. From consideration of

TABLE 10

Calculated Total Absorbance of Solutions Containing
Complexes of Iron(III)[a] as a Function
of Acidity and Anion

Total Acid Concentration, $\underline{M}$	Total Absorbance for $FeNH_4(SO_4)_2-H_2SO_4$ System[b]	Total Absorbance for $FeCl_3-HCl$ System[c]
	At 300 nm	
10^{-4}	0.439	0.482
10^{-3}	0.233	0.282
10^{-2}	0.262	0.102
10^{-1}	0.500	0.955
1	0.681	0.260
10	0.698	0.358
	At 280 nm	
10^{-4}	0.380	0.491
10^{-3}	0.258	0.332
10^{-2}	0.270	0.191
10^{-1}	0.433	0.177
1	0.577	0.304
10	0.590	0.449

[a]Excluding the iron(III)-oxalate complexes.
[b]Contains $1x10^{-4}$ $\underline{M}$ C_2O_4, $3x10^{-4}$ $\underline{M}$ $FeNH_4(SO_4)_2$ and H_2SO_4.
[c]Contains $1x10^{-4}$ $\underline{M}$ C_2O_4, $3x10^{-4}$ $\underline{M}$ $FeCl_3$ and HCl.
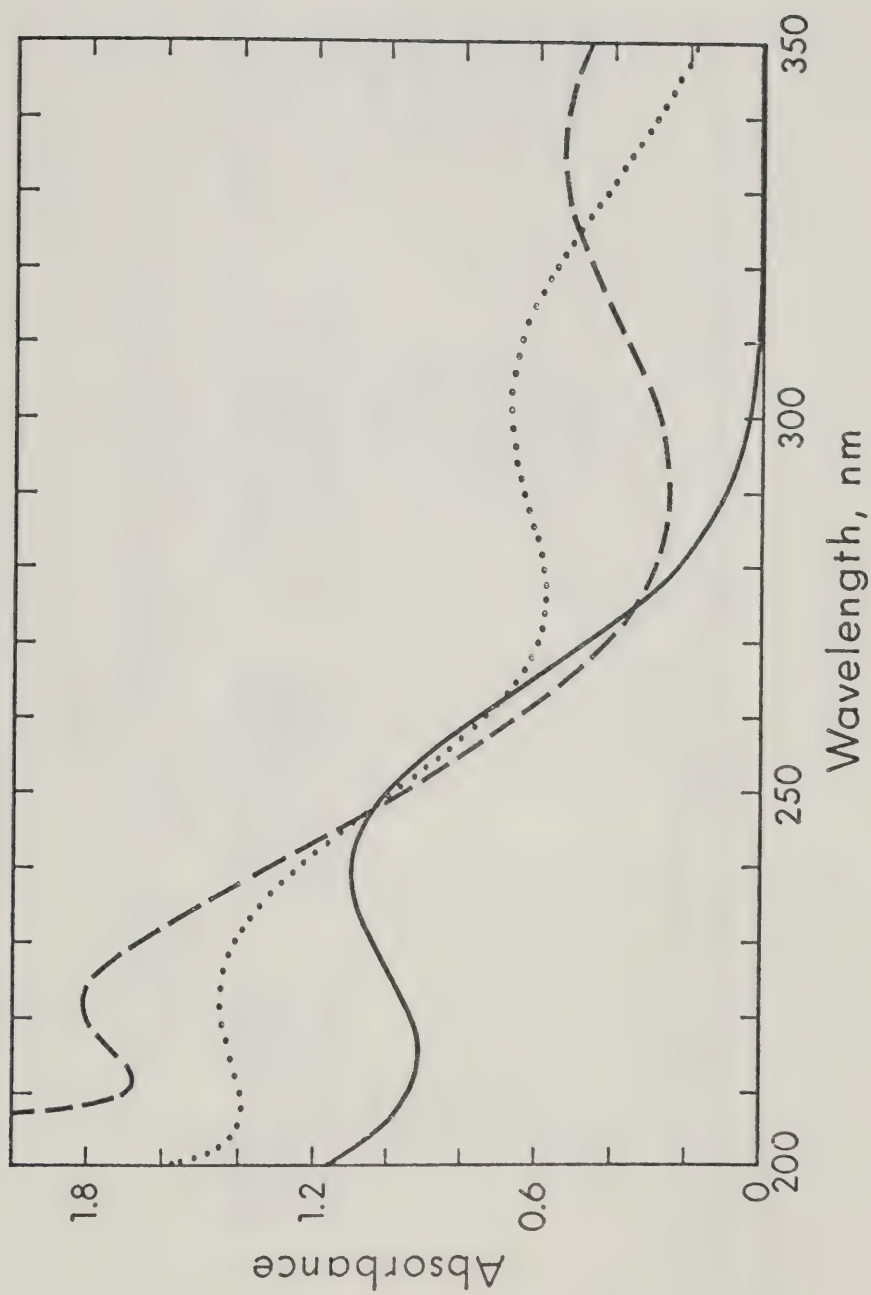
Figure 30   Effect of Anion on Spectra of Iron(III).

$\cdots\cdots$, $2.72\text{x}10^{-4}$ $\underline{M}$ FeNH$_4$(SO$_4$)$_2$ in 1 $\underline{M}$ H$_2$SO$_4$;

$-\cdot-\cdot$, $2.41\text{x}10^{-4}$ $\underline{M}$ FeCl$_3$ in 1 $\underline{M}$ HCl; $\underline{\quad\quad}$, $3.02\text{x}10^{-4}$ $\underline{M}$

Fe(ClO$_4$)$_3$ in 1 $\underline{M}$ HClO$_4$.

TABLE 11

Molar Absorptivities of $FeNH_4(SO_4)_2$ in 1 $\underline{M}$ H_2SO_4 and
$FeCl_3$ in 1 $\underline{M}$ HCl at Selected Wavelengths

Wavelength, nm	Relative Energy[a] (Medium Pressure Mercury Lamp)	Relative Energy[a] (Low Pressure Mercury Lamp)	Molar Absorptivity $FeNH_4(SO_4)_2$ in 1 $\underline{M}$ H_2SO_4	Molar Absorptivity $FeCl_3$ in 1 $\underline{M}$ HCl
254	17.7[b]	100	3.23×10^3	3.44×10^3
265	15.3	—	2.41×10^3	2.16×10^3
297	16.6	—	2.44×10^3	1.10×10^3
303	23.9	—	2.48×10^3	1.24×10^3
313	49.9	—	2.30×10^3	1.60×10^3
336	100	—	1.26×10^3	2.27×10^3

[a]Radiation intensity relative to most intense line, which is set arbitrarily at 100.

[b]Reversed radiation.

this information, together with the spectral data from Figure 30, it was concluded that the results of Tables 9 and 10 apply, in general, to the ultraviolet region employed in the experimental work. The precision of the absorbances in these calculations was limited by the uncertainties in the estimates of the molar absorptivities of each of the species present. Also, corrections for the amount of iron(III) complexed to oxalate were not made, which caused somewhat lower results. The data in Table 11 show little difference between background absorptivity for the iron(III) sulfate and iron(III) chloride solutions for the low pressure lamp. (This is confirmed experimentally in Chapter 5.) However, for the medium pressure lamp, lower absorptivities for the chloride species result at all wavelengths except 336 and 254 nm.

Iron(III)-Carboxylate Spectra

Spectra of the iron(III) complexes of three carboxylic acids were obtained under conditions where the presence of other complexes was minimized. For this purpose potassium oxalate, sodium citrate or potassium sodium tartrate was added to a solution of iron(III) perchlorate in 1 M perchloric acid. Perchlorate was chosen as the anion because it forms only weak iron(III) complexes of low absorbance compared to sulfate or

chloride. Figure 31 shows the spectra of a solution of iron(III) perchlorate in perchloric acid with and without added oxalate. Some photodecomposition may have taken place prior to the iron-oxalate spectra being run, although precautions were taken to protect the solutions from exposure to light.

Computer calculations showed that in 1 $\underline{M}$ HClO$_4$ and 3×10^{-4} $\underline{M}$ Fe(ClO$_4$)$_3$ only 18.7% of the total oxalate is present as FeOx$^+$ when the analytical oxalate concentration is 1×10^{-4} $\underline{M}$. In Figure 31 the spectrum of the iron(III) solution containing 1×10^{-4} $\underline{M}$ oxalate shows a slightly higher absorbance in the region 350 to 270 nm compared to the solution containing no oxalate. To increase the amount of FeOx$^+$ formed spectra were run with 1×10^{-3} and 1×10^{-2} $\underline{M}$ oxalate added. In doing this, the concentrations of the di- and tri-oxalatoferrate(III) complexes were also increased. Therefore, the absorbance increases seen are not totally due to the monooxalato-ferrate(III). The absorbance due to that complex could be calculated if the concentrations and molar absorbances were known for the Fe(Ox)$_2^-$ and Fe(Ox)$_3^{-3}$ complexes. Figure 32 shows the spectra for solutions of 1×10^{-4}, 1×10^{-3} and 1×10^{-2} $\underline{M}$ potassium oxalate without iron(III) or acid present. Comparing spectra of the iron(III) perchlorate and potassium oxalate solutions
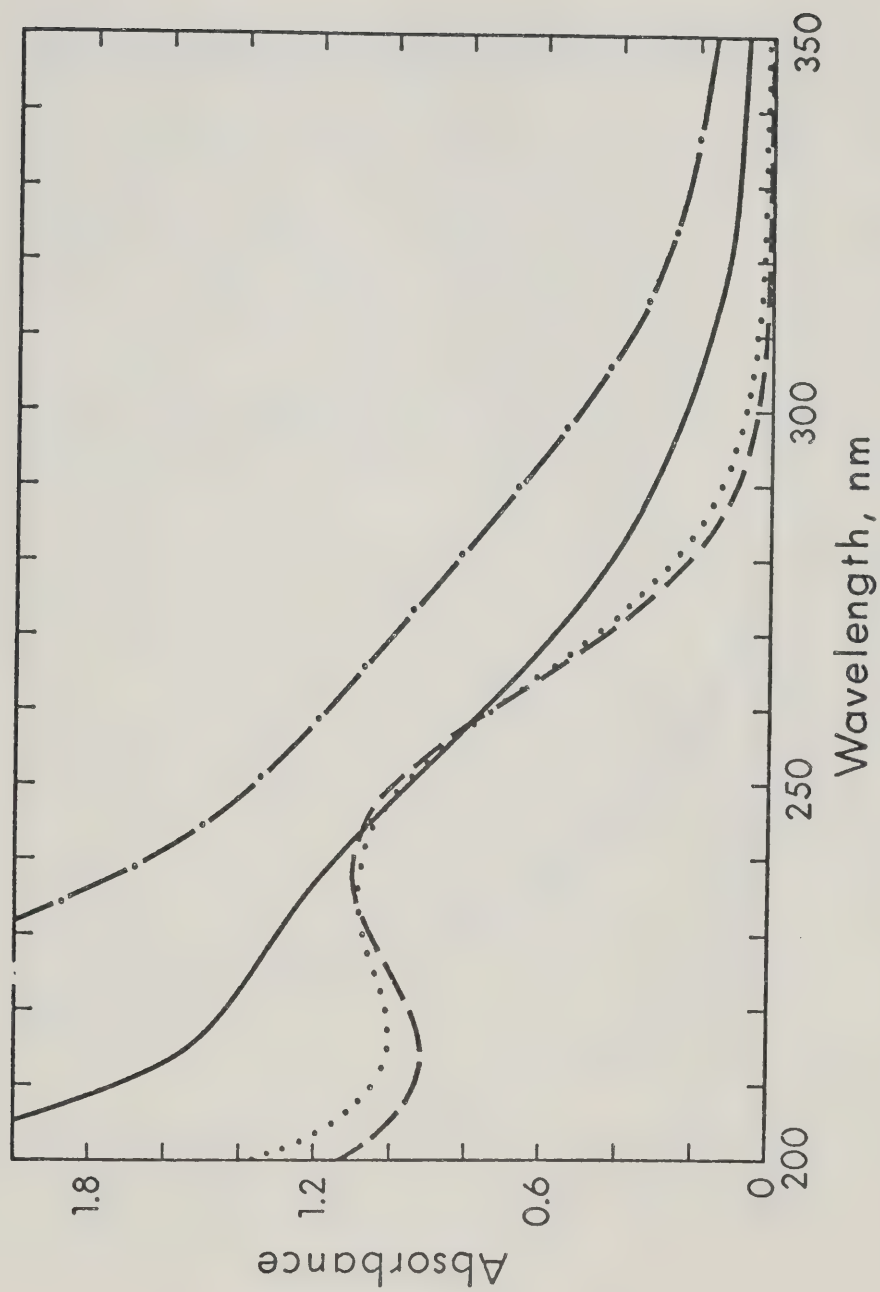
Figure 31 Spectra of Iron(III) Perchlorate in Perchloric Acid with Various Concentrations of Potassium Oxalate. All solutions contain 3.02×10^{-4} $\underline{M}$ Fe(ClO$_4$)$_3$ in 1 $\underline{M}$ HClO$_4$. ————; no oxalate present; ·····, 1×10^{-4} $\underline{M}$ oxalate present; ————, 1×10^{-3} $\underline{M}$ oxalate present; —·—·—, 1×10^{-2} $\underline{M}$ oxalate present.
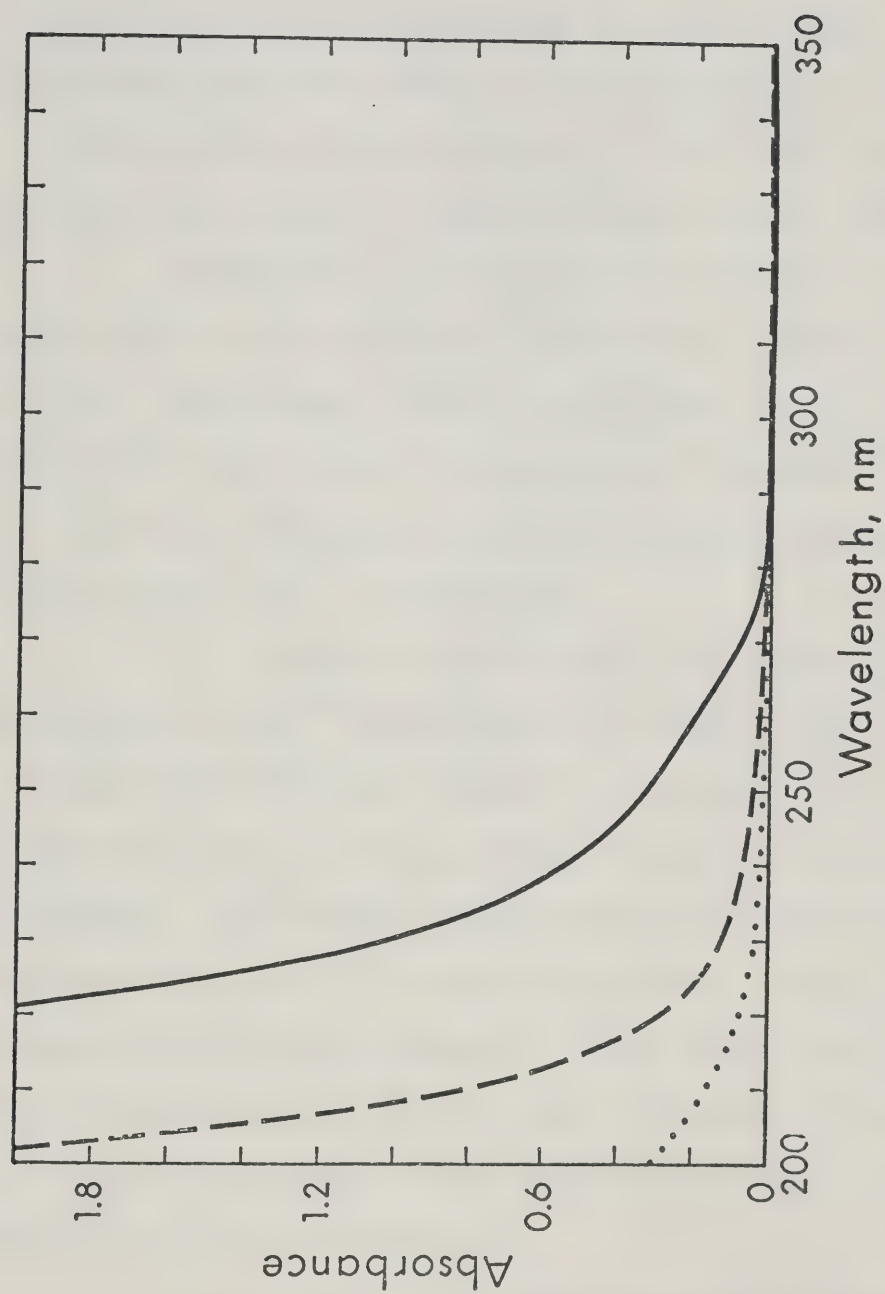
Figure 32 Spectra of Aqueous Potassium Oxalate Solutions.
......, 1x10^{-4} $\underline{M}$ oxalate; — —, 1x10^{-3} $\underline{M}$ oxalate;
———, 1x10^{-2} $\underline{M}$ oxalate.

with those of the mixtures it is evident that the
enhancement must be due to complex formation. No
attempts were made to subtract the absorbance of the
background species from the spectra obtained in Figure 31
to obtain molar absorptivities for the $FeOx^+$ complex
because the amount of complex formed was so small.

When $1x10^{-4}$ $\underline{M}$ citrate and tartrate solutions
were added to an iron(III) perchlorate solution, little,
if any, enhancement in the ultraviolet region was evident.
Therefore the extent to which these compounds interfere
by absorbing radiation in this wavelength region under
these conditions is negligible.

To simulate experimental conditions more
accurately, $1x10^{-4}$ $\underline{M}$ solutions of each of the three
carboxylate salts were added to a solution of iron(III)
ammonium sulfate in 1 $\underline{M}$ sulfuric acid and the spectra
recorded. Very little difference in the spectra as
compared to iron(III) ammonium sulfate with no added
carboxylate salt was apparent. This shows that in relatively
high concentrations of acid the formation of the iron(III)
carboxylate species is low and hence cannot be detected
easily by spectrophotometry.

In an effort to enhance the absorbance of the
iron(III)-carboxylate complexes, the spectrum of a
solution of iron(III) ammonium sulfate in 0.01 $\underline{M}$ sulfuric

acid was recorded. Figure 33 presents this spectrum and similar ones containing 1×10^{-4} and 1×10^{-3} $\underline{M}$ added oxalate. Computer calculations predict that, in a solution containing 3×10^{-4} $\underline{M}$ iron(III) ammonium sulfate, 1×10^{-4} $\underline{M}$ oxalate and 0.01 $\underline{M}$ sulfuric acid, 93.0% of the oxalate is in the form of $FeOx^+$, but that an increase in the level of H_2SO_4 to 1 $\underline{M}$ decreases the fraction of oxalate present as $FeOx^+$ to only 1.65%. For similar citrate and tartrate solutions (3×10^{-4} $\underline{M}$ iron(III) ammonium sulfate, 1×10^{-4} $\underline{M}$ citrate or tartrate, and 0.01 $\underline{M}$ sulfuric acid) the percentage of carboxylate complexed as the monocarboxylateferrate(III) is 90.1 and 40.2% respectively. While slight enhancement of the spectra can be seen for added citrate and tartrate (Figures 34 and 35) it is not as significant as the oxalate enhancement, lending further evidence to the applicability of the determination of oxalate in the presence of other carboxylic acids.
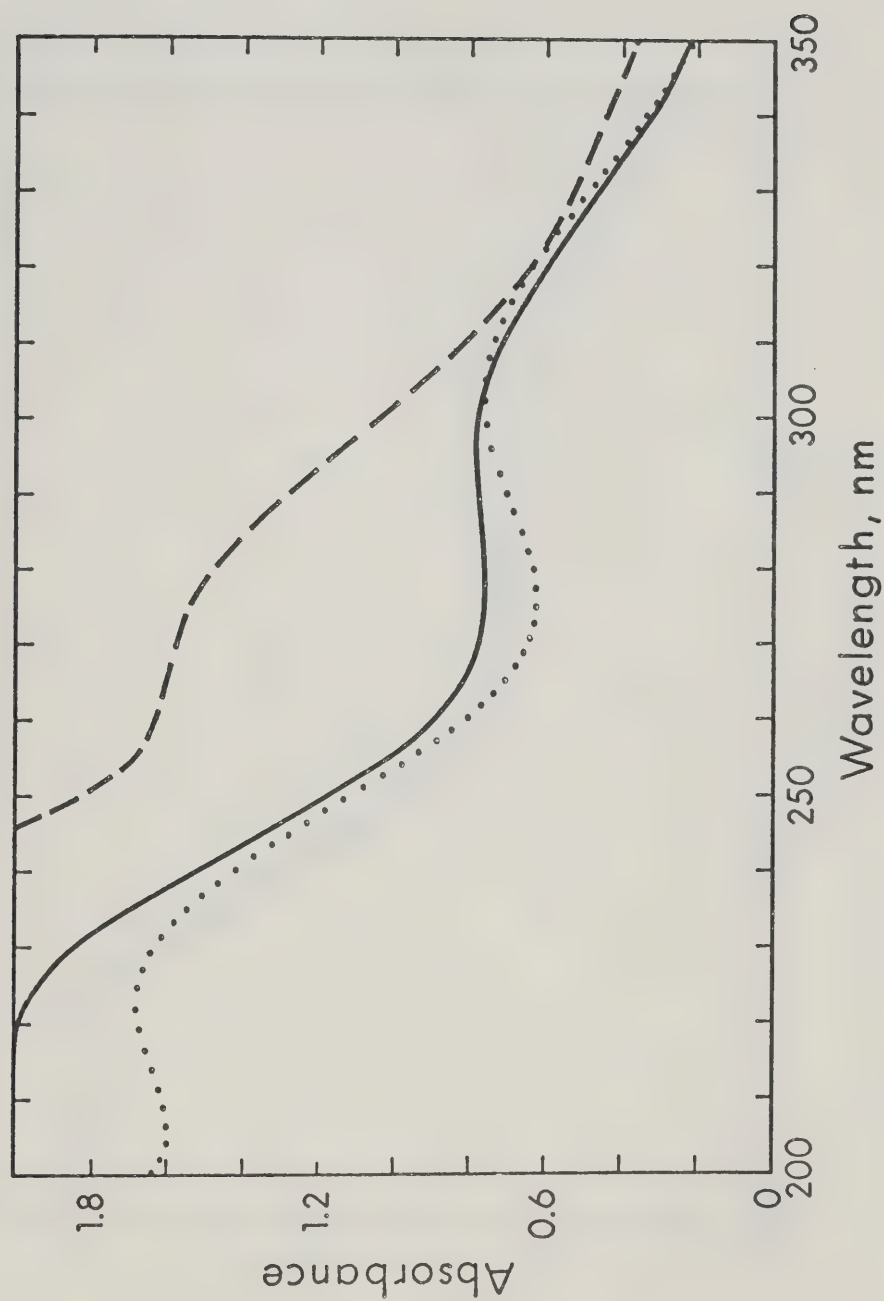
Figure 33   Spectra of Iron(III) Ammonium Sulfate in Sulfuric acid with Various Concentrations of Potassium Oxalate. All solutions contain 3.20×10^{-4} $\underline{M}$ FeNH$_4$(SO$_4$)$_2$ in 1×10^{-2} $\underline{M}$ H$_2$SO$_4$.
·······, no oxalate present; ———, 1×10^{-4} $\underline{M}$ oxalate present; ———— , 1×10^{-3} $\underline{M}$ oxalate present.
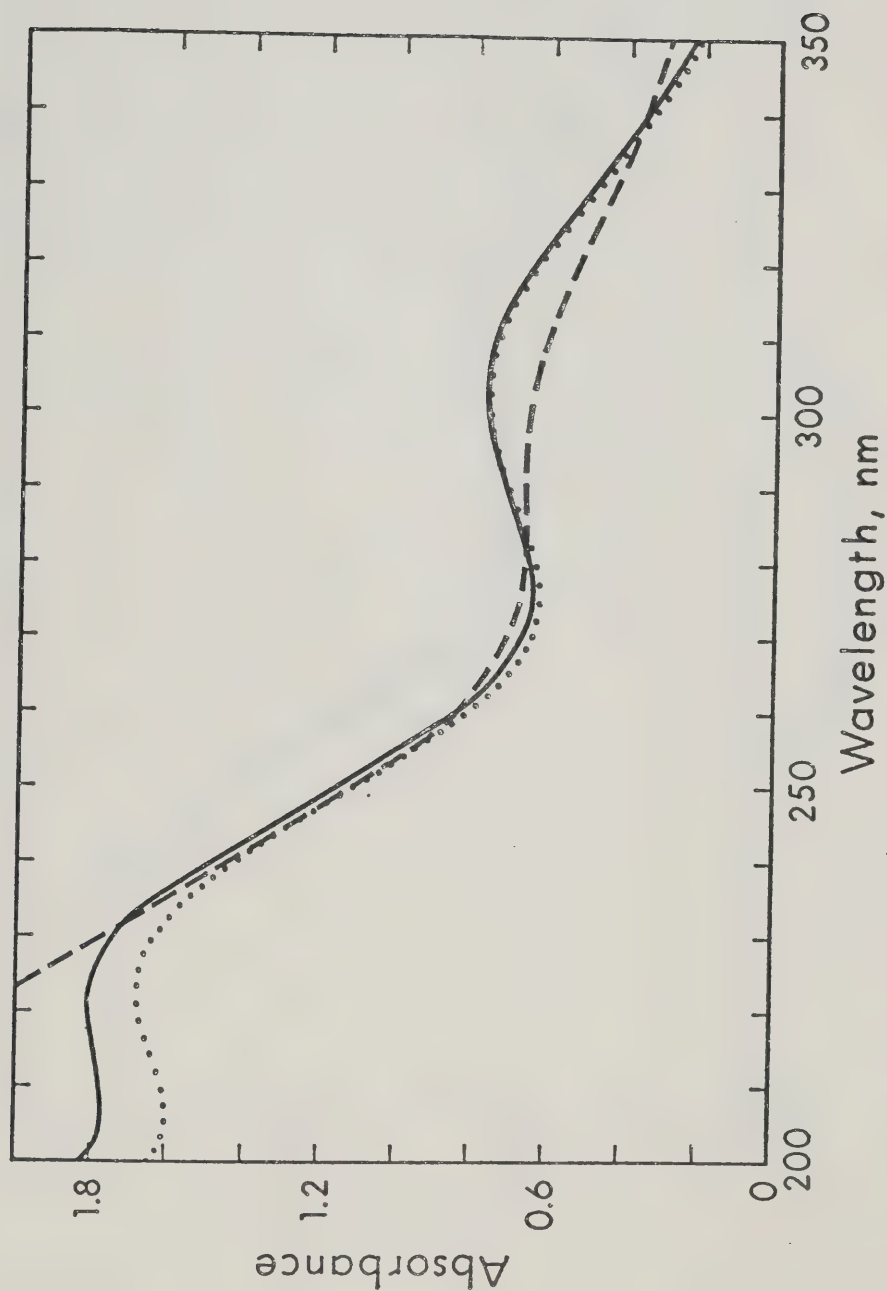
Figure 34 Spectra of Iron(III) Ammonium Sulfate in Sulfuric Acid with Various Concentrations of Sodium Citrate. All solutions contain 3.20×10^{-4} M $FeNH_4(SO_4)_2$ in 1×10^{-2} M H_2SO_4. ·····, no citrate present; ———, 1×10^{-4} M citrate present, ———, 1×10^{-3} M citrate present.
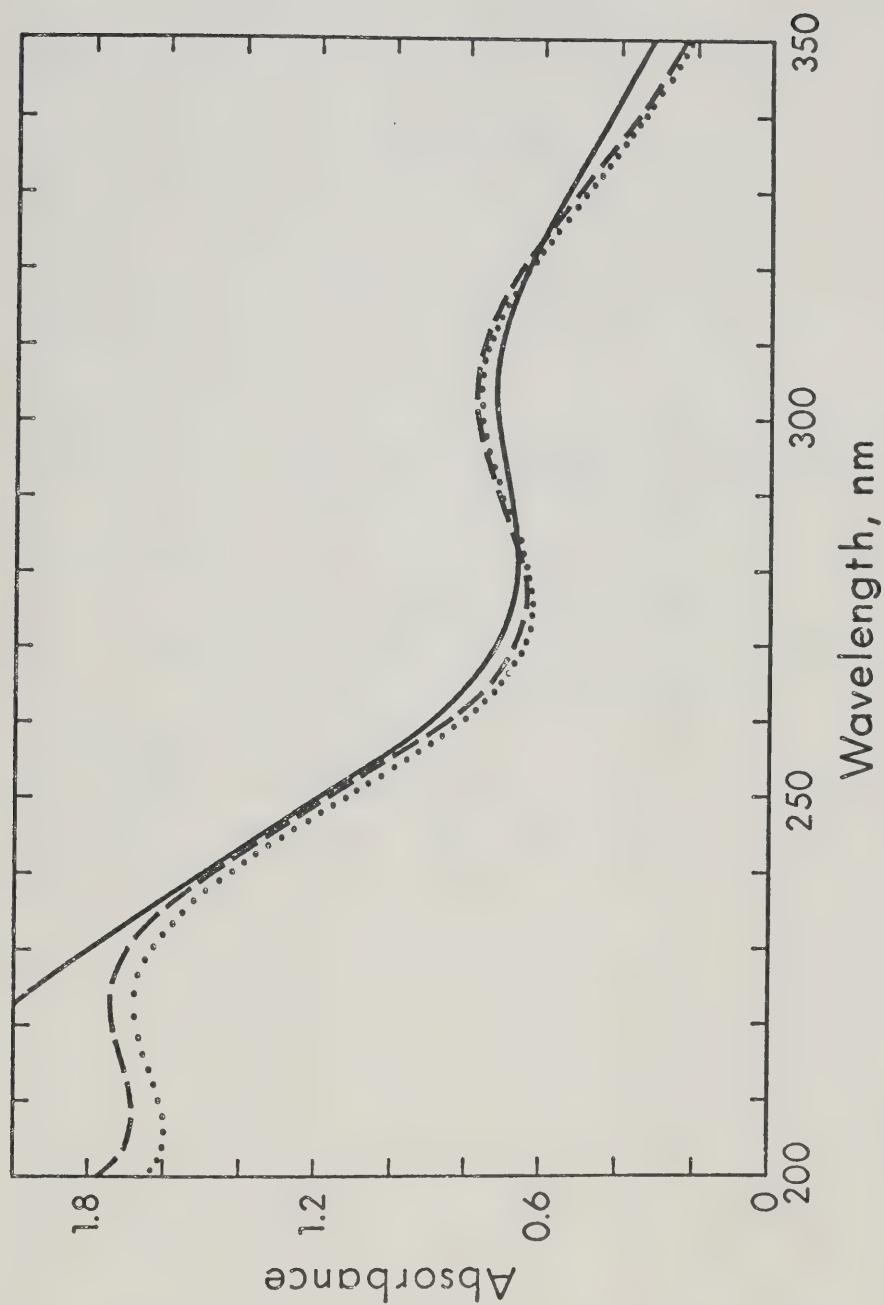
Figure 35 Spectra of Iron(III) Ammonium Sulfate in Sulfuric Acid with
Various Concentrations of Potassium Sodium Tartrate. All
solutions contain 3.20×10^{-4} $\underline{M}$ $FeNH_4(SO_4)_2$ in 1×10^{-2} $\underline{M}$ H_2SO_4.
••••••, no tartrate present; ———, 1×10^{-4} $\underline{M}$ tartrate
present; ———, 1×10^{-3} $\underline{M}$ tartrate present.

SUMMARY

The spectra of solutions of several iron(III) salts and of solutions containing mixtures of iron(III), acid and various carboxylate salts were measured. The importance of optimizing the iron(III):oxalate ratio and of considering the effects of the kind and concentration of acid present when analyzing for oxalate is discussed in light of the spectral and previous information. Having optimized the theoretical conditions _via_ computer calculations in Chapter 3 and spectral analysis in this chapter, the carbon dioxide evolved from irradiated iron(III)-oxalate or iron(III)-carboxylate solutions was measured by a gas chromatographic means in Chapter 5 in an attempt to avoid the drawbacks associated with the pCO_2 gas electrode detection system.

CHAPTER 5

GAS CHROMATOGRAPHIC MEASUREMENT OF CARBON DIOXIDE EVOLVED IN THE IRON(III)-OXALATE REACTION

INTRODUCTION

From the work that was performed using the gas electrode it became evident that the determination of the carbon dioxide produced in the iron(III)-oxalate reaction was a promising approach, but that the pCO_2 gas sensing electrode had several drawbacks. Other methods of analysis for carbon dioxide were therefore evaluated.

Methods for Determination of Carbon Dioxide

Many of the methods discussed below are reviewed by Charlot and Bezier[87].

Titrations. Carbon dioxide (carbonic acid) can be titrated with an alkaline solution to a HCO_3^- endpoint or excess standard base can be added and a back-titration performed. Care must be exercised when titrating that no carbon dioxide is lost to or gained from the atmosphere. Unless a catalyst such as carbonic anhydrase is added the titration must be carried out slowly.

Gas Phase Analysis. An indirect method which has been used to measure carbon dioxide involves bubbling the gas into a solution of sodium hydroxide or of sodium hydroxide

and barium chloride and measuring the resulting conductance. A simple, but not too accurate, method has been suggested based on the measurement of the turbidity of the barium carbonate precipitate formed when carbon dioxide is bubbled through a semisaturated solution of barium chloride.

Carbon dioxide in a gas mixture can be measured by passage into an unbuffered solution of known initial pH, such as a sodium bicarbonate solution. The pH of the resultant solution is then measured with a glass electrode and the carbon dioxide concentration is calculated from the pH change. Alternatively, gas phase carbon dioxide can be measured colorimetrically after absorption into an alkaline carbonate-bicarbonate buffer containing phenolphthalein.

Alkalimeter Methods. An alkalimeter has been used to measure the amount of carbon dioxide, bicarbonate and carbonate in a sample by measurement of the decrease in weight after purging the carbon dioxide evolved upon acidification. Similarly, a direct weight-gain method in which the carbon dioxide is trapped in a tube containing solid alkali can be used.

Infrared Analysis. A nondispersive infrared method has successfully been used in an automated mode to measure gaseous carbon dioxide[88]. Two parallel chambers, one of

which contains the unknown sample and the second of which
contains a carbon dioxide-free sample, precede two smaller
chambers containing pure carbon dioxide. Infrared radiation
passes through both sets of chambers. The difference in
the temperature of the two carbon dioxide chambers, which
is a measure of the amount of carbon dioxide in the sample,
is detected by the displacement of a membrane between the
two. This method requires either separation of the carbon
dioxide into a gaseous phase, or use of a liquid matrix
that absorbs no infrared radiation in the region of
interest.

Manometric and Gas Volume Analysis. Both manometric and
gas volumetric measurements have been made of the carbon
dioxide evolved upon acidification of a solution of the
sample. Neither of these methods is specific for carbon
dioxide since both sense the total amount of gaseous
species produced.

Gas Chromatographic Analysis. Gas chromatography has
been used to measure quantatively gases in liquid samples.
Many different experimental designs have been proposed[89].
A liquid sample can be injected onto a precolumn desiccant
which absorbs the solvent but allows the gases to pass
to and be separated on the chromatographic column. Or,
the water in an aqueous sample can be converted to a

noninterfering substance such as acetylene by reaction with calcium carbide. These methods are of limited use because a small concentrated sample is required. Other methods liberate the gas from solution by boiling the acidified sample, by vacuum extraction, or by passing carrier gas over the agitated sample. The sample vessel can be part of the flow system or the analysis can be performed on the head gas.

With the increasing concern over the presence of organic contaminants in water, many of which are carcinogenic, environmental laboratories have been using gas chromatography, often in combination with mass spectroscopy, to analyze for the volatile constituents of selected waters. Stripping is preferred over liquid extraction for removal of these substances because the reproducibility is better. Furthermore, stripping is more suitable for routine work than liquid extraction[90]. Depending on the kinds of compounds under investigation, the procedure used for stripping may vary from evaporation in a stream of inert gas at room temperature to a steam distillation[91]. One general method is to pass the carrier gas, after trapping impurities in a cold trap, over or through the sample, which can be heated if desired. A salting-out agent such as sodium sulfate can also be used to aid in sample volatilization[92]. The

lower the vapor pressure of the compound, the greater the time necessary for its extraction. Hence, for environmental analysis, stripping time is an important variable. This can be controlled by holding the stripped gases in a closed-loop until the extraction is completed and then introducing a portion of the head gas into the gas chromatograph. Another technique frequently used is to trap the volatiles on an adsorbent at a low temperature and then warm the cold trap to introduce the gases to the gas chromatographic column.

Molecular species in urine have been separated by the latter procedure using programmed-temperature gas chromatography. One hundred and seventy low molecular weight constituents in urine have been resolved[93].

Gas Chromatographic Determination of Carbon Dioxide

The method that was chosen for the analysis of the carbon dioxide evolved from the photochemical iron(III)-oxalate reaction was a gas chromatographic procedure based on that described by Swinnerton, Linnenbom and Cheek[94]. They determined carbon dioxide, among other products, in irradiated solutions and further suggested the general applicability of their method to routine oceanographic and water pollution work. A stream of helium, after passage through a fritted glass disc, stripped the dissolved gases out of the liquid sample and

into a gas chromatographic column. The sample was
introduced into the stripping cell by hypodermic syringe
through an injection port fitted to the top of the cell.
A tube of Drierite between the cell and gas chromatographic
column removed water vapor prior to chromatographic
separation of the carbon dioxide on a column of 30% HMPA
(hexamethylphosphoramide) on 60- to 80-mesh Columpak. A
second column of 60- to 80-mesh Columpak followed by 40-
to 60-mesh Molecular Sieve 13X was used to separate O_2,
N_2, CH_4 and CO. The second column quantitatively absorbed
the carbon dioxide. A thermal conductivity detector was
used. Other workers[95] used this method, modified in that
only one silica gel column was used, to measure carbon
dioxide in sea water and reported a reproducibility of
$\pm$ 0.7%.

Several different columns are suitable for
separating carbon dioxide[96]. A 4 meter long, 4 millimeter
diameter column of 40/60 mesh silica gel at 30°C with an
argon carrier gas flow rate of 60 ml/min will elute
carbon dioxide with a retention time of 15.5 minutes.
Hydrogen, oxygen and nitrogen are eluted in less than 2
minutes. Activated charcoal (75/100 mesh), 0.35 meters
in length and 4 millimeters in diameter, will elute
carbon dioxide in 5 minutes at 40°C when the carrier gas
is nitrogen. Hydrogen is eluted in less than 2 minutes

in this system. Most molecular sieves absorb carbon
dioxide at room temperature and programmed-temperature
gas chromatography must be used to elute the gas.

The gas chromatographic method of analysis is
rapid, especially for a relatively volatile component such
as carbon dioxide, simple, accurate, applicable to small
sample volumes and relatively insensitive to the sample
matrix. Selectivity for carbon dioxide over other
possible interfering volatiles can be assured by proper
choice of the chromatographic column and conditions.

EXPERIMENTAL

Initial Configuration

Because only carbon dioxide was to be measured,
a system similar to that of Park, Kennedy and Dobson[95]
could be used. A stream of helium gas was passed through
a pressure regulator and then to one side of a thermal
conductivity cell (GOW-MAC Instrument Co., Model TR 11B)
which was operated at maximum sensitivity and a filament
current of 220 milliamperes. Stainless steel tubing,
1/16 in. o.d., was used for most connections, being
attached to glass with Kovar seals and to metal with
Swagelok fittings. After passage through one side of a
four-way stopcock the helium was bubbled through a 10- to
20-μm frit in the bottom of an approximately 15-ml sample
compartment (glass blown in the Department of Chemistry
glass shop) and purged gases from the liquid sample.
These solutions were injected into the sample compartment
through a septum on one end of a Swagelok tee. The other
end of the tee was used as an exit for the helium gas,
which next passed through a 1-cm i. d., 30-cm long
column of 8-mesh indicating Drierite (W. A. Hammond
Drierite Company) with pieces of glass wool at either end.
A ground-glass joint near one end of the column facilitated
replacement of the Drierite. The ends of the column were
reduced to 8-mm openings that were fitted with one-hole

silicone rubber stoppers through which 1/16 in. stainless
steel tubing was passed. After the Drierite column the
gas was passed through the second half of the four-way
stopcock to a U-shaped 90 x 0.6 cm i.d. silica gel column
(40- to 60-mesh, Fisher Chemical) via a one-hole silicone
rubber stopper. From the separating column the gas passed
to the second side of the thermal conductivity unit and
thence to a soap-bubble flow meter. A Hewlett-Packard
7101BM strip chart recorder, operated at a chart speed of
15 cm/hr, was used to monitor the readings of the
detector. A maximum sensitivity of 1 mV full scale was
possible with this recorder.

        The four-way stopcock could be positioned so
that the helium gas went directly from the reference side
of the thermal conductivity cell to the silica gel column
or so that its path also included the fritted sample
container and Drierite. With this design a continuous
flow of helium was maintained through the detector so as
to prevent any damage to its filaments. The gas flow rate
dropped sharply when the sample compartment was included
in the flow path because of the resistance to flow of the
porous glass frit in the base of the compartment. The
porosity was selected on the basis of the finest porosity
that, by breaking the gas stream into small bubbles,
would provide high stripping efficiency without providing

too high a resistance to gas flow.

A 5 in. 20-gauge needle was used to inject samples. Attempts to use a syringe and needle to withdraw the samples after analysis were not successful because the high gas pressure in the sample compartment caused the syringe contents to be expelled as soon as the syringe needle was withdrawn from the septum. Therefore the septum was generally removed and samples withdrawn at atmospheric pressure. The air introduced during this procedure was displaced after the septum was replaced by purging with helium carrier gas. Several modifications were made to this initial design; these are discussed before a diagram of the final design is included.

Syringe Chaney Adaptor

Because large uncertainties in sample volumes are introduced when conventional hypodermic syringes are used to deliver volumes of 1 to 5 ml, Chaney adaptors were fitted by the Chemistry Department machine shop to 5-ml and 1-ml syringes.

The design chosen for the 5-ml Chaney adaptor was a flat brass cap which fitted over the top of the Teflon covered plunger. A stainless steel rod used to select the delivery volume passed through the cap and could be adjusted and then held in place with a set screw.

The flared end of the barrel of the syringe was ground down on one side to allow the rod to pass easily beside it when the liquid in the syringe was discharged.

A similar design in stainless steel was used for the 1-ml syringe. Because of its smaller size a stainless steel cap was also placed on the barrel of the syringe to provide adequate area for the rod to rest upon while adjusting the sample volume. A threaded rod of larger diameter than that used on the 5-ml syringe was used to provide more rigidity.

Before each injection the syringe was overfilled with sample, inverted, tapped lightly to displace air bubbles, and then adjusted to the correct volume which was predetermined by the position of the set-screw anchored rod. The syringe needle was then inserted through the septum and the liquid delivered.

Initial Configuration Used for Iron(III)-Oxalate Analysis

Modifications were made to the sample container so that a low pressure Pen-Ray lamp, Model 11SC-1 (Ultra Violet Products Inc.) could be placed into a quartz finger sealed into the sample container. Aluminum foil was placed around the container to minimize photodecomposition of the solution prior to or after irradiation, to reflect ultraviolet light back into the solution and to prevent eye damage. Pen-Ray lamps are small, low

pressure, cold cathode mercury gaseous discharge lamps made of double bore quartz tubing. These cool burning lamps emit approximately 90% of their output as the 254-nm mercury line with the other 10% coming from lines at 313, 365, 405, 436 and 546 nm. The emitting portion of the lamp is 2 1/8 in. long with an outside diameter of 1/4 inch. Although the rated output of the lamp is only 5.5 watts, the lamp was confined in a tube during use, and to minimize possible heating effects, a slow stream of compressed air was passed across the finger entrance near the base of the lamp.

During irradiation of the sample, the helium flow was diverted from the sample chamber. This increased the sensitivity of the method by allowing carbon dioxide to accumulate throughout the entire irradiation for introduction onto the column in a small volume. The volume of solution falling below the frit during a normal irradiation time was small and it could easily be swept back into the sample chamber by the flow of helium. To expedite this return of solution, the volume of the cell below the frit was held to a minimum, and capillary tubing, sloping upward, was used to connect the frit to the four-way stopcock.

With the system designed in this manner, a solution of iron(III) and acid could be introduced into

the sample chamber, followed by a sample solution
containing oxalate. A stream of helium was then passed
through the chamber to displace any carbon dioxide
initially present in the system. The four-way stopcock
was then turned so that the gas flow bypassed the chamber
while the Pen-Ray lamp was irradiating the sample. During
this time carbon dioxide accumulated in the sample cell.
At the conclusion of the irradiation, the four-way stopcock
was turned so that the flow of helium passed through the
fritted sample container carrying the carbon dioxide out
through the Drierite to the gas chromatographic column.

Although many experiments were done with this
experimental set-up, it still possessed several
disadvantages. One was that there was no easy way to
clean the cell. When urine samples were injected into
this system, for example, a yellowish residue accumulated
on the walls, especially just above the liquid level. A
variety of cleaning solutions, including acids, Contrad 70
and dichromate, did not remove the material. It acted
as a filter and lowered the amount of irradiation reaching
the sample, and also caused the stripping efficiency to
vary from sample to sample. Therefore, a new cell was
designed which would allow disassembly for cleaning.

Modified Sample Container

A ground-glass joint was incorporated initially into the sample compartment to permit dissembly for cleaning. However, the pressure of the flowing helium was so great that an adequate seal was impossible to obtain. This was replaced, therefore, with an O-ring joint and number 35 clamp. Another modification that simplified dissembly of the sample cell was the inclusion of Cheminert fittings (Chromatronix, Inc.) to join the gas inlet at the bottom of the sample container to the four-way stopcock. The basic fitting of the Cheminert system is a "tube end fitting" consisting of a threaded polypropylene bushing, rubber spring washer and two stainless steel washers. Tubing is inserted through these parts and the end of the tubing is flanged at right angles. Using Cheminert fittings, small diameter Teflon tubing can be joined to capillary glass that has been modified with an external groove to accept the fittings. With this arrangement the sample cell could be removed readily from the system by disconnecting the silicone stopper fitting at the Drierite column inlet and the Cheminert fitting below the sample chamber. During dissembly the helium flow was diverted from the sample cell and Drierite.

One further modification was a new method of injection and removal of samples. Previously, it was necessary to take off the septum and remove the analyzed solutions with a syringe. Because of the possibility of incomplete reaction when oxalate was analyzed, each sample was removed before a new one was irradiated. Thus, oxalate analyses were quite slow since the air had to be flushed out prior to each irradiation. In the new design an inlet tube was placed just above the frit. A serum cap fitted over this tube served as the septum for sample injection. With this arrangement a ½ in. 26 gauge needle could be used with the Chaney-adapted syringes to introduce the samples. An injection error occurred in this system when the syringe was withdrawn from the serum cap after injection of the sample. A small drop of solution emerged on the needle tip, apparently because of the high pressure inside the cell. However, this error was not large. A 1½ in. 22-gauge needle epoxyed into a piece of rubber tubing was used to remove samples after completion of each analysis. The needle was inserted through the septum to the frit and the internal pressure in the cell forced the liquid out the tube into a waste beaker.

In this new diagram the o.d. of the quartz finger, which was situated as close as possible to the

frit, was increased to 1.5 cm. The i.d. of the sample container remained 2.3 cm. The increased volume of the quartz tube meant that the volume of the sample chamber was decreased. As a result, the height of solution in the cell was greater than before, and the area of solution exposed to irradiation was increased. This provided more efficient decomposition of oxalate. Most analyses were performed using 5 ml of oxalate sample solution and 1 ml of an acidified iron(III) solution, i.e., using the 5 and 1 ml syringes to their maximum capacity to minimize injection errors.

The final design that was used for analysis, including a new position of the Drierite (discussed in the Results and Discussion Section), is given in Figure 36.

The peaks obtained with this system were very sharp and consequently peak heights were measured rather than areas. In the diagrams which follow the peak heights were obtained at or corrected to a recorder range of 1 mV per 25 cm.

Regent grade chemicals and distilled water were used as received.
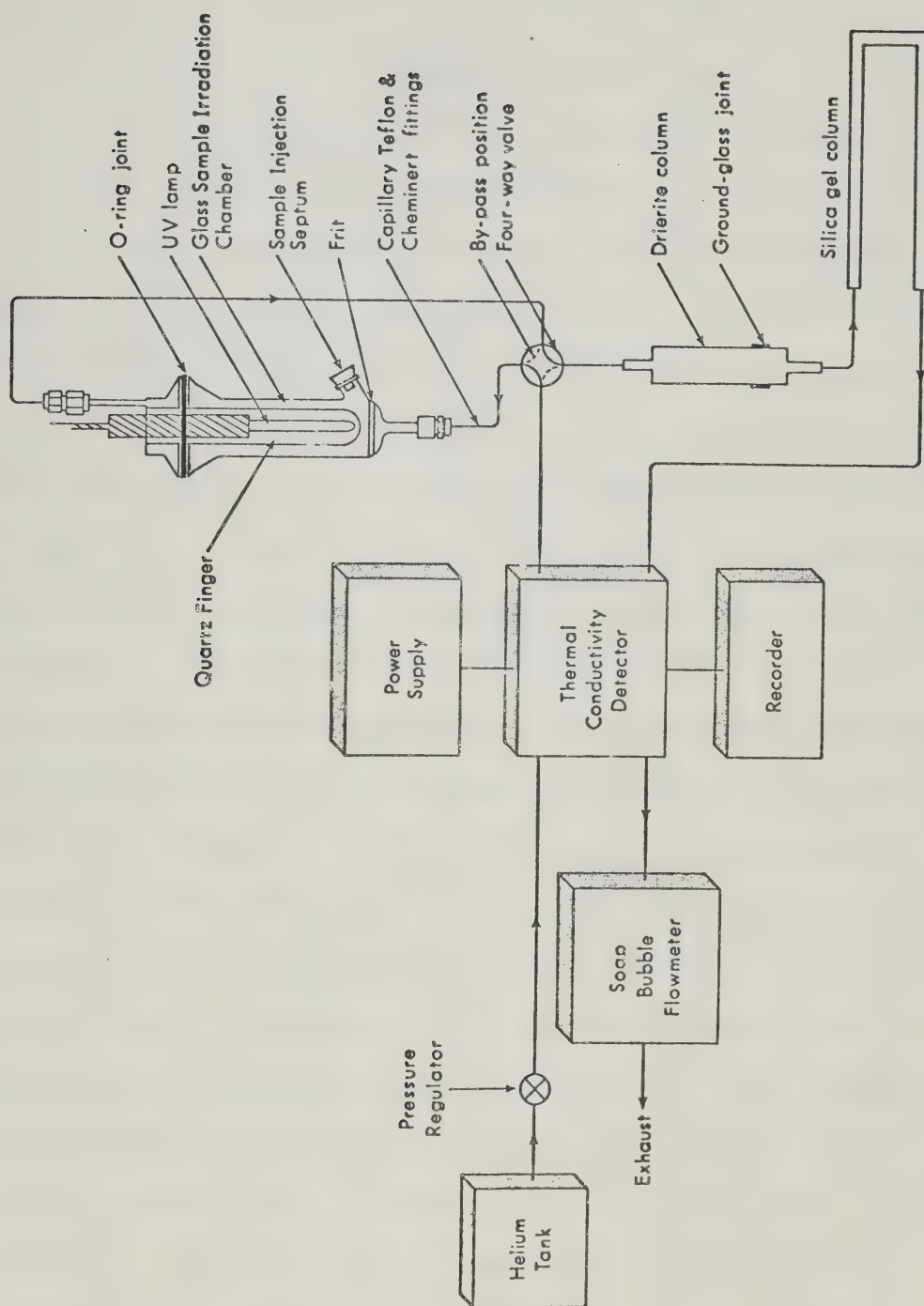
Figure 36 Apparatus for Determination of Oxalate by Gas Chromatographic Measurement of Carbon Dioxide generated by Photolytic Decomposition of Iron(III)-Oxalate.

RESULTS AND DISCUSSION

Method of Injection

The pCO_2 electrode responds to the concentration (partial pressure) of carbon dioxide in a sample and not to the absolute amount present, as the gas chromatograph does. Thus, in the latter method of analysis the method and volume of injection of the samples are critical. Initially, the volume between two air bubbles in a syringe was used as a measure of the amount of solution injected, but with this technique the air passed through the system quickly, emerging as a peak before the carbon dioxide. Because of the magnitude of the air peak obtained with this procedure, often time was insufficient for a baseline to be reestablished before the carbon dioxide emerged. Another injection technique which was tried involved filling the syringe and needle with solution without air bubbles present. This method involved a large error in adjusting the syringe volume before each injection. Further errors arose in that the plunger had to be firmly held while injecting the needle through the septum because of the high pressure inside the sample chamber. However, if it were held too firmly some sample was lost from the needle tip before it passed through the septum. Conversely, if it were not held

firmly enough, helium from the sample chamber entered the barrel and caused a small increase in the volume of sample injected due to displacement by helium of that portion of the sample which usually remained in the needle.

Considerable improvement to the injection technique was seen on addition of Chaney adaptors to the syringe. The relative standard deviation for five measurements of the weight of 5 ml of water delivered from one 5-ml syringe decreased from 0.254% before to 0.038% after incorporation of the Chaney adaptor. For six measurements of the weight of 1 ml of water delivered with the Chaney-adapted 1-ml syringe the relative standard deviation was 0.101%. The improvement in accuracy during analysis was more significant because loss or gain of sample before injection was minimized.

Bicarbonate Analysis

To test the system initially, acidified samples of bicarbonate were injected without the use of the Chaney adaptor. Reproducibility of $\pm$ 5% could be achieved by introducing acid to the sample chamber, purging to remove any air, and then adding a solution of known concentration of bicarbonate to generate the carbon dioxide in situ. In one trial, sets of two or three 1×10^{-3} and 1×10^{-4} $\underline{M}$ bicarbonate samples were run alternately. A relative error of 2% for the first and 4.5% for the second concentration

was observed. This indicated that sample carryover and
interaction between subsequent samples were not a problem
in this system.

Linear calibrations over all concentration ranges
could be obtained. Since background carbon dioxide was
not removed from the distilled water this did, however,
restrict the lower limit of the calibrations. This
background was not a problem with oxalate analysis as
the iron(III) and oxalate solutions could be introduced
into the system and any residual carbon dioxide displaced
by the carrier gas before irradiation. Since the
bicarbonate reacted immediately with the acid to produce
carbon dioxide, an initial purging of the total solution
in the cell could not be done for the bicarbonate analysis.
Although the distilled water used to prepare bicarbonate
samples could be made carbon dioxide-free by boiling or
purging before use, the oxalate method was still found
to be easier and since oxalate was the species of
analytical interest, time was not spent trying to
perfect the bicarbonate analysis at low concentrations.

Oxalate Analysis

Before the quartz finger was incorporated into
the experimental design the only way to analyze for low
concentrations of oxalate was in a continuous-flow mode
using AutoAnalyzer components. The experiment was run as

described in Chapter 2 except that instead of flowing
under a $\underline{p}CO_2$ electrode the irradiated solutions were
collected in small jars, one jar for each sample, then
injected into the purging unit for carbon dioxide measure-
ment. Reproducibilities of $\pm$ 10% could be obtained for
samples of 1 ml of an irradiated 5×10^{-4} $\underline{M}$ oxalate solution or
of $\pm$ 3.3% for a 2-ml sample of 7.5×10^{-4} $\underline{M}$ oxalate solution.

Residual Carbon Dioxide Problem. Most oxalate analyses,
however, were performed using the quartz finger and
Pen-Ray lamp. This system worked well except that acidified
distilled water seemed to contain a relatively constant
residual amount of carbon dioxide which appeared after
each irradiation and purging. Similarly, when a dilute
solution of oxalate, iron(III) and acid was analyzed,
apparent carbon dioxide peaks of about the same size were
obtained under three different sets of conditions. These
were: (1) diverting the helium flow so as to bypass the
sample chamber and Drierite tube for several minutes;
(2) diverting the helium flow for the same length of time
while irradiating the sample; and (3) using the same
sample again and diverting the carrier gas flow from the
solution for the same length of time. As the time the
sample chamber and Drierite were isolated from the flow
was increased, the size of the carbon dioxide peak
increased, independent of whether the lamp was on or the

sample had been previously cycled.

Efficiency of Stripping. One possible explanation for
this behavior was that the stripping of the carbon dioxide
from the solution was not 100% efficient. To test this
hypothesis a second, nonstripping method of injection of
carbon dioxide samples into the system was tried. An
Aerograph heated gas chromatographic inlet equipped with
a Hot Watt 120 Volt-100 watt pencil heater was inserted
into the system between the sample chamber and Drierite
tube. The inlet temperature was set at about 220°C with
a Variac-controlled resistance heater. With this arrangement
small volumes of concentrated bicarbonate solutions could
be injected into the heated inlet, the sample plus
solvent vaporized, and the carbon dioxide produced from
bicarbonate decomposition,

$$2NaHCO_3 \xrightarrow{\Delta} Na_2CO_3 + CO_2 + H_2O$$
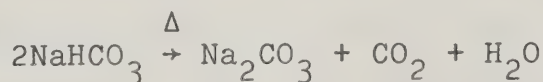
carried to the chromatographic column and detector.

Samples of 0.5 and 1.0 $\underline{M}$ $NaHCO_3$ solutions were
injected into the heated inlet with a 5-µl Unimetrics
syringe. Similarly a Chaney-adapted 5-ml syringe was
used to inject 2.5×10^{-4} and 5×10^{-5} $\underline{M}$ $NaHCO_3$ solutions
into an acid solution in the stripping chamber. The
total millimoles of carbon dioxide produced in each

system should be the same if both are 100% efficient in introducing carbon dioxide to the chromatographic column. However, the stripping method gave slightly higher peaks. The presence of residual carbon dioxide in the much larger solution volumes that were used in the stripping method accounted for this difference. When boiled, then cooled, water was used to prepare the sodium bicarbonate solutions the results of the heating and stripping experiments were comparable. Thus, the persistancy of the carbon dioxide peak was not due to incomplete stripping.

Effect of the Position of the Drierite. The only component not yet tested, the Drierite column, was then checked by moving it so that it was located outside the sample cell loop. Helium then flowed continuously through the Drierite whether the sample cell was in or out of the flow stream. With this arrangement the extraneous peaks disappeared, indicating that they could have been the result of adsorption and desorption of carbon dioxide on the Drierite. Additional support for this explanation was provided by the observation that when acidified iron(III)-oxalate solutions were irradiated for times from one to twenty minutes, more carbon dioxide appeared to be given off as the irradiation time was increased. Even at 20 minutes irradiation time

a plateauing of the amount of carbon dioxide given off was not evident. The primary reason for this was not because of incomplete reaction but because adsorption and desorption of carbon dioxide on the Drierite produced larger peaks as the time the Drierite was isolated from the helium stream increased.

Another indicator of this adsorption/desorption phenomenon was the gradual shift of the baseline throughout a set of experiments. Although before and after an analysis a straight baseline was obtained, that after the analysis was slightly higher possibly because of a constant bleeding of carbon dioxide from the Drierite. This was one reason why peak heights rather than peak areas were chosen to analyse the results. With a continuous flow of helium passing through the Drierite, baseline shift was not as severe.

In this new position the Drierite had to be changed more often and was replaced each day with material that had been dried for 1 to 2 days at 200°C.

Percentage Reaction. A 5-minute irradiation time was chosen for most analyses. Although not sufficient for complete conversion of the oxalate to carbon dioxide it was selected as a compromise between the extent of reaction needed to obtain satisfactory results and analysis time. This time was chosen after a series of measurements in

which 5 ml of a 1.01×10^{-4} M potassium oxalate solution
was irradiated in the presence of 1 ml of 1.13×10^{-3} M
iron(III) ammonium sulfate in 0.6 M HCl for varying times.
Table 12 gives the percentage reaction, assuming that a
20-minute irradiation gave 100% conversion of oxalate to
carbon dioxide. From this table it is evident that the
rate of carbon dioxide generation is rapid at the
beginning of the reaction, then declines. Thus, after a
5 minute irradiation, over 90% of the oxalate has reacted
and the remaining oxalate reacts only slowly. Some
variation in irradiation time after 5 minutes will not
lead to large errors in oxalate concentration. A
disadvantage of longer irradiation times is that the
temperature of the iron-oxalate solutions is increased
due to heating from the Pen-Ray lamp. This increases the
possibility of seepage of solution below the frit as the
gas in the cell expands due to the higher temperature.

Increase in the Speed of Analysis. Air accompanied the
introduction of each oxalate sample into the irradiation
cell because the septum was removed and/or because of
dissolved gases in the solution. Before the position of
the Drierite was changed, more reproducible results were
obtained if the irradiation step was postponed until the
carbon dioxide from the air was measured by the detector.

TABLE 12

Percentage Reaction of an Iron-Oxalate
Solution as a Function of Time

Time, in minutes	Percentage Reaction[a]
½	62
1	76
2	83
3	88
6	95
10	98
15	99
20	100

[a]Based on assumption that a 20-minute irradiation
gives 100% conversion of oxalate to carbon dioxide.
Five ml of 1.01×10^{-4} $\underline{M}$ potassium oxalate and 1 ml
of 1.13×10^{-3} $\underline{M}$ iron(III) ammonium sulfate in 0.6 $\underline{M}$
hydrochloric acid were used.

In the new design this waiting period was no longer necessary. After sample injection, purging with helium was necessary only until the oxygen and nitrogen peaks appeared on the recorder; at this point the helium flow could be set to bypass the cell and irradiation could be started. During this step the carbon dioxide in the Drierite and silica gel columns was purged from the system. This procedure increased the speed of analysis because the oxygen and nitrogen peaks emerged in a minute or two but the carbon dioxide peak took about 15 minutes (depending on the flow rate used).

Effect of Helium Flow Rate. After many analyses the initial section of the Drierite became hydrated and the flow rate of helium decreased. When the Drierite column was located immediately behind the sample cell in the samply loop this was a particular problem as the desiccant caked appreciably. However, the final procedure adopted relieved this problem, either because the changed position of the Drierite allowed the continual flow of helium to distribute the water more evenly over the length of the column or because fresh Drierite was substituted into the system each day. The seriousness of the initial problem can be appreciated from Figure 37, a graph of flow rate versus peak height which was obtained with the Drierite in its initial position
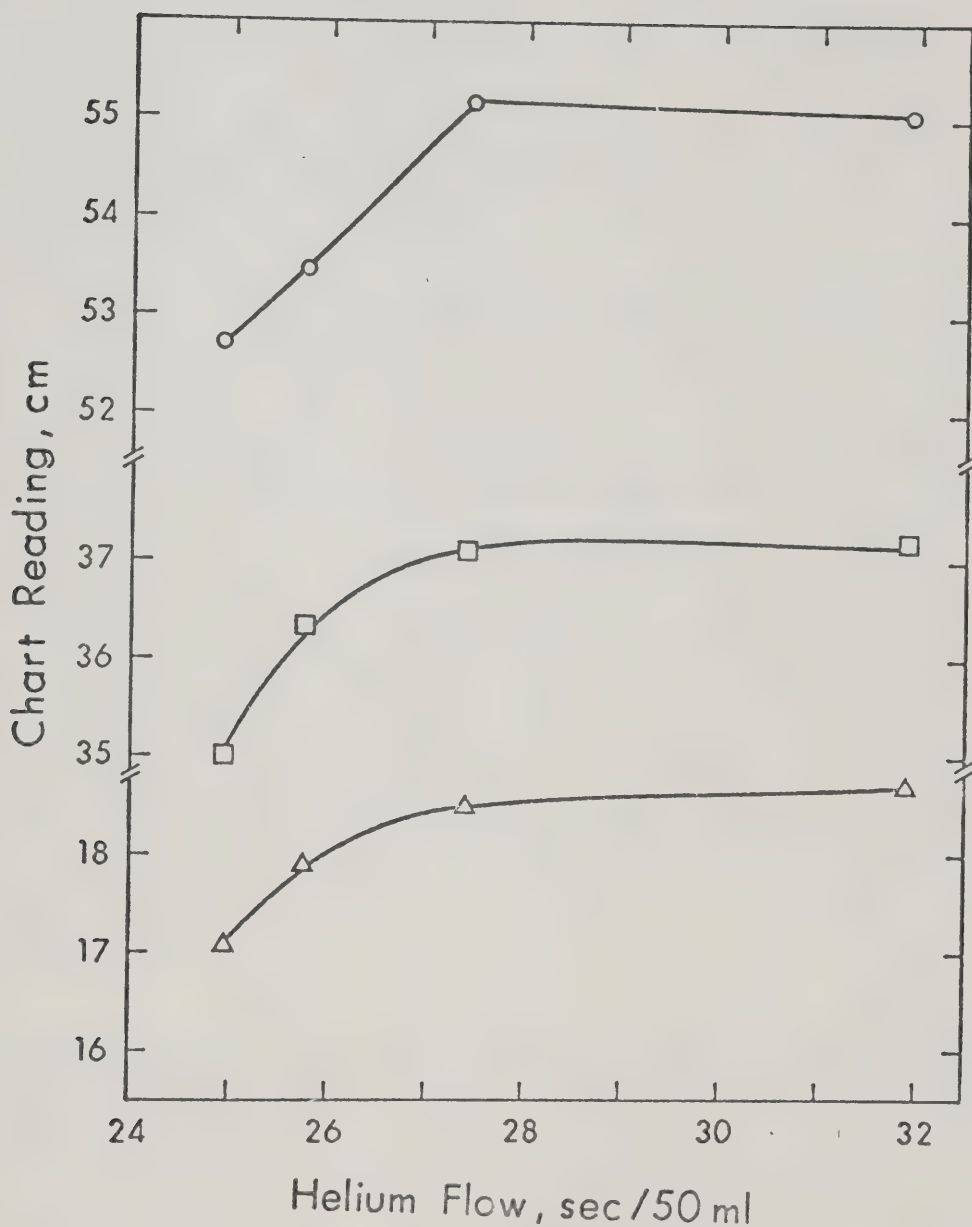
Figure 37   Plot of Detector Response to Carbon
Dioxide versus Flow for Three
Oxalate Samples: o $3x10^{-4}$ $\underline{M}$ Ox,
□ $2x10^{-4}$ $\underline{M}$ Ox, △ $1x10^{-4}$ $\underline{M}$ Ox.

immediately behind the sample compartment in the sample
loop. With decreasing flow rate the peak height
increased. A flow rate of 28 sec/50 ml or slower was
optimum in the sense that slight changes in flow rate did
not produce major changes in peak height. This was
confirmed experimentally using 5 ml of $1x10^{-4}$ $\underline{M}$ oxalate
with 1 ml of $3.14x10^{-3}$ $\underline{M}$ iron(III) ammonium sulfate in
4 $\underline{M}$ H_2SO_4. At a flow rate of 21 sec/50 ml the relative
standard deviation for 4 analyses was 5.11% while at a
flow rate of 26 sec/50 ml it was 2.80% and at 35 sec/50 ml
it was only 0.87%. However, most analyses were performed
at a faster flow rate so the peaks would emerge in less
time. Perturbations in flow rate, such as that introduced
when the flow path of the helium was changed to include
or omit the sample chamber, were evident on the recorder.
But, the time necessary for equilibrium to be reestablished
was very short.

Radiation Source. The gas electrode work was performed
using a medium pressure 140-watt Hanovia lamp while the
gas chromatographic experiments used a low pressure
5.5 watt Pen-Ray lamp. These lamps differ, not only in
wattage but in spectral output, the low pressure lamp
having its major wavelength of output at 254 nm, and the
medium pressure lamp at 365 to 366 nm. The effect of
wattage on the amount of carbon dioxide generated was

investigated in Chapter 2. To ascertain the importance
of the wavelength of the radiation, a second Pen-Ray lamp,
Model 11SC-1L, was obtained and studied. This lamp was
the same as the low pressure model but contained, in
addition, a fluorescent sleeve and filter that absorbed
visible light and converted the 254 nm radiation to a
band peaking at 366 nm. The diameter of this lamp, 3/8
inch, was larger than the 1/4 inch diameter of the low
pressure lamp. Table 13 shows results of a comparison of
the two lamps. It is seen that at sulfuric acid molarities
below about 1 $\underline{M}$ the amount of carbon dioxide produced
was approximately the same for both lamps, indicating
that the wavelength of radiation was not critical. The
low pressure lamp was used throughout the remainder of
the work because of greater availability of replacements.

Effect of Acidity. The data in Table 13 were obtained
using 5 ml of oxalate (1.40×10^{-4} $\underline{M}$) in water, 1 ml of
iron(III) ammonium sulfate (2.14×10^{-3} $\underline{M}$) and 1 ml of
sulfuric acid solutions of varying concentration. After
the nitrogen and oxygen peaks emerged, the stopcock was
turned to divert the helium flow while the samples were
irradiated for 15 minutes each. As predicted in the
computer studies, with increasing pH larger amounts of
carbon dioxide were produced. A final acidity of 0.5 $\underline{M}$
or less in sulfuric acid appeared optimum from these data.

TABLE 13

Comparison of Radiation Sources and Effect of
Acid Concentration on Oxalate Analysis

Molarity of added H_2SO_4 [a]	Final Molarity in H_2SO_4 [b]	Recorder Peak Height[c], cm	
		Model 11SC-1 (254 nm)	Model 11SC-1L (366 nm)
7	1.001	19.10	12.82
3.5	0.501	23.00	21.54
0.7	0.101	24.40	24.82
0.35	0.0514	25.14	25.88
H_2O	0.00143	26.86	26.28

---

[a] The solution contained 5 ml of 1.40×10^{-4} M oxalate, 1 ml of 2.14×10^{-3} M iron(III) ammonium sulfate and 1 ml of acid of the indicated concentration.

[b] Because the samples were analyzed in the order in the list the actual acidity may be slightly higher due to some residual acid in the cell from the previous analysis.

[c] The solutions were irradiated for 15 minutes.

<u>Temperature Control</u>. Although straight line calibrations
generally were obtained with this system, the
reproducibility was not as good as desired. The carbon
dioxide peak heights usually trended in one direction
during the analysis of a series of oxalate samples of the
same concentration. Furthermore, a sloping baseline that
made it difficult to estimate the peak height accurately
was often evident. Changes in temperature of the
chromatographic column were suspected as the cause so
thermostatting of the silica gel column by immersion in
a large cylinder of water was arranged. The cylinder
was placed on a magnetic stirrer to provide circulation
of water. Heating water, circulated through a three-turn
copper coil immersed in the cylinder and connected to a
Haake R20 circulating thermostat unit, was used to control
the bath temperature. A temperature of 41 to 42°C was
chosen, enough above room temperature to allow adequate
temperature control, but not so high that the carbon
dioxide peak was not well separated from the other gases.
Once equilibrium was established the column water bath
temperature fluctuated by only a few tenths of a degree
over many days of monitoring. A small amount of Sparkleen
was added to the cylinder water to prevent corrosion of
the heating coil, and the top of the cylinder was
insulated with a layer of Fiberglas covered with

aluminum foil to minimize heat loss and water evaporation.
Initially, with no auxiliary heating, the temperature of
the thermal conductivity detector was 41°C. Using a
Variac its temperature was raised above the column
temperature to about 60°C. Although the detector was
insulated, its temperature did not remain as constant as
the column. The reproducibility of successive runs
improved markedly with these changes, although some
baseline drift occurred on occasion. This was attributed
primarily to variability in the detector temperature.

The increase in precision produced by
thermostatting the column can be appreciated by comparing
a set of experiments done before and after the
modification. Five-minute irradiations were done on 5 ml
of potassium oxalate solutions of concentration 1.4×10^{-5},
4.2×10^{-5}, 7.0×10^{-5}, 9.8×10^{-5} and 1.4×10^{-4} $\underline{M}$ in combination
with 1 ml of 2.14×10^{-3} $\underline{M}$ iron(III) ammonium sulfate in
0.01 $\underline{M}$ H_2SO_4. Prior to thermostatting, thirteen
measurements were made in order of increasing, decreasing,
then increasing oxalate concentration. A least squares
analysis of the data gave an overall absolute standard
deviation of fit of the straight line of 1.14 cm chart
reading. A baseline drift was evident. When eleven
solutions (concentrations used were 4.0×10^{-5}, 5.0×10^{-5},
8.0×10^{-5} and 1.0×10^{-4} $\underline{M}$ in oxalate and 2.25×10^{-3} $\underline{M}$

iron(III) ammonium sulfate in 0.1 $\underline{M}$ H_2SO_4) were similarly
run after thermostatting, the overall absolute standard
deviation had decreased to 0.216 cm chart reading and all
points were within 2.2% of the readings obtained for the
initial four oxalate solutions. Thus no hysteresis effect
was observed with the gas chromatographic experiments and
thermostatting the system made a substantial improvement.

Optimization of Iron:Oxalate Ratios. The optimum ratio of
iron(III) to oxalate determined for the $\underline{p}CO_2$ electrode in
Chapter 2 could not be applied to the gas chromatographic
method because in the latter method oxygen was not
available to reoxidize iron(II) to iron(III) and thereby
allow recycling of the iron. Iron(II) is oxidized to
iron(III) in water when irradiated with UV radiation [97]
however, and so the ratio had to be redetermined. For
this purpose a set of seven solutions 0.6 $\underline{M}$ in HCl and
ranging from 0.53 to 5.3×10^{-4} $\underline{M}$ in $FeCl_3$ were prepared.
To 1 ml of each solution in turn was added 5 ml of
1.0×10^{-4} $\underline{M}$ potassium oxalate, the mixture purged of air
with helium and irradiated for 5 minutes. The optimum
Fe:Ox ratio was found to be between 2:1 and 20:1.
Figure 38 shows the effect of Fe:Ox ratio on the
detector signal; it also includes a similar run in which
the $FeCl_3$ in 0.6 $\underline{M}$ HCl was replaced by $FeNH_4(SO_4)_2$ in
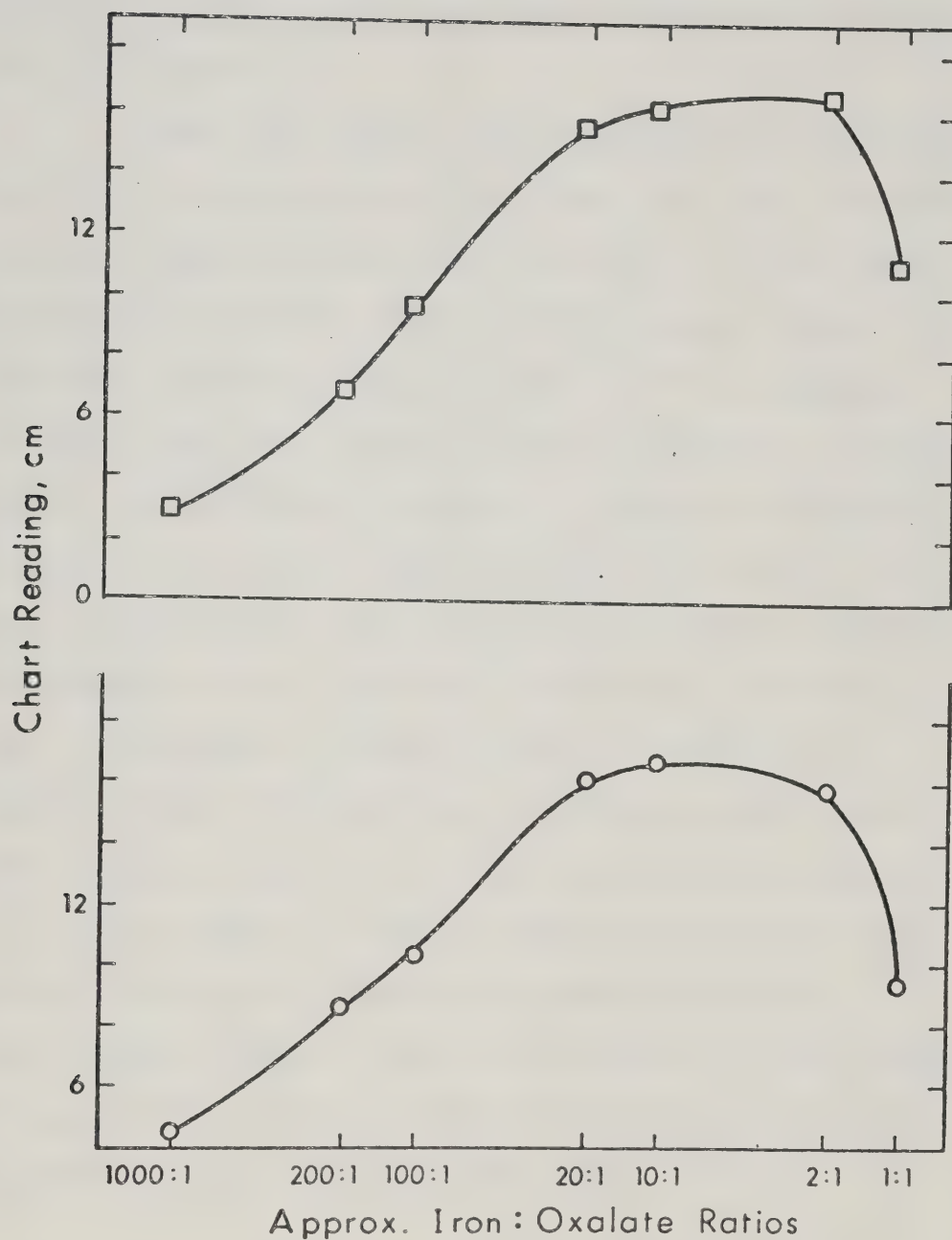
Figure 38 Optimization of the Iron:Oxalate Ratios
for 1×10^{-4} $\underline{M}$ Oxalate: □ in 0.1 $\underline{M}$ HCl;
o in 0.1 $\underline{M}$ $\overline{H}_2SO_4$.

0.6 $\underline{M}$ H_2SO_4. It can be seen that the results for the two acids are similar.

When the oxalate concentration was increased to $1x10^{-3}$ $\underline{M}$ in the presence of the same iron(III) chloride solutions, the 2:1 Fe:Ox ratio appeared to give larger readings than the 10:1 or 20:1 Fe:Ox ratios (Figure 39). A similar result was obtained with $1x10^{-2}$ $\underline{M}$ oxalate. This low Fe:Ox ratio was probably more satisfactory at higher oxalate concentrations because of increased screening of irradiation by higher concentrations of absorbing species. When the experiment with the $1x10^{-3}$ $\underline{M}$ oxalate solution was repeated with a 10-minute irradiation instead of a five, an increase in carbon dioxide evolution was observed under all conditions. Increasing the iron:oxalate ratio slightly above 2:1 did not cause such a dramatic fall in the amount of carbon dioxide given off as was evident with only a 5-minute irradiation period. Iron:oxalate ratios as close as possible to those found optimum in the 5-minute irradiation period were used whenever possible in subsequent work.

Comparison of Hydrochloric and Sulfuric Acids. A comparison was made of hydrochloric and sulfuric acid as the source of hydrogen ions. In Chapter 2 it was found that either acid could be used satisfactority. To
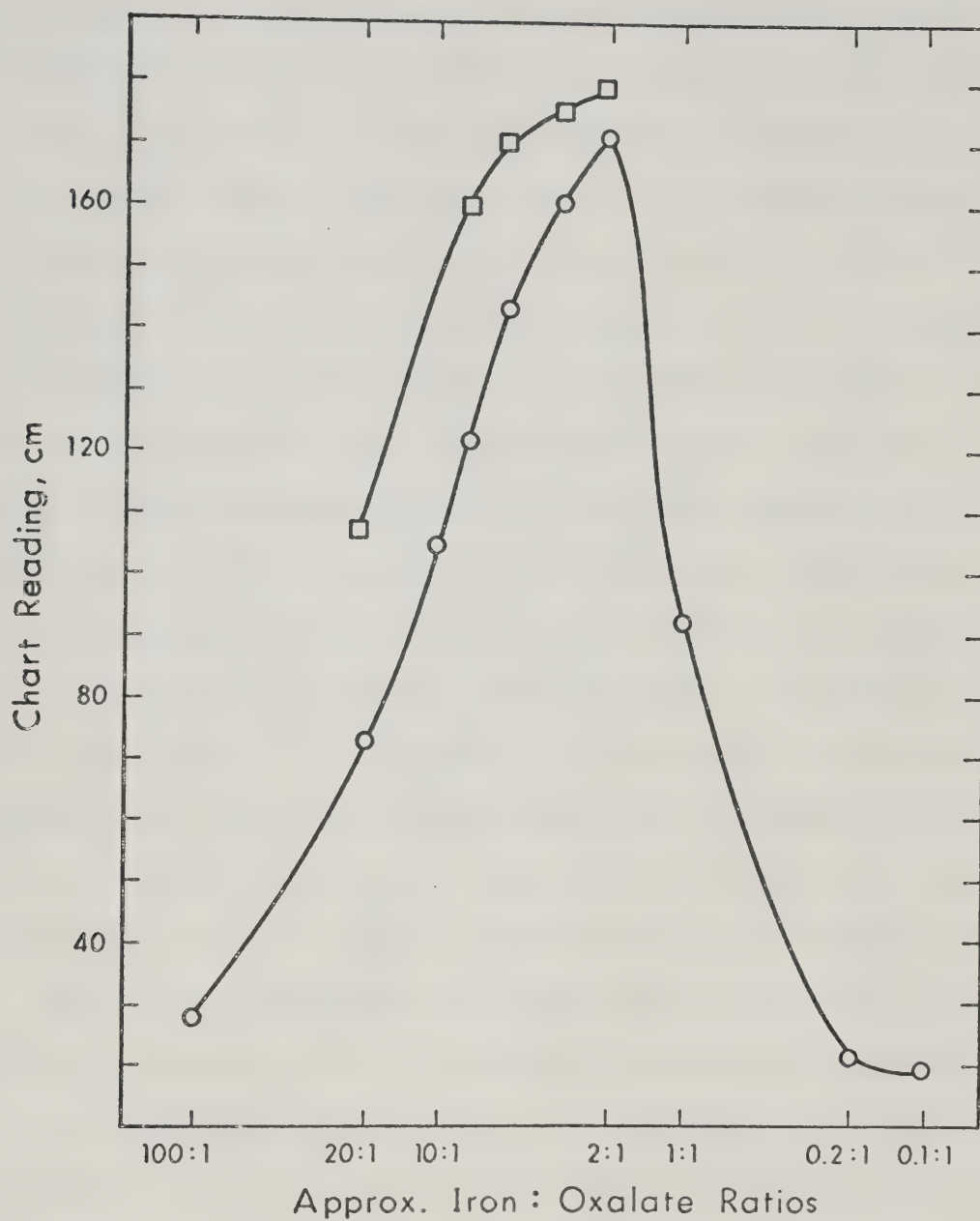
Figure 39 Optimization of the Iron:Oxalate Ratios for 1×10^{-3} $\underline{M}$ Oxalate in 0.1 $\underline{M}$ HCl: ○ 5 minutes irradiation, □ 10 minutes irradiation.

investigate this point in the gas chromatographic method
of detection several runs were made using solutions of
4.61×10^{-3} $\underline{M}$ iron(III) ammonium sulfate in hydrochloric
and sulfuric acids. When the final acid concentration
in a solution containing 5 ml of a 1.01×10^{-4}, 2.02×10^{-4}
or 3.03×10^{-4} $\underline{M}$ oxalate solution added to 1 ml of iron(III)
ammonium sulfate was 0.10 $\underline{M}$ no difference in carbon
dioxide production could be detected between the two
acids. But when the acidity of the final solution was
increased to 0.75 $\underline{M}$, more carbon dioxide was generated
in a 5-minute irradiation in a hydrochloric acid solution
than in a similar sulfuric acid solution. At higher
acidities less of the oxalate is present as the iron(III)
complex, and conditions for production of carbon dioxide
are not optimum. Thus, the experimental results are in
agreement with the computer calculations of Chapter 3 and
4. The results obtained are depicted in Figure 40. At
254 nm, the wavelength of maximum irradiation intensity
for low pressure mercury lamp, the absorbance of iron(III)
chloride solutions is less than that of iron(III) sulfate
solutions; this allows more irradiation to reach the
iron-oxalate complex.

Many of the calibration plots in this study
gave a positive intercept. In all cases the intercept
became larger under conditions where the iron-oxalate
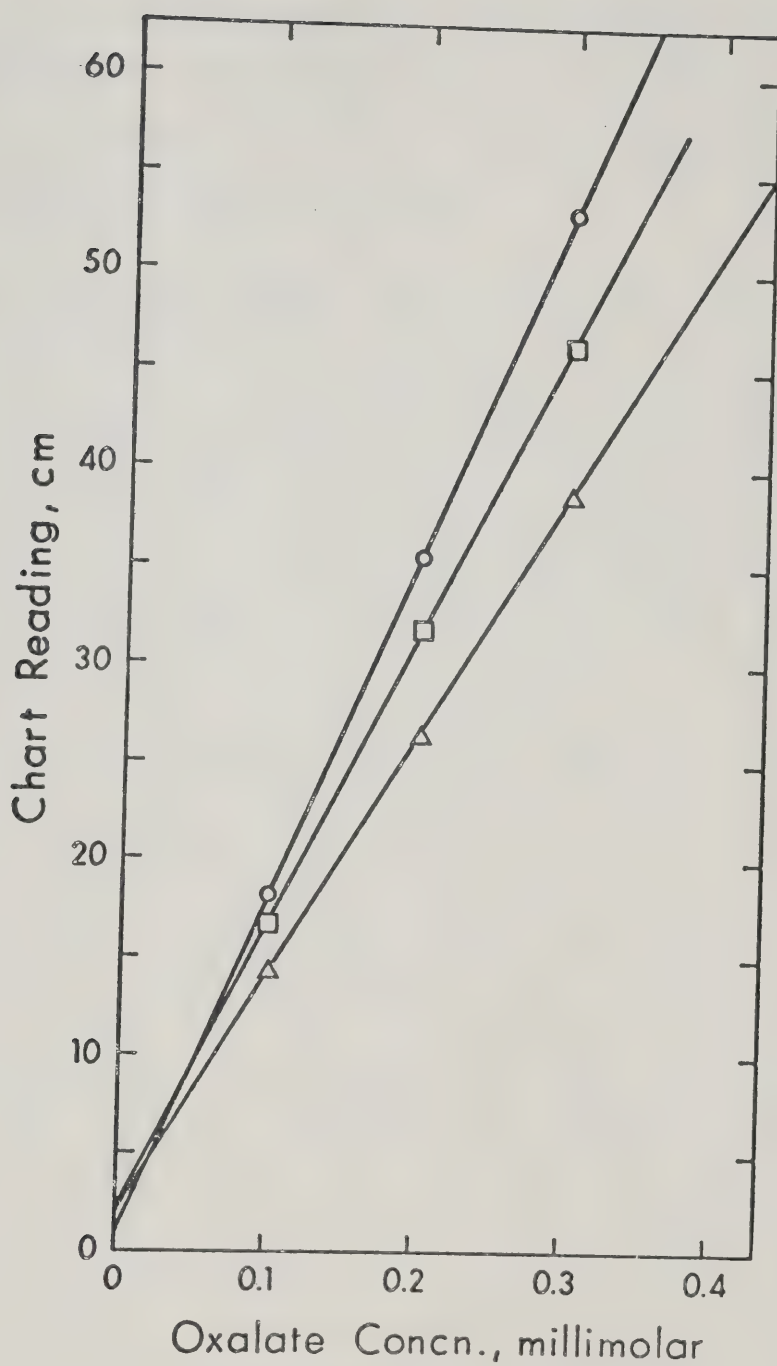
Figure 40   Effect of Concentration of Hydrochloric
            and Sulfuric Acid on the Iron(III)-
            Oxalate Reaction: o 0.10 $\underline{M}$ H_2SO_4 and
            HCl; □ 0.70 $\underline{M}$ HCl, △ 0.70 $\underline{M}$ H_2SO_4.

reaction was less complete. At 100% reaction a straight line calibration through the origin is predicted. This positive intercept leads to an error if standard additions are performed on unknown samples.

Effect of Different Salts. An investigation was undertaken of the effect of different salts and the corresponding increase in ionic strength on the iron-oxalate reaction. Several 5×10^{-4} $\underline{M}$ potassium oxalate solutions were prepared containing up to 0.7 $\underline{M}$ sodium sulfate, sodium chloride or sodium perchlorate. After an initial purge the iron-oxalate solutions were irradiated for 5 minutes and then the carbon dioxide peak heights measured. Since the acidity in the final solution was held constant at 0.36 $\underline{M}$ H_2SO_4 it was the major contributor to the ionic strength, the added salts causing only a small perturbation. In each case the readings for the solutions containing differing amounts of salt are within 4% of the average for the set. Not only was the ionic strength changed slightly, but also there were different complexes formed, each with its own absorptivity. As there was no trend in the readings, it was concluded that random errors were the source of the observed differences in readings. The high acidity (0.36 $\underline{M}$) and the high Fe:Ox ratio (5:1) were both likely reasons for the large random errors, as neither condition was optimum.

Effect of Metal Ions. A number of metal ions, in
addition to iron, react with oxalate. Analytical chemists
have long used the insolubility of calcium oxalate for
gravimetric separation of both calcium and oxalate.
Magnesium oxalate is also insoluble but tends to form
supersaturated solutions. One of the more insoluble
oxalate salts is thorium oxalate. (The logarithm of the
solubility product is -21.38[98].) A complex with aluminum
is also formed by oxalate ions. To investigate the
effect of these metal ions on the iron-oxalate reaction a
1.02×10^{-2} $\underline{M}$ potassium oxalate solution was prepared which
was diluted to give a set of solutions 5.10×10^{-5}, 1.02×10^{-4}
and 2.04×10^{-4} $\underline{M}$ in oxalate. Stock solutions of the metal
ion salts to be tested were also prepared. An approximately
8.60×10^{-3} $\underline{M}$ solution of $CaCl_2 \cdot 6H_2O$ was prepared. The
nitrate salt was not chosen because of the oxidizing
power of nitrate ion in acid solution. Stock magnesium
solution was prepared as 9.91×10^{-3} $\underline{M}$ $MgCl_2 \cdot 6H_2O$ and the
aluminum solution was 5.00×10^{-3} $\underline{M}$ $Al_2(SO_4)_3 \cdot K_2SO_4 \cdot 2H_2O$.
The B.D.H. thorium chloride label did not specify the
number of waters of hydration present, but The Merck
Index[56] says that generally thorium chloride is hydrated
with 7 to 9 moles of water. Therefore, 100 ml of
solution containing 0.5085 g of the B.D.H. material was
prepared. Assuming a molecular weight of 500, the

molarity of this solution is 1.02×10^{-2} $\underline{M}$. Each metal

ion stock solution was diluted by a factor of ten twice

to give a final solution 100 times more dilute. An

iron(III) ammonium sulfate solution (1.52×10^{-3} $\underline{M}$) in

0.7 $\underline{M}$ H_2SO_4 was used as the source of iron(III). A

standard oxalate calibration plot was prepared by

injecting into the sample chamber 1 ml of the iron(III)

solution, 2.5 ml water and then 2.5 ml of the oxalate

solution. After removal of the residual gases by

purging with helium, the solution was irradiated for

5 minutes. To test for interference by metal ions 1 ml

of the iron(III) solution was injected into the sample

chamber, followed by 2.5 ml of metal ion stock solution

and lastly 2.5 ml of 2.04×10^{-4} $\underline{M}$ oxalate solution. The

results obtained are shown in Table 14. An oxalate

calibration was repeated between the test for aluminum

and thorium interference; it showed a slight downward

shift in carbon dioxide signal, likely due to oxalate

instability. This change was taken into account when

calculating the extent of interference. From the table

it can be seen that calcium and magnesium ions present no

interference at concentrations up to approximately 50

times that of oxalate. At the higher concentrations

aluminum and thorium ions cause a decrease in the amount

of carbon dioxide measured. If these ions were in a

TABLE 14

Effect of Foreign Ions on the
Iron(III)-Oxalate Reaction

Metal Ion	Ratio, Metal Ion:Oxalate[a]	% Interference
Ca^{+2}	0.4:1	< 1
	4:1	< 1
	40:1	< 1
Mg^{+2}	0.49:1	~ 1
	4.9:1	~ 1
	49:1	~ 1
Al^{+3}	0.49:1	< 1
	4.9:1	1.2
	49:1	22.5
Th^{+4}	0.5:1	~ 1
	5:1	~ 1
	50:1	8.8

[a] 2.04×10^{-4} $\underline{M}$ oxalate solution was used throughout.

solution to be analyzed a chelating agent to tie them up preferentially would likely decrease their interference.

Effect of Urea. Urea was also tested as a possible interference in the iron-oxalate reaction as it sometimes occurs in combination with oxalate and is an important constituent in urine. Solutions 1 $\underline{M}$ in urea were prepared in water and in 1 $\underline{M}$ H_2SO_4. Five-minute irradiations of these solutions produced only a small amount of carbon dioxide. Ten minutes of further irradiation increased the amount of gas given off by a factor of 2 or 3 only. Urea can be produced by reaction between carbon dioxide and ammonia; under the conditions used here, the back reaction is not observed to any significant extent.

The urea solutions were then tested as interferences in combination with oxalate and iron(III) and acid. Even at many hundreds of times the oxalate concentration the difference in readings when urea was present could be attributed to random error..

Effect of Other Carboxylic Acids

Investigation as Interferences. Because the gas chromatographic method worked well for oxalate samples, the effect of other carboxylic acids was investigated. To determine whether any of the molecular carboxylic

acids would be swept out of solution during purging and separated on the column or whether they decomposed to carbon dioxide during irradiation, 0.01 $\underline{M}$ solutions of sodium formate, sodium acetate, potassium oxalate, sodium citrate and potassium sodium tartrate were prepared in 1 $\underline{M}$ H_2SO_4. Five ml of each of these solutions were injected, the solutions purged with helium and then irradiated for 5 minutes. Iron(III) was not added for this run. Only small peaks were obtained so the solutions were irradiated for a further 10 minutes. The readings obtained after a total of 15 minutes of irradiation represented less than 1% decomposition of the acids. No chromatographic peaks corresponding to the molecular acids were evident.

The effect of other carboxylic acids as interferences was investigated in a similar manner to the method used to observe the effect of metal ions on the iron-oxalate reaction. Two effects were possible with the carboxylic acids. Firstly, they could complex with iron(III), thereby decreasing the amount of iron(III) available to complex with the oxalate and causing low results; or, secondly, they could complex with iron(III) and react photochemically to produce carbon dioxide and thus act as a positive interference.

To test for interference 1 ml of a 2.14×10^{-3} $\underline{M}$ iron(III) ammonium sulfate solution in 0.6 $\underline{M}$ H_2SO_4 was injected into the irradiation chamber. Then 2.5 ml of the carboxylate salt or acid to be tested for interference (or water when the oxalate calibration was performed) was added followed by 2.5 ml of potassium oxalate solution. The carboxylates were added as metal salts whenever convenient so as to avoid pH changes. Three oxalate solutions of concentrations 1×10^{-4}, 2×10^{-4} and 3×10^{-4} $\underline{M}$ were used to establish the calibration graph. The 2×10^{-4} $\underline{M}$ oxalate solution was used in combination with the carboxylate to be tested. The absolute percentage errors found with the eight different carboxylates tested are shown in Table 15.

The reactivity of sodium formate is especially great. Others did not observe this[34]. Several different lots of Fisher Brand chemicals were tested; all yielded large interferences. Generally the 1:1 and 10:1 interfering carboxylate:oxalate errors were 10% or less.

Determination of Other Carboxylic Acids. Because the reactivity of several of the carboxylic acids with iron(III) on irradiation was appreciable, a brief preliminary study was made of the conditions necessary to adapt the method to the determination of tartrate and citrate. This was done in the following way. Five

TABLE 15

Interference in the Iron(III)-Oxalate

Reaction due to the Presence of Other Carboxylates

Carboxylate Added	Ratio, Carboxylic Acid:Oxalate[a]	Absolute Percentage Error
Sodium citrate	1:1	5
	10:1	9
	100:1	60
Potassium sodium tartrate	1:1	6
	10:1	10
	100:1	85
Succinic acid	1:1	2
	10:1	1
	100:1	4
Sodium propionate	1:1	3
	10:1	5
	100:1	2
Malic acid	1:1	7
	10:1	8
	100:1	20
Sodium formate	1:1	5
	10:1	37
	100:1	49
Sodium acetate	1:1	0
	10:1	2
	100:1	7
Malonic acid	1:1	2
	10:1	10
	100:1	86

[a]Potassium oxalate was added as 2.5 ml of a 2×10^{-4} $\underline{M}$ oxalate solution. One ml of 2.14×10^{-3} $\underline{M}$ iron(III) ammonium sulfate in 0.6 $\underline{M}$ H_2SO_4 was used. The carboxylate salt or acid was added in 2.5 ml volume.

ml of the solution to be analyzed was injected into 1 ml of 0.20 $\underline{M}$ $FeNH_4(SO_4)_2$ in 0.06 $\underline{M}$ H_2SO_4. After purging the residual gases from the solution, a 5-minute irradiation generated carbon dioxide which was analyzed in a similar manner to the oxalate experiments. Calibrations obtained are shown in Figure 41. A high iron(III) concentration was chosen so that one iron(III) solution could be used throughout the analysis. This, likely, gave rise to the nonlinearity of the calibration. Over shorter concentration ranges an optimum iron(III) concentration could be chosen and more carbon dioxide would be evolved for the low concentration samples during the same 5-minute irradiation. The critical dependence on the amount of iron(III) present is similar to that for oxalate. A low acid concentration was chosen so formation of the iron(III)-carboxylate complexes, which are weaker for these acids than for oxalic, would not be hindered. When the acidity of the iron(III) solution was increased to 0.7 $\underline{M}$ H_2SO_4 more scatter was evident, especially at higher carboxylic acid concentrations, and the amount of carbon dioxide given off was diminished.
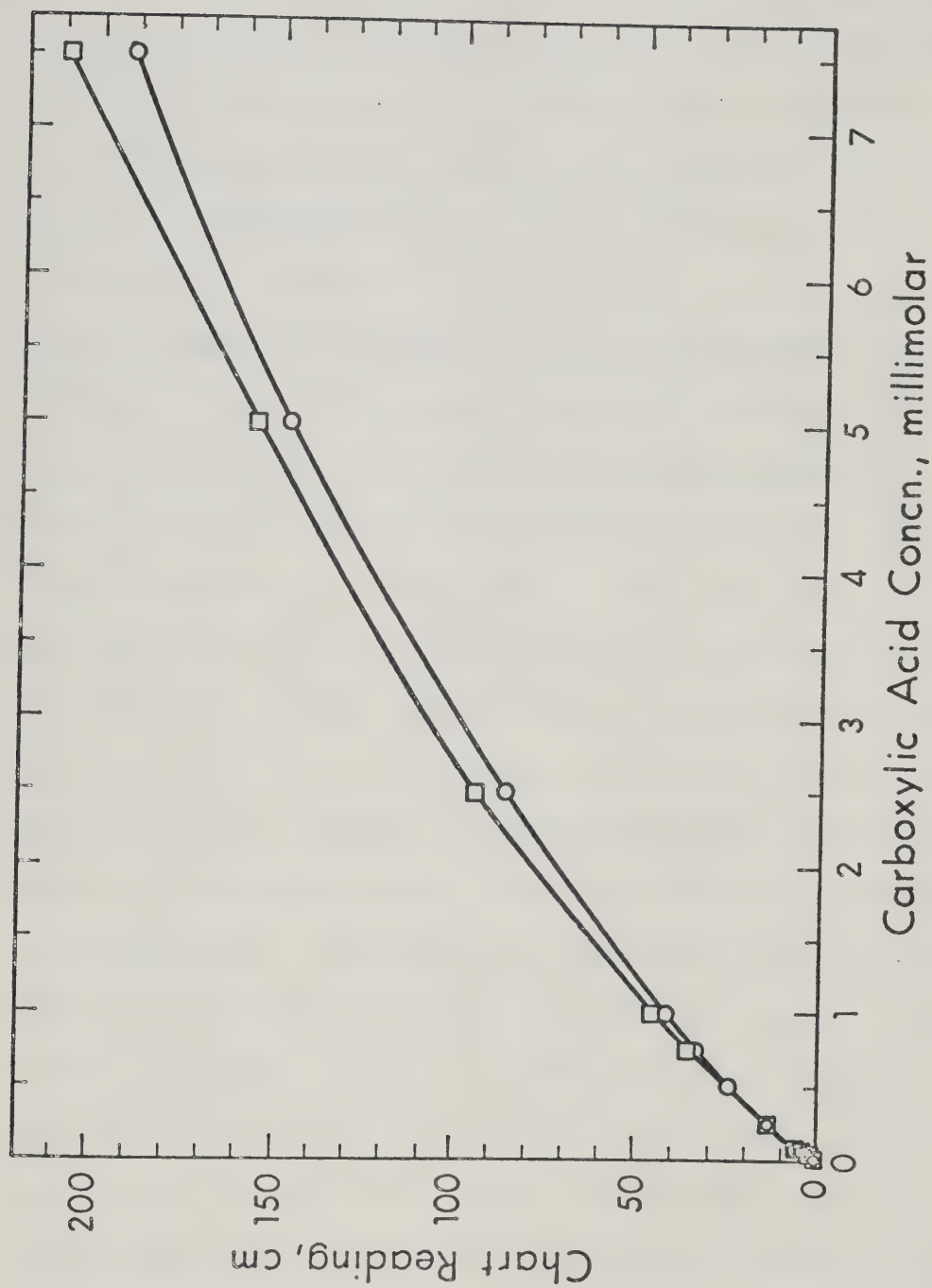
Figure 41 Calibration Plots for Sodium Citrate and Potassium Sodium
Tartrate using Photochemical Decomposition of the Iron(III)
Complexes: □ sodium citrate; ○ potassium sodium tartrate.

SUMMARY

After a review of the methods available for
the determination of carbon dioxide, a gas chromatographic
method of detection of the carbon dioxide produced in
the iron(III)-oxalate reaction is described. The carbon
dioxide is generated _in situ_ in an irradiation cell using
a Pen-Ray low pressure mercury lamp; the resultant gas
purged from the reaction solution with helium, carried
through a column of calcium sulfate (Drierite) to remove
water vapor, separated on a silica gel column and
measured with a thermal conductivity detector. This
simple apparatus avoided many of the problems of the pCO_2
gas electrode, such as hysteresis and interference from
low molecular weight organic acids and aromatic compounds.
The procedure for estimating oxalate concentration was
optimized with respect to concentration of iron(III),
kind and concentration of acid, and time and wavelength
of irradiation. Potential interferences from several ions
that interact with oxalate, and from carboxylic acids that
react in a manner similar to oxalate, were assessed. It
was shown that this system also could be used to analyze
for citric and tartaric acids. Advantages include
simple operation, the speed with which results can be
obtained relative to some other methods, freedom from

many interferences, a wide range of applicability and high
sensitivity. Disadvantages include that it is non
automated (applicability to continuous analysis would
be complicated), that it requires close temperature
control and that all operating conditions must be
carefully controlled if 100% efficiency is to be
achieved.

Having optimized the iron(III)-oxalate
reaction for use in simple aqueous solutions, some
preliminary data for a more complex system, oxalate
determination in human urine, are presented in
Chapter 6.

CHAPTER 6

DETERMINATION OF URINARY OXALATE

INTRODUCTION

Background on Kidney Stones

Kidney stones have been known for centuries. Most urinary tract calculi in humans are composed of calcium oxalate (as the mono or dihydrate), calcium phosphate (as hydroxyapatite), uric acid, magnesium ammonium phosphate, cystine or mixtures of these substances. Calcium phosphate stones tend to occur in patients with infected urines, where the pH is elevated. Oxalate stones, often found in patients with no urinary infection, are particularly important since wholly or partially they form two thirds of all calculi. Hypercalciuria (high calcium levels) and hyperoxaluria (high oxalate levels) are two causes of oxalate stones, yet there is often no satisfactory explanation for their occurrence in otherwise "normal" patients.

Theories of Stone Formation. The theories of stone formation and non formation are many and varied. Several reviews have covered this subject extensively[99,100,101] and some theories will be mentioned here. The precipitation-crystallization theory postulates stone

formation as a result of salt precipitation from supersaturated solution. While it is generally agreed that most urines are supersaturated with stone-forming substances this has not been proved experimentally. Early workers measured total calcium and oxalate (rather than ionic concentrations) and used these values to calculate ion products. Raaflaub[102] developed a method to determine free calcium concentrations using the dye tetramethylmurexide but as yet there is no known method to measure ionic oxalate, estimated to be 50% of the total. It has been recognized that various components of urine are more soluble in urine than in a water solution. The solubility of calcium oxalate in urine is increased by ions such as citrate, which complexes with calcium, and magnesium, which complexes with oxalate. If calcium and oxalate ion activities in urine could be measured the supersaturation theory could be proved or disproved.

A major problem lies in the fact that some individuals tend to form a few large stones that cause serious problems, and others many small ones that are passed at home. It has been proposed that stones form around a foreign body that acts as a nucleus. Some organic material is present in all stones, and the suggestion has been made that this material plays a major role in stone formation by providing a medium in which

the dissolved ions combine and crystallize, or a medium which controls crystallization. Others attribute stone formation to the calcium-binding properties of certain mucoproteins of the organic matrix.

An inhibitory theory suggests that polyphosphate and/or pyrophosphates and/or polypeptides excreted by non-stone formers act as a crystal poison. According to this theory stone formers excrete less of this substance.

Still others propose a protective colloid theory which states that colloids can coat crystal micelles and prevent growth. The absorbed matrix has also been suggested as a means of protecting the crystal phase from dissolution during periods when the urine is undersaturated.

There appears to be little concrete evidence to attribute stone formation to only one theory.

If a better analytical method for urinary oxalate were available perhaps additional evidence could be provided to prove or disprove the supersaturation theory. Since oxalate measurement appears to be the limiting factor, a review was undertaken of the methods to determine oxalate concentrations in urine.

Methods for Determining Urinary Oxalate

The basic difficulty in measuring this acid is its low level ($\sim 10^{-4}$ $\underline{M}$) in urine and the abundance of

potential interferences in the complex urinary matrix.
Because of the low sensitivity of many methods often
oxalate must first be concentrated and it is usually
separated because of the variety of interferences present
in urine which could cause inaccurate results. The
separation step causes considerable difficulty. Few
workers add a correction for nonquantitative extraction
or precipitation. It appears that a correction factor,
perhaps determined by radioisotope measurements, should be
applied to all results.

A classic method for oxalate involves oxidation
with potassium permanganate. The determination can be
completed by measuring the evolved carbon dioxide[103],
performing a back titration with sodium thiosulfate[104],
or colorimetrically determining the end point[105]. Various
procedures proposed to increase the specificity of the
reaction include preliminary esterification and distillation
to separate oxalate from interferences before gasometric
determination of the carbon dioxide[106].

Yarbro and Simpson[107] found that an extraction
time of 18 hours was necessary for the complete recovery
of urinary oxalic acid by diethyl ether extraction. To
avoid phosphate coprecipitation and obtain 98-100% recovery,
calcium oxalate was precipitated at a pH of 4.0 to 4.5.
The oxalate concentration was then measured with a

permanganate-thiosulfate titration. The above procedure
was modified in that after the calcium oxalate was
precipitated at pH 6.0 it was converted to glycolic acid
with zinc and then measured colorimetrically with
chromotropic acid[108]. Recoveries of 88-94% were reported.
A 98 ± 1% recovery in the diethyl ether extraction step
can be obtained if ammonium sulfate is added to the
acidified urine and the extraction carried out for 6 hours
at 70°C[109]. A 5-minute extraction with tri-n-butyl
phosphate was a later improvement[110]. The oxalate was
then precipitated by addition of calcium sulfate,
reduced to glyoxylic acid and treated with resorcinol to
form a colored fluorescent complex. Endo[111] also used a
resorcinol fluorometric analysis for urinary oxalate.
Alternatively oxalate can be reduced to glycolic acid and
measured with chromotropic acid[112].

Precipitated calcium oxalate can be determined
by an automated method involving measurement of the
reduction in the absorbance of the red
uranium(IV)-4-(2-pyridylazo)resorcinol complex. A
correction was applied to take into account incomplete
precipitation of the oxalate[113]. Pernet and Pernet[114,115]
converted urinary oxalate, precipitated as the calcium
salt, to glyoxylic acid with zinc and hydrochloric acid
and added phenylhydrazine, hydrochloric acid and hydrogen

peroxide so they could estimate the oxalate colorimetrically[116]. After decarboxylation to formic acid, urinary oxalate has been measured colorimetrically using indole[117].

Numerous methods have been proposed which use the oxalate specific enzyme, oxalate decarboxylase, obtained from <u>Collybia velutipes</u>. In the first of these[118], precipitated calcium oxalate was incubated with the enzyme and manometric readings of the evolved carbon dioxide were used to complete the analysis. A direct enzymatic determination[119] using a Warburg respirometer has been performed after preconcentration of the urine. In an automated method[26] requiring special equipment and chemicals the evolved carbon dioxide was measured colorimetrically. Inhibition of the enzyme due to sulfate and phosphate was overcome by adding these ions to the standard solutions. A simpler colorimetric method[120] utilized a closed conical flask containing urine, buffer and enzyme. After 18 hours at 37°C the carbon dioxide present in an alkaline buffer in a cuvette was measured with a glass electrode. For small amounts of oxalate the evolved formate could be measured using tetrahydrofolate synthetase[121]. Oxalate decarboxylase can also be coupled with the NAD^+-requiring enzyme formate dehydrogenase and the absorbance of NADH measured[122].

Another relatively selective technique which has been used successfully is isotope dilution. The counting can be done on the precipitated calcium oxalate[123,124] or after conversion of the oxalate to glycolate[125]. A double isotope labelling experiment using calcium-45 and carbon-14 labelled oxalate has also been used.

More unusual methods, such as polarography[127], have been tried, while centrifuge tubes have been developed that permit washing of the calcium oxalate precipitate and analysis by cerate oxidimetry[128]. In this procedure radioisotope-determined factors were used to correct for incomplete precipitation. Extracted or separated oxalate, after conversion to the diethyl or methyl derivative, has been measured by gas chromatography[129,130,131].

The difference between the excess calcium ions present in the urinary supernatant at pH 5 and 2, as measured by atomic absorption, was used by Menachè[132] as a routine micromethod to determine oxalic acid. The calcium in precipitated calcium oxalate can be measured by atomic absorption[133] or complexometrically[134].

After a tri-n-butyl phosphate extraction and precipitation of oxalate as calcium oxalate, Dutt and Mottola[135] analyzed the oxalate with a standard addition technique and observed the effect of oxalate on the rate of oxidation of tris(1,10 phenanthroline)-iron(II) complex by

chromium(VI) in relatively low concentrations of sulfuric acid.

Discussion of Three Important Methods of Measuring
Urinary Oxalate

One clinical laboratory in Edmonton uses a combination of extraction and precipitation to separate and concentrate urinary oxalate. Their method involves heating the acidified samples at 100°C for 30 minutes to hydrolyze any oxaluric acid that may be present. The cooled filtered solution, an oxalate standard and a blank are then extracted with diethyl ether. The ether is added to a small volume of water, then evaporated. To the remaining solution calcium chloride and an ethanol-acetic acid mixture is added. After 24 hours the solution is centrifuged and the supernatant removed. The precipitate is dissolved in sulfuric acid and titrated with potassium permanganate at 60°C.

A second laboratory uses a somewhat different but equally time consuming method[133]. Whereas the first laboratory uses only 25 ml of urine, the second needs a 100-ml sample for each analysis. Because of the low oxalate levels an oxalate spike is added to each urine sample. A standard potassium oxalate in water is carried through the analysis as well. The oxalate is precipitated as calcium oxalate directly from pH 5.0 urine and the solutions are allowed to stand 3 to 7 days at 4°C to form

the precipitate. The supernatant liquid is removed and the precipitate is washed several times with calcium oxalate saturated water, then dissolved in sulfuric acid and the calcium determined by atomic absorption. A calibration curve is run on standards prepared from pure calcium carbonate in acid.

Several sources of error are evident in both of these procedures. Koch and Strong[128] state that the fraction of oxalate precipitated as calcium oxalate depends both on the amount present in solution and the length of time allowed for the precipitate to form. One day is insufficient for complete formation of the precipitate, and even after 3 days precipitation is incomplete. The standards used in both of these methods, pure potassium or sodium oxalate in water, do not mimic the complicated urinary matrix. (Recently, the second procedure has been modified in that standard additions are now used. Although an improvement, the method is still not very reproducible or reliable.)

Hogkinson and Williams[112] determined oxalate in urine by adding calcium sulfate and ethanol to pH 7 urine and allowing the precipitate to form overnight. After decantation the precipitate was dissolved in sulfuric acid, zinc wire added to reduce the oxalate to glycolic acid and the solution heated in boiling water for 30

minutes. A spectrophotometric determination with
chromotropic acid in sulfuric acid was then performed.
The method was investigated in the laboratory as it
appeared quite promising. The procedure was followed as
outlined, except that zinc pellets were used because of
the unavailability of zinc wire. Removal and washing of
the pellets with only 0.5 ml of 1% chromotropic acid
solution was difficult, however. Also, extreme care had
to be exercised due to the high concentrations of sulfuric
acid used. The precision obtained for the method when
using oxalate in water was poorer than the 2% claimed for
the method. An earlier method of Hodgkinson and Zarembski[109]
which used zinc dust was also tried. The zinc dust
settled to the bottom of the tube and a portion of the
supernatant could be easily transferred for reaction with
the chromotropic acid. The precision obtained was no
better than with the zinc pellet method.

After assessment of the long analysis time and
poor precision of the methods available, an attempt was
made to analyze urinary oxalate by the iron(III)-oxidation
method presented in Chapters 2 and 5. A method that is
more rapid and that avoids the problems of prior
separation of the oxalate is greatly needed.

EXPERIMENTAL

The analysis of urine for oxalate using both the pCO_2 electrode and the gas chromatographic stripping method to measure the carbon dioxide produced by the iron(III) reduction was investigated. The experimental conditions used are those outlined in Chapters 2 and 5.

While the low oxalate levels present in urine are not a problem for the gas chromatographic detector, they were below the linear region of the pCO_2 gas sensing electrode. Furthermore, citrate is present in most urines at higher concentrations than oxalate. The normal citric acid level in urine is about 800 mg/day while the normal oxalic acid level is about 30 mg/day. However, the citric acid interference can be minimized by decreasing the pH of the samples, as discussed earlier. Other major urinary components, such as sodium and potassium chloride and urea, did not interfere with the iron(III)-oxalate reaction or with the measurement of evolved carbon dioxide.

Some carbon dioxide is evolved from urine samples on acidification; this can be removed before the samples are introduced into the analytical procedure by purging with an inert gas. In addition, some background carbon dioxide appeared to be evolved upon irradiation, likely from components such as citric acid.

The only practical way to analyze urine samples appeared to be via a standard addition technique. This procedure will compensate for ionic strength effects, the presence of agents capable of complexing with iron(III) and the high absorbance of the solution. The urine was diluted to the same total volume with either water or spikes of standard oxalate solutions. The standard addition equation which was used in the gas electrode determination of the carbon dioxide was derived from the Nernst equation:

$$E_1 = E^O + S \log [C_x(V_x/V_{tot})]$$

$$E_2 = E^O + S \log [C_x(V_x/V_{tot}) + C_s(V_s/V_{tot})]$$

where E_1 and E_2 are two millivolt readings, without and with added spike, E^O is the standard electrode potential, S is the slope, C_x and C_s are the concentrations of the unknown and spike solution, V_x and V_s are the corresponding volumes, and V_{tot} is the total volume. Subtracting and rearranging,

$$\frac{\Delta E}{S} = \log \left(\frac{C_x(V_x/V_{tot}) + C_s(V_s/V_{tot})}{C_x(V_x/V_{tot})} \right)$$

$$\Delta E = E_2 - E_1$$

Taking the antilog of each side and rearranging,

$$C_x(V_x/V_{tot})(10^{\Delta E/S}) - C_x(V_x/V_{tot}) = C_s(V_s/V_{tot})$$

or,

$$C_x = C_s(V_s/V_{tot})(10^{\Delta E/S} - 1)^{-1}$$

The urinary oxalate concentration was obtained from the x-axis intercept on the standard addition plot for the gas chromatographic method of detection of the evolved carbon dioxide.

RESULTS AND DISCUSSION

pCO_2 Electrode as the Detector

A difficulty encountered in the use of standard additions for the determination of carbon dioxide was the high degree of dependence of the equation on the values of ΔE and S. As mentioned in Chapter 2 the pCO_2 electrode displayed a memory effect when lower concentration samples followed ones of higher concentration. Thus if a urine with water added were analyzed alternatively with spiked urine samples the value obtained, in millivolts, for the nonspiked sample continually increased. The initial value did not appear to be the correct one to use because if this first non-spiked solution were run consecutively several times, increasing millivolt readings were also obtained. This may be due to diffusion of molecular species in the urine across the gas permeable membrane. In addition, plots of oxalate concentration against millivolt readings gave varying slopes, especially at low concentrations where non-Nernstian behavior becomes significant. In the standard-addition equation small changes in ΔE and S result in large changes in C_x.

A major problem with urinary oxalate analysis is knowledge of the "true" value of the oxalate concentration. A number of analyzed samples were

obtained from the University of Alberta Hospital, but all had been stored at 4°C for at least a week and usually much longer. Hence their composition may have changed through decomposition or precipitation. Because of this, and because of the uncertainties in their method of analysis, no confidence could be placed in their values.

The data obtained with the pCO_2 electrode was too scattered to determine whether the electrode was responding in a Nernstian manner because the Nernst equation included both C_x and the spiked values in the logarithmic term.

In theory, with enough standard addition spikes, the three unknowns in the Nernst equation, E^O, S and C_x, could be evaluated. But because of the large differences in the magnitude of these terms -- E^O about 100 mV, S less than 60 mV and C_x about 10^{-4} to 10^{-5} $\underline{M}$ - this was not practical. Furthermore, this method assumes a linear calibration, which may not be valid.

A bisection method was also investigated. In this approach the Nernst equation is rearranged to yield a set of equations of the type:

$$\frac{C_x + C_{s2}}{C_x + C_{s1}}^{(E_{3-1}/E_{2-1})} - \frac{C_x + C_{s3}}{C_x + C_{s1}} = 0$$

where C_x is the unknown concentration, C_{s1}, C_{s2} and C_{s3} are the concentrations of the three spike solutions used

and E_{3-1} and E_{2-1} are the differences in millivolt readings between those obtained with spikes three and one and with two and one. In deriving this equation S and E^o are assumed constant. This assumption may not be valid at the low concentrations of oxalate present in the urine. The value of the exponential term in the above equation is critical also; a small error leads to a large error in oxalate concentration.

Changes in iron(III) concentration, acidity, type of lamp and speed of analysis in the pCO_2 electrode system did not improve the results. Thus it appears that this method should be reevaluated if a more reliable pCO_2 electrode becomes available.

Gas Chromatographic Method of Analysis

A brief preliminary study was made of the gas chromatographic method of Chapter 5 in an attempt to measure urinary oxalate. The addition of several drops of Antifoam B, a silicone emulsion (J. T. Baker Chemical Co.), to the urine samples was necessary to reduce its tendency to foam during helium purging.

A synthetic urine mixture was prepared which contained over twenty of the major components present in urine. From analysis of this solution the optimum iron(III)-oxalate ratio was found to be about 20:1. This

is much higher than the 2:1 ratio found optimum for aqueous solutions of oxalate and can be explained as due to the high absorbance of the urine solution. The spectrum of a urine sample, diluted by half with water and with no iron(III) added, is shown in Figure 42. The absorbance is significantly higher at all wavelengths than that for a pure potassium oxalate solution (Figure 32). Even a further addition of 10 ml of water to 1 ml of the urine mixture still resulted in high absorbances for the solution.

To avoid the added complication of the unknown rate of decomposition and/or precipitation of the oxalate or other substances in freshly collected human urine as well as variation from person to person and day to day Hycel No. 928-000 dried human urine was used as the source of urine. Four vials (lot number 2951AI) which reconstituted to 25 ml each were purchased. The urine is a pooled sample for which the analyzed values of many components are available. Although an oxalate value was not included, use of these samples provided a reproducible sample for study.

When 2.5 ml of a Hycel urine sample was mixed with 1 ml of iron(III) in 0.6 $\underline{M}$ HCl the pH of the resulting solution was approximately 1, at the limit if interference from citrate is to be minimized. Since this acidity could be attained from the acid in the iron(III)
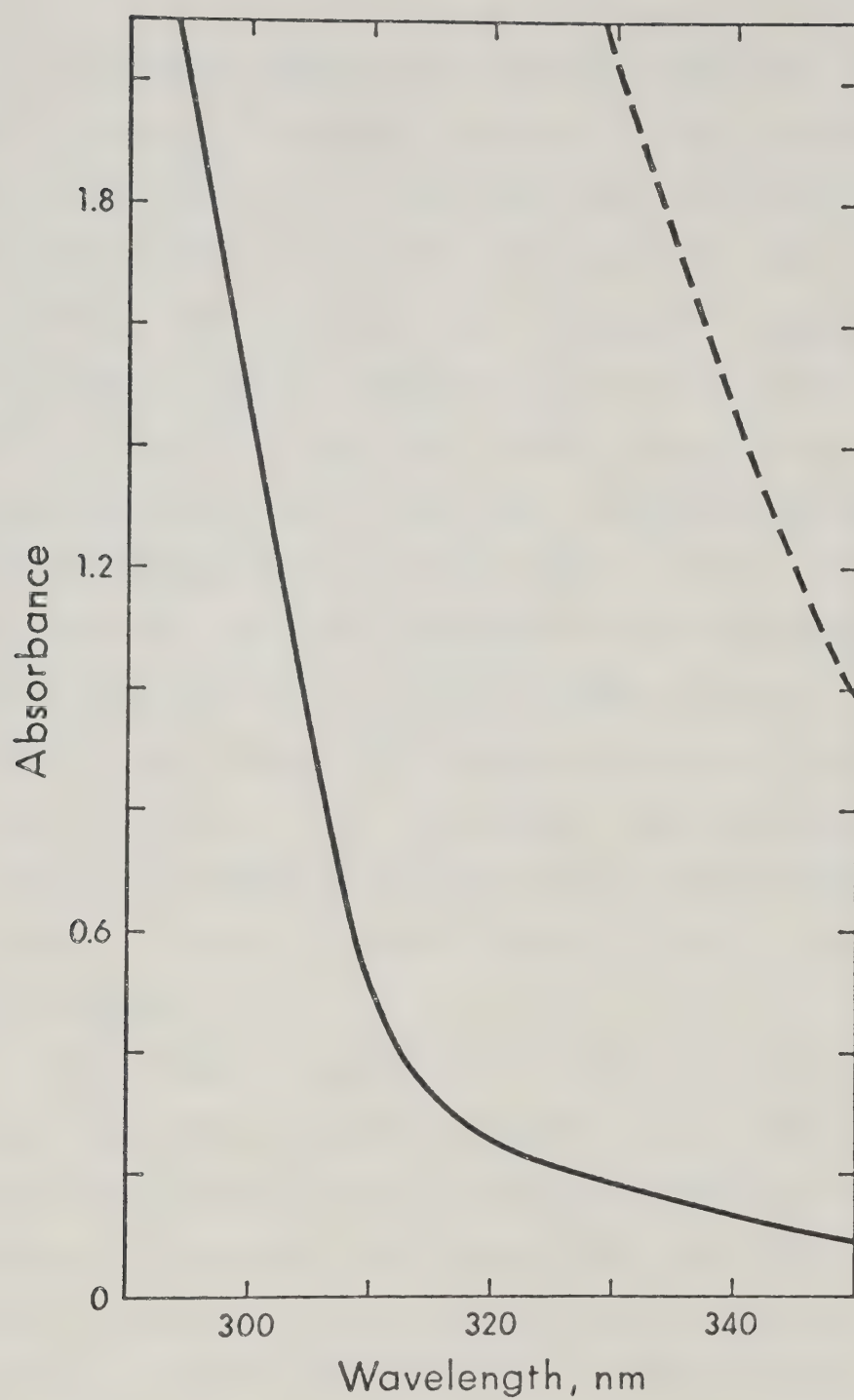
Figure 42   Spectra of a Human Urine Sample:
••••••, urine diluted 1:1 with water;
————, urine diluted 1:20 with water.

solution, the urine sample itself was not acidified for the first analysis. Therefore 2.5 ml of urine, an equal volume of water and 1 ml of 0.6 $\underline{M}$ HCl were irradiated for 5 minutes after the residual gases had been flushed out of the system. Then the water was replaced by varying concentrations of oxalate spikes and the 0.6 $\underline{M}$ HCl was replaced by 1.5×10^{-2} $\underline{M}$ iron(III) in 0.6 $\underline{M}$ HCl. An apparent oxalate concentration of 40 mg/l was calculated for this sample after taking the background carbon dioxide into account. However, when this background was added to an aqueous oxalate calibration a lower urinary oxalate concentration was obtained by reading the value of the urine with water only added as a spike. This discrepancy is the result of screening by strongly absorbing components in the urine. Oxalate in water cannot be used to calibrate for urine samples.

Urine samples spiked with oxalate do not react quantitatively; each additional 5 minutes of irradiation yielded a significantly large peak up to 20 minutes total irradiation. In contrast, individual peaks for each additional 5 minutes irradiation were small and relatively constant when no additional oxalate or iron(III) was present. This, again, shows the difference in behavior between urinary oxalate and aqueous oxalate samples.

A similar analysis procedure was used on a second vial of urine control, except that a 20-ml portion of the urine was acidified with a few drops of 7 $\underline{M}$ H_2SO_4 to duplicate the conditions under which urines are often received by clinical laboratories. Although a lower urinary oxalate concentration might have been expected for this sample because of the higher acidity, experimentally a value of 63 mg/l was obtained. No explanation could be provided for this.

The third vial was analyzed in a similar manner to the first vial except a 20-minute irradiation was used instead of a 5-minute irradiation as it appeared 5 minutes was not enough time for a complete iron(III)-oxalate reaction to occur. This experiment yielded a 77 mg/l value for the oxalate concentration of the sample.

The three straight-line calibrations which were obtained are shown in Figure 43. Since a value for the oxalate concentration was not available these results could not be compared, and so no further work in this area was carried out. Once a value for the oxalate concentration is known, the effect of acid and iron(III) concentration and other variables can be determined. It appears as if the dried urine controls are the best choice for development work because storage and decomposition problems and variation from person to person are avoided.
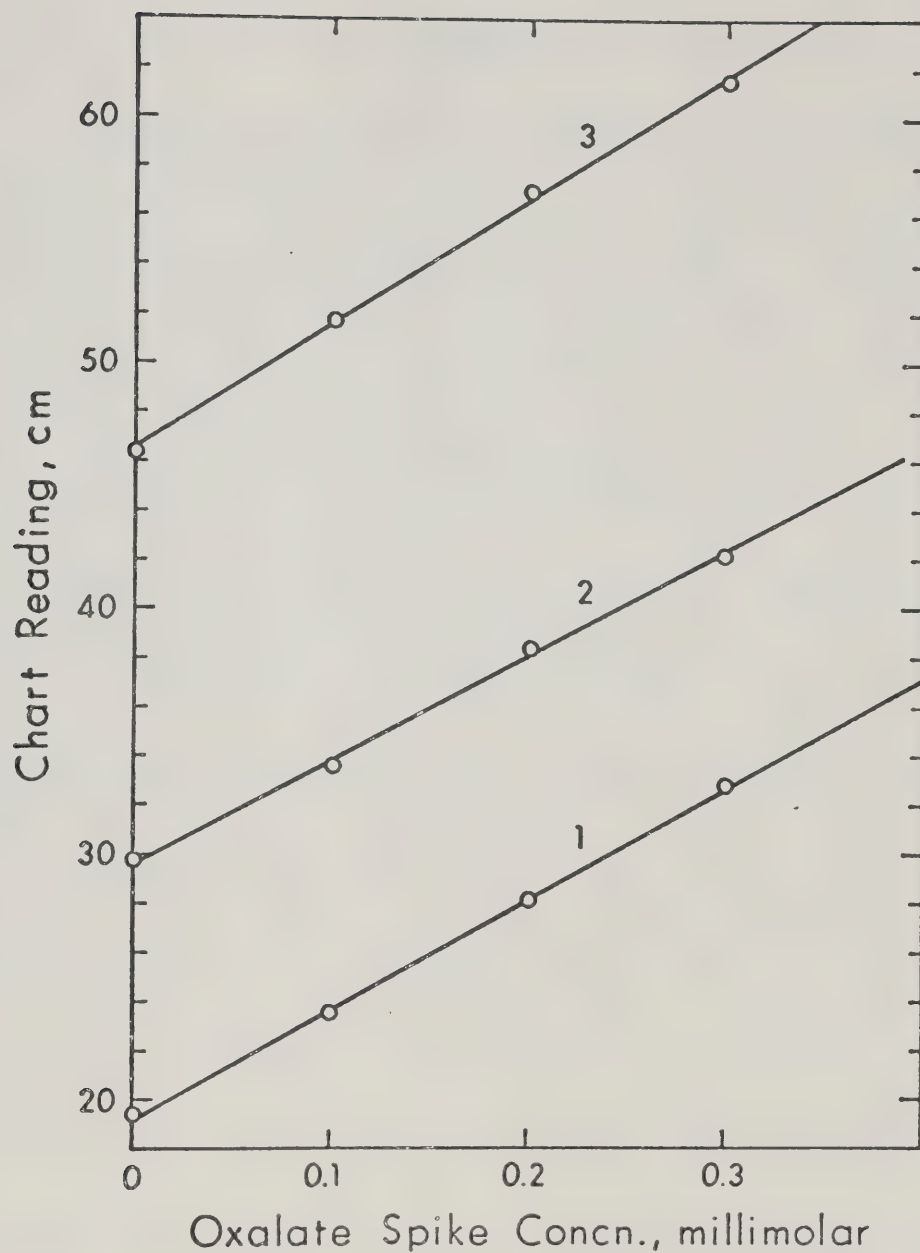
Figure 43   Analysis of Oxalate-Spiked Hycel Urine
Sample: 1, 2 and 3 refer to results
obtained for first, second and third
vials of urine.

SUMMARY

After a survey of the methods available for the determination of oxalate in urine, a brief investigation was made of its measurement using the iron(III)-oxalate reaction and determination of the evolved carbon dioxide with either a pCO_2 electrode or in a gas chromatographic method. While the oxalate concentration appeared to be in the non Nernstian range of the pCO_2 electrode, the gas chromatographic method is sufficiently sensitive to be able to measure the carbon dioxide evolved. Because of the high background absorbance in urine, higher concentrations of iron(III) and longer irradiation times must be used than was found optimum for simple aqueous solutions. Assessment of the accuracy of the method is hampered by lack of a reference method with which to compare results.

REFERENCES

1. A. Hodgkinson, _Clin. Chem._, _16_, 547 (1970).

2. I. Sarudi, _Pharm. Zentralh. Deut._, _106_, 217 (1967).

3. E. Pap and L. Szekeres, _Chemist-Analyst_, _53_, 108 (1964).

4. A. K. Mukherji, _Anal. Chim. Acta_, _40_, 354 (1968).

5. W. Selig, _Microchem. J._, _15_, 452 (1970).

6. Z. Gregorowicz and W. Hertyk, _Zeszyty Nauk. Politech. Slask., Chem._, No. _13_, 3 (1963).

7. I. Al. Crisan and R. Krausz, _Stud. Univ. Babes-Bolyai, Ser. Chem._, _12_, 19 (1967).

8. P. S. Dubey and K. N. Tandon, _Indian J. Chem._, _6_, 115 (1968).

9. E. Bakacs-Polgar and I. Kurcz-Csiky, _Z. Anal. Chem._, _199_, 247 (1964).

10. J. Bergerman and J. S. Elliot, _Anal. Chem._, _27_, 1014 (1955).

11. Z. D. Draganic, _Anal. Chim. Acta_, _28_, 394 (1963).

12. F. Burriel-Martí, J. Ramírez-Muñoz and E. Fernández-Caldas, _Anal. Chem._, _25_, 583 (1953).

13. R. E. Neas and J. C. Guyon, _Anal. Chem._, _44_, 799 (1972).

14. D. A. Britton and J. C. Guyon, _Anal. Chim. Acta_, _44_, 397 (1969).

15. V. P. Calkins, _Ind. Eng. Chem._, _Anal. Ed._, _15_, 762 (1943).

16. S. Miyazaki, Y. Suhara and T. Kobayashi, _J. Chromatogr._, _39_, 88 (1969).

17. K. S. Lee and O. Samuelson, _Anal. Chim. Acta_, _37_, 359 (1967).

18. T. S. Rumsey and C. H. Noller, J. Chromatogr., 24, 325 (1966).

19. D. J. Curran and K. S. Fletcher (III), Anal. Chem., 41, 267 (1969).

20. A. I. Ryaguzov, I. V. Aleksandrova and I. B. Cherepenina, Zh. Anal. Khim., 27, 2469 (1972).

21. V. A. Bork and K. S. Sal'nikova, Zh. Anal. Khim., 23, 901 (1968).

22. A. G. Kornienko, L. A. Mirkind and M. Ya. Fioshin, Zh. Anal. Khim., 21, 1501 (1966).

23. M. Ignaczak and A. Grzejdziak, Soc. Sci. Lodz. Acta Chim., 18, 135 (1974).

24. S. Kihara, T. Yamamoto and K. Motojima, Bunseki Kagaku, 21, 496 (1972).

25. G. G. Guilbault, S. H. Sadar, R. McQueen, Anal. Chim. Acta, 45, 1 (1969).

26. C. F. Knowles and A. Hodgkinson, Analyst, 97, 474 (1972).

27. C. A. Parker, Proc. Roy. Soc. (London), A220, 104 (1953).

28. S. Suzuki, K. Matsumoto, K. Harada and E. Tsubura, Photogr. Sci. Eng., 12, 2 (1968).

29. C. A. Parker and C. G. Hatchard, J. Phys. Chem., 63, 22 (1959).

30. G. G. Rao and V. M. Rao, Current Sci., 13, 317 (1944).

31. G. G. Rao and V. M. Rao, Proc. Natl. Inst. Sci. India, 12, 217 (1946).

32. G. G. Rao and G. Aravamudan, Anal. Chim. Acta, 13, 415 (1955).

33. G. G. Rao, G. Aravamudan and N. C. Venkatamma, Z. Anal. Chem., 146, 161 (1955).

34. W. M. Riggs and C. E. Bricker, Anal. Chem., <u>38</u>, 897 (1966).

35. G. G. Guilbault and F. R. Shu, Anal. Chem., <u>44</u>, 2161 (1972).

36. R. W. Stow and B. F. Randall, Amer. J. Physiol., <u>179</u>, 678 (1954).

37. R. W. Stow, F. Baer and B. F. Randall, Arch. Phys. Med. Rehabilitation, <u>38</u>, 646 (1957).

38. K. H. Gertz and H. H. Loeschcke, Naturwissenschaften, <u>45</u>, 160 (1958).

39. J. W. Severinghaus and A. F. Bradley, J. Appl. Physiol., <u>13</u>, 515 (1958).

40. C. H. Hertz and B. Siesjö, Acta Physiol. Scand., <u>47</u>, 115 (1959).

41. K. Ishitani, Oyô Denki Kenkyûsho Ihô, <u>11</u>, 261 (1959).

42. S. R. Gambino, Clin. Chem., <u>7</u>, 336 (1961).

43. P. Rispens and W. Hoek, Clin. Chim. Acta, <u>22</u>, 291 (1968).

44. R. L. Gelder and J. F. Neville Jr., Amer. J. Clin. Pathol., <u>55</u>, 325 (1971).

45. J. W. Severinghaus, Acta Anaes. Scand. (Supp. XI), <u>6</u>, 207 (1962).

46. J. W. Ross, J. H. Riseman and J. A. Krueger, Pure Appl. Chem., <u>36</u>, 473 (1973).

47. J. Ružička and E. H. Hansen, Anal. Chim. Acta, <u>69</u>, 129 (1974).

48. H. Shimazono and O. Hayaishi, J. Biol. Chem., <u>227</u>, 151 (1957).

49. B. L. Bengtsson, Anal. Biochem., <u>19</u>, 144 (1967).

50. E. Emiliani and B. Riera, Biochim. Biophys. ʼ a, <u>167</u>, 414 (1968).

51. E. B. Vaisey, V. H. Cheldelin and R. W. Newburgh, Arch. Biochem. Biophys., 95, 66 (1961).

52. J. Chiriboga, Biochem. Biophys. Res. Commun., 11, 277 (1963).

53. J. Chiriboga, Arch. Biochem. Biophys., 116, 516 (1966).

54. B. Halliwell, Biochem. J., 129, 497 (1972).

55. R. H. Müller, Anal. Chem., 41,(12), 113A (1969).

56. P. G. Stecher, (Ed.), "The Merck Index", 8th ed., Merck and Co., Inc., Rahway, N.J.,(1968).

57. J. W. Swinnerton and W. W. Miller, J. Chem. Educ., 36, 485 (1959).

58. M. Deneux, R. Meilleur and R. L. Benoit, Canad. J. Chem., 46, 1383 (1968).

59. E. Bottari and L. Ciavatta, Gazzetta, 95, 908 (1965).

60. R. A. Whiteker and N. Davidson, J. Amer. Chem. Soc., 75, 3081 (1953).

61. S. Ahrland and L. Brandt, Acta Chem. Scand., 22, 1579 (1968).

62. O. E. Zvyagintsev and S. B. Lyakhmanov, Zhur. neorg. Khim., 13, 1230 (1968).

63. E. Rabinowitch and W. H. Stockmayer, J. Amer. Chem. Soc., 64, 335 (1942).

64. G. A. Gamlen and D. O. Jordan, J. Chem. Soc., 1953, 1435.

65. R. E. Hamm, S. M. Shull, Jr. and D. M. Grant, J. Amer. Chem. Soc., 76, 2111 (1954).

66. K. S. Rajan and A. E. Martell, Inorg. Chem., 4, 462 (1965).

67. L. G. Sillén and A. E. Martell, (Eds.), "Stability Constants of Metal-Ion Complexes", Special Publication No. 17 and No. 25, The Chemical Society, London, 1964 and 1971.

68. H. Tsubota, Bull. Chem. Soc. Japan, 35, 640 (1962).

69. D. D. Perrin, J. Chem. Soc., 1959, 1710.

70. L. Sommer and K. Pliska, Coll. Czech. Chem. Comm., 26, 2754 (1961).

71. D. Banerjea and I. P. Singh, Z. anorg. Chem., 331, 225 (1964).

72. D. D. Perrin, J. Amer. Chem. Soc., 82, 5642 (1960).

73. K. S. Rajan and A. E. Martell, J. Inorg. Nuclear Chem., 29, 523 (1967).

74. C. Bertin-Batsch, Ann. Chim. (France), 7, 481 (1952).

75. R. K. Cannan and A. Kibrick, J. Amer. Chem. Soc., 60, 2314 (1938).

76. C. F. Timberlake, J. Chem. Soc., 1964, 5078.

77. E. Campi, Ann. Chim. (Italy), 53, 96 (1963).

78. C. F. Timberlake, J. Chem. Soc., 1964, 1229.

79. J. Stary, Analyt. Chim. Acta, 28, 132 (1963).

80. O. Vartapetian, Ann. Chim. (France), 2, 916 (1957).

81. S. D. Bhardwaj and G. V. Bakore, J. Indian Chem. Soc., 38, 967 (1961).

82. J. E. Powell and W. F. S. Neillie, J. Inorg. Nucl. Chem., 29, 2371 (1967).

83. T. Nozaki and H. Kurihara, Nippon Kagaku Zasshi, 82, 707 (1961).

84. T. Nozaki, F. Hori and H. Kurihara, Nippon Kagaku Zasshi, 82, 713 (1961).

85. C. F. Baes, Jr. and R. E. Mesmer, "The Hydrolysis of Cations", John Wiley and Sons, Inc., New York, 1976, p. 257.

86. J. G. Calvert and J. N. Pitts, Jr., "Photochemistry", John Wiley and Sons, Inc., New York, 1966, p. 696.

87. G. Charlot and D. Bézier, "Quantitative Inorganic Analysis", 3rd ed., Authorized translation by R. C. Murray, John Wiley and Sons, Inc., New York, 1957, pp. 376-379.

88. G. Charlot and D. Bézier, "Quantitative Inorganic Analysis", 3rd ed., Authorized translation by R. C. Murray, John Wiley and Sons, Inc., New York, 1957, p. 318.

89. A. Tolk, W. A. Lingerak, A. Kout and D. Börger, Anal. Chim. Acta, 45, 137 (1969).

90. K. Grob, K. Grob, Jr. and G. Grob, J. Chromatogr., 106, 299 (1975).

91. K. Grob and G. Grob, J. Chromatogr., 90, 303 (1974).

92. J. Novák, J. Žlutický, V. Kubelka and J. Mostecký, J. Chromatogr., 76, 45 (1973).

93. B. J. Dowty, L. E. Green and J. L. Laseter, Anal. Chem., 48, 946 (1976).

94. J. W. Swinnerton, V. J. Linnenbom and C. H. Cheek, Anal. Chem., 34, 483 (1962).

95. K. Park, G. H. Kennedy and H. H. Dobson, Anal. Chem., 36, 1686 (1964).

96. G. Zweig and J. Sherma, (Eds.), "Handbook of Chromatography", Vol. I, CRC Press, Cleveland, 1972, p. 130.

97. T. Rigg and J. Weiss, J. Chem. Phys., 20, 1194 (1952).

98. A. I. Moskvin and L. N. Essen, Russ. J. Inorg. Chem., 12, 359 (1967).

99. S. N. Gershoff, Metab., Clin. Exptl., 13, 875 (1964).

100. B. E. C. Nordin and A. Hodgkinson, Advan. Internal Med., 13, 155 (1967).

101. W. C. Thomas, Jr., J. Urol., 113, 423 (1975).

102. J. Raaflaub, Z. Physiol. Chem., 328, 198 (1962).

103. D. D. Van Slyke and J. Sendroy, Jr., J. Biol. Chem., 84, 217 (1929).

104. S. Maugeri, Z. physiol. Chem., 217, 138 (1933).

105. N. V. Dmitrieva, Gigiena Truda i Prof. Zabolevaniya, 10, 59 (1966).

106. E. C. Dodds and E. J. Gallimore, Biochem. J., 26, 1242 (1932).

107. C. L. Yarbro and R. E. Simpson, J. Lab. Clin. Med., 48, 304 (1956).

108. E. F. Dempsey, A. P. Forbes, R. A. Melick and P. H. Hennema, Metab., Clin. Exptl., 9, 52 (1960).

109. A. Hodgkinson and P. M. Zarembski, Analyst, 86, 16 (1961).

110. P. M. Zarembski and A. Hodgkinson, Biochem. J., 96, 717 (1965).

111. R. Endo, Kyosai Iho, 17, 552 (1968).

112. A. Hodgkinson and A. Williams, Clin. Chim. Acta, 36, 127 (1972).

113. H. Baadenhuijsen and A. P. Jansen, Clin. Chem. Acta, 62, 315 (1975).

114. J. L. Pernet and A. Pernet, Ann. Biol. Clin. (Paris), 20, 737 (1962).

115. J. L. Pernet and A. Pernet, Ann. Biol. Clin. (Paris), 23, 1189 (1965).

116. G. Devoto and P. Salis, Med. Lav., 65, 389 (1974).

117. E. R. Hausman, J. S. McAnally and G. T. Lewis, Clin. Chem., 2, 439 (1956).

118. G. G. Mayer, D. Markow and F. Karp, Clin. Chem., 9, 334 (1963).

119. M. E. Ribeiro and J. S. Elliot, Invest. Urol., 2, 78 (1964).

120. P. C. Hallson and G. A. Rose, Clin. Chim. Acta, 55, 29 (1974).

121. W. B. Jakoby, Methoden Enzym. Anal., 3. Neubearbeitete Erweiterte Aufl., 2, 1587 (1974).

122. J. Costello, M. Hatch and E. Bourke, J. Lab. Clin. Med., 87, 903 (1976).

123. B. M. Dean and W. J. Griffin, Nature, 205, 598 (1965).

124. D. A. Gibbs and R. W. E. Watts, J. Lab. Clin. Med., 73, 901 (1969).

125. T. D. R. Hockaday, E. W. Frederick, J. E. Clayton and L. H. Smith, Jr., J. Lab. Clin. Med., 65, 677 (1965).

126. O. P. Foss, In Vitro Proced. Radioisotop. Med., Proc. Symp., 121 (1969).

127. Ch. Vittu and J. Cl. Lemahieu, Ann. Biol. Clin. (Paris), 23, 913 (1965).

128. G. H. Koch and F. M. Strong, Anal. Biochem., 27, 162 (1969).

129. G. Charransol and P. Desgrez, J. Chromatogr., 48, 530 (1970).

130. M. Th. Duburque, J. M. Melon, J. Thomos, E. Thomas, R. Pierre, G. Charransol and P. Desgrez, Ann. Biol. Clin. (Paris), 28, 95 (1970).

131. R. H. Harrocks, E. J. Hindle, A. Lawson, D. H. Orrell and A. J. Poole, Clin. Chim. Acta, 69, 93 (1976).

132. R. Menaché, Clin. Chem., 20, 1444 (1974).

133. J. Fraser and D. J. Campbell, Clin. Biochem., 5, 99 (1972).

134. A. L. Giterson, P. A. M. Slooff and H. Schouten, Clin. Chim. Acta, 29, 342 (1970).

135. V. V. S. E. Dutt and H. A. Mottola, Biochem. Med., 9, 148 (1974).

APPENDIX 1

COMPUTER PROGRAM USED TO CALCULATE IONIC CONCENTRATIONS

```
 2      C        THIS PROGRAM IS A SPECIALIZED IMPLEMENTATION OF
 3      C        THE NEWTON RAPHSON METHOD TO CALCULATE CONCENTRATIONS
 4      C        OF IONIC SPECIES BY VARYING THE CHEMICAL EQUILIBRIUM
 5      C        AND MASS BALANCES.
 6      C        NUMERICALLY THE PROBLEM TO SOLVE IS THE FOLLOWING-
 7      C
 8      C        |--                          -| |--   --|
 9      C        |    D'F      D'F     D'F  | |        |
10      C        |    ----     ----    ---- | | -DF   |
11      C        |    DX       DY      DZ   | |        |
12      C        |                          | |        |
13      C        |    D'G      D'G     D'G  | |        |
14      C        |    ----     ----    ---- | | -DG   |
15      C        |    DX       DY      DZ   | |        |
16      C        |                          | |      |
17      C        |    D'H      D'H     D'H  | |        |
18      C        |    ----     ----    ---- | | -DH   |
19      C        |    DX       DY      DZ   | |        |
20      C        |--                          -| |--   --|
21      C
22      C        THE ABOVE MATRIX OBTAINED BY A TAYLOR'S EXPANSION
23      C        IN 3 UNKNOWNS IS SOLVED USING THE GAUSSIAN ELIMATION
24      C        METHOD
25      C
26      C        PROGRAM WRITTEN - JANUARY 1976
27      C
28      C        USER - JEAN COOLEY
29      C
30      C        REFERENCE - JOURNAL OF CHEMICAL EDUCATION 36(10) 485 1959
31      C
32      C ****************************************************************
33              SUBROUTINE SOLVE(NR,IOK)
34              IMPLICIT REAL*8(A-H,O-Z)
35              REAL*8 FX(15),XX(20),DT(60),N,M,CO(20,20),BB(20),A(20),
36             *IDEGRE
37              COMMON /N1/ FX,XX,DT,N,M,CO,BB,A,IDEGRE
38              REAL*8 MULT(50),MAX
39      C****GAUSSIAN ELIMINATION ALGORITHM
40      C*****NR IS DIMENSION OF SQUARE MATRIX
41      C*****CO IS COEFFICIENT MATRIX, BB RIGHT HAND SIDE OF EQUATIONS
42      C*****A IS SOLUTION VECTOR
43              DO1 J=1,NR
44      C****PERFORM ALGORITHM FOR ALL ROWS J
45              MAX=0.0
46              II=J
47      C****II IS ROW IDENTIFIER FOR MAX ELEMENT
48              DO2 I=J,NR
49      C****MAXIMUM ELEMENT IN COLUMN FOUND
50              COMP=DABS(CO(I,J))
51              IF(COMP.GT.MAX)II=I
52              IF(COMP.GT.MAX)MAX=COMP
53            2 CONTINUE
54      C****ROW EXCHANGE PERFORMED
55              TEMP=BB(J)
56              BB(J)=BB(II)
57              BB(II)=TEMP
58              DO 3 JJ=1,NR
59              MULT(JJ)=CO(J,JJ)
60              CO(J,JJ)=CO(II,JJ)
61            3 CO(II,JJ)=MULT(JJ)
```

```
 62            DO 4 I=J,NR
 63      C****STORE MULTIPLIERS
 64          4 MULT(I)=CO(I,J)
 65            DO 5 I=J,NR
 66            DO 9 JJ=J,NR
 67            IF ( DABS(MULT(J)).LT.1.0E-7) GOTO 99
 68      C****USE MULTIPLIERS ON DIFFERENT ROWS
 69            IF(I.EQ.J)CO(J,JJ)=CO(J,JJ)/MULT(J)
 70            IF(I.GT.J)CO(I,JJ)=CO(I,JJ)-MULT(I)*CO(J,JJ)
 71          9 CONTINUE
 72      C****USE MULTIPLIERS ON RHS
 73            IF(I.EQ.J)BB(I)=BB(I)/MULT(J)
 74            IF(I.GT.J)BB(I)=BB(I)-MULT(I)*BB(J)
 75          5 CONTINUE
 76          1 CONTINUE
 77      C****BACK SUBSTITUTE IN TRIANGULAR MATRIX
 78            DO 7 I=1,NR
 79            II=NR-I+1
 80            SUM=0.0
 81            IF(II.EQ.NR)GO TO 7
 82            K=II+1
 83            DO 8 JJ=K,NR
 84            SUM=SUM+CO(II,JJ)*A(JJ)
 85          8 CONTINUE
 86          7 A(II)=BB(II)-SUM
 87            IOK=1
 88            RETURN
 89         99 WRITE(6,609) MULT(J)
 90        609 FORMAT('0 PIVOT ELEMENT TOO SMALL - SINGULAR MATRIX?',D20.10)
 91            IOK=0
 92            RETURN
 93            END
 94            DOUBLE PRECISION FUNCTION F1(ITER)
 95            IMPLICIT REAL*8(A-H,O-Z)
 96            COMMON /N2/A7,A8,A9,A10,A11,A21,A22,A23,A24,A25,A26,A27,A28
 97            COMMON /N3/S,T,V,X,Y,Z,C1,C2,C3,C4,C20,C31,A29,A30,A31,A32
 98            COMMON /N4/T2,T3,V2,V3,X2,X3,Y2,Y3,Z2,Z3,Z4
 99            F1=T+T*Y*A7+T*V*A11+T*V2*A21+T*Z*A22+T*Z2*A23+T*Z3*A24
100          #    +T*A26/X-C1+T*Y2*A27+T*Y3*A28+T*Z4*A25+T*S*A30
101            RETURN
102            END
103            DOUBLE PRECISION FUNCTION F2(ITER)
104            IMPLICIT REAL*8(A-H,O-Z)
105            COMMON /N2/A7,A8,A9,A10,A11,A21,A22,A23,A24,A25,A26,A27,A28
106            COMMON /N3/S,T,V,X,Y,Z,C1,C2,C3,C4,C20,C31,A29,A30,A31,A32
107            COMMON /N4/T2,T3,V2,V3,X2,X3,Y2,Y3,Z2,Z3,Z4
108            F2=V+X*V*A8+T*V*A11+2*T*V2*A21-C2
109            RETURN
110            END
111            DOUBLE PRECISION FUNCTION F3(ITER)
112            IMPLICIT REAL*8(A-H,O-Z)
113            COMMON /N2/A7,A8,A9,A10,A11,A21,A22,A23,A24,A25,A26,A27,A28
114            COMMON /N3/S,T,V,X,Y,Z,C1,C2,C3,C4,C20,C31,A29,A30,A31,A32
115            COMMON /N4/T2,T3,V2,V3,X2,X3,Y2,Y3,Z2,Z3,Z4
116            F3=X+X*Y*A8+X*Y*A10+2*X2*Y*A9-C3+3*X3*S*A31+2*X2*S*A32+X*S*A29
117            RETURN
118            END
119            DOUBLE PRECISION FUNCTION F4(ITER)
120            IMPLICIT REAL*8(A-H,O-Z)
121            COMMON /N2/A7,A8,A9,A10,A11,A21,A22,A23,A24,A25,A26,A27,A28
```

```
122            COMMON /N3/S,T,V,X,Y,Z,C1,C2,C3,C4,C20,C31,A29,A30,A31,A32
123            COMMON /N4/T2,T3,V2,V3,X2,X3,Y2,Y3,Z2,Z3,Z4
124            F4=Y+X2*Y*A9+X*Y*A10+T*Y*A7-C4+2*T*Y2*A27+3*T*Y3*A28
125            RETURN
126            END
127            DOUBLE PRECISION FUNCTION F5(ITER)
128            IMPLICIT REAL*8(A-H,O-Z)
129            COMMON /N2/A7,A8,A9,A10,A11,A21,A22,A23,A24,A25,A26,A27,A28
130            COMMON /N3/S,T,V,X,Y,Z,C1,C2,C3,C4,C20,C31,A29,A30,A31,A32
131            COMMON /N4/T2,T3,V2,V3,X2,X3,Y2,Y3,Z2,Z3,Z4
132            F5=Z+T*Z*A22+2*T*Z2*A23+3*T*Z3*A24-C20+4*T*Z4*A25
133            RETURN
134            END
135            DOUBLE PRECISION FUNCTION F6(ITER)
136            IMPLICIT REAL*8(A-H,O-Z)
137            COMMON /N2/A7,A8,A9,A10,A11,A21,A22,A23,A24,A25,A26,A27,A28
138            COMMON /N3/S,T,V,X,Y,Z,C1,C2,C3,C4,C20,C31,A29,A30,A31,A32
139            COMMON /N4/T2,T3,V2,V3,X2,X3,Y2,Y3,Z2,Z3,Z4
140            F6=X3*S*A31+X2*S*A32+X*S*A29+T*S*A30-C31
141            RETURN
142            END
143            DOUBLE PRECISION FUNCTION DF1S(ITER)
144            IMPLICIT REAL*8(A-H,O-Z)
145            COMMON /N2/A7,A8,A9,A10,A11,A21,A22,A23,A24,A25,A26,A27,A28
146            COMMON /N3/S,T,V,X,Y,Z,C1,C2,C3,C4,C20,C31,A29,A30,A31,A32
147            DF1S=T*A30
148            RETURN
149            END
150            DOUBLE PRECISION FUNCTION DF1T(ITER)
151            IMPLICIT REAL*8(A-H,O-Z)
152            COMMON /N2/A7,A8,A9,A10,A11,A21,A22,A23,A24,A25,A26,A27,A28
153            COMMON /N3/S,T,V,X,Y,Z,C1,C2,C3,C4,C20,C31,A29,A30,A31,A32
154            COMMON /N4/T2,T3,V2,V3,X2,X3,Y2,Y3,Z2,Z3,Z4
155            DF1T=1+Y*A7+V*A11+Y2*A21+Z*A22+Z2*A23+Z3*A24+A26/X
156       *        +Y2*A27+Y3*A28+Z4*A25+S*A30
157            RETURN
158            END
159            DOUBLE PRECISION FUNCTION DF1V(ITER)
160            IMPLICIT REAL*8(A-H,O-Z)
161            COMMON /N2/A7,A8,A9,A10,A11,A21,A22,A23,A24,A25,A26,A27,A28
162            COMMON /N3/S,T,V,X,Y,Z,C1,C2,C3,C4,C20,C31,A29,A30,A31,A32
163            DF1V=T*A11+2*T*V*A21
164            RETURN
165            END
166            DOUBLE PRECISION FUNCTION DF1X(ITER)
167            IMPLICIT REAL*8(A-H,O-Z)
168            COMMON /N2/A7,A8,A9,A10,A11,A21,A22,A23,A24,A25,A26,A27,A28
169            COMMON /N3/S,T,V,X,Y,Z,C1,C2,C3,C4,C20,C31,A29,A30,A31,A32
170            COMMON /N4/T2,T3,V2,V3,X2,X3,Y2,Y3,Z2,Z3,Z4
171            DF1X=-T*A26/X2
172            RETURN
173            END
174            DOUBLE PRECISION FUNCTION DF1Y(ITER)
175            IMPLICIT REAL*8(A-H,O-Z)
176            COMMON /N2/A7,A8,A9,A10,A11,A21,A22,A23,A24,A25,A26,A27,A28
177            COMMON /N3/S,T,V,X,Y,Z,C1,C2,C3,C4,C20,C31,A29,A30,A31,A32
178            COMMON /N4/T2,T3,V2,V3,X2,X3,Y2,Y3,Z2,Z3,Z4
179            DF1Y=T*A7+2*T*Y*A27+3*T*Y2*A28
180            RETURN
181            END
```

```
182          DOUBLE PRECISION FUNCTION DF1Z(ITER)
183          IMPLICIT REAL*8(A-H,O-Z)
184          COMMON /N2/A7,A8,A9,A10,A11,A21,A22,A23,A24,A25,A26,A27,A28
185          COMMON /N3/S,T,V,X,Y,Z,C1,C2,C3,C4,C20,C31,A29,A30,A31,A32
186          COMMON /N4/T2,T3,V2,V3,X2,X3,Y2,Y3,Z2,Z3,Z4
187          DF1Z=T*A22+2*T*Z*A23+3*T*Z2*A24+4*T*Z3*A25
188          RETURN
189          END
190          DOUBLE PRECISION FUNCTION DF2T(ITER)
191          IMPLICIT REAL*8(A-H,O-Z)
192          COMMON /N2/A7,A8,A9,A10,A11,A21,A22,A23,A24,A25,A26,A27,A28
193          COMMON /N3/S,T,V,X,Y,Z,C1,C2,C3,C4,C20,C31,A29,A30,A31,A32
194          COMMON /N4/T2,T3,V2,V3,X2,X3,Y2,Y3,Z2,Z3,Z4
195          DF2T=V*A11+2*V2*A21
196          RETURN
197          END
198          DOUBLE PRECISION FUNCTION DF2V(ITER)
199          IMPLICIT REAL*8(A-H,O-Z)
200          COMMON /N2/A7,A8,A9,A10,A11,A21,A22,A23,A24,A25,A26,A27,A28
201          COMMON /N3/S,T,V,X,Y,Z,C1,C2,C3,C4,C20,C31,A29,A30,A31,A32
202          DF2V=1+T*A11+X*A8+4*T*V*A21
203          RETURN
204          END
205          DOUBLE PRECISION FUNCTION DF2X(ITER)
206          IMPLICIT REAL*8(A-H,O-Z)
207          COMMON /N2/A7,A8,A9,A10,A11,A21,A22,A23,A24,A25,A26,A27,A28
208          COMMON /N3/S,T,V,X,Y,Z,C1,C2,C3,C4,C20,C31,A29,A30,A31,A32
209          DF2X=V*A8
210          RETURN
211          END
212          DOUBLE PRECISION FUNCTION DF2Y(ITER)
213          IMPLICIT REAL*8(A-H,O-Z)
214          COMMON /N2/A7,A8,A9,A10,A11,A21,A22,A23,A24,A25,A26,A27,A28
215          COMMON /N3/S,T,V,X,Y,Z,C1,C2,C3,C4,C20,C31,A29,A30,A31,A32
216          DF2Y=0
217          RETURN
218          END
219          DOUBLE PRECISION FUNCTION DF2Z(ITER)
220          IMPLICIT REAL*8(A-H,O-Z)
221          COMMON /N2/A7,A8,A9,A10,A11,A21,A22,A23,A24,A25,A26,A27,A28
222          COMMON /N3/S,T,V,X,Y,Z,C1,C2,C3,C4,C20,C31,A29,A30,A31,A32
223          DF2Z=0
224          RETURN
225          END
226          DOUBLE PRECISION FUNCTION DF3S(ITER)
227          IMPLICIT REAL*8(A-H,O-Z)
228          COMMON /N2/A7,A8,A9,A10,A11,A21,A22,A23,A24,A25,A26,A27,A28
229          COMMON /N3/S,T,V,X,Y,Z,C1,C2,C3,C4,C20,C31,A29,A30,A31,A32
230          COMMON /N4/T2,T3,V2,V3,X2,X3,Y2,Y3,Z2,Z3,Z4
231          DF3S=3*X3*A31+2*X2*A32+X*A29
232          RETURN
233          END
234          DOUBLE PRECISION FUNCTION DF3T(ITER)
235          IMPLICIT REAL*8(A-H,O-Z)
236          COMMON /N2/A7,A8,A9,A10,A11,A21,A22,A23,A24,A25,A26,A27,A28
237          COMMON /N3/S,T,V,X,Y,Z,C1,C2,C3,C4,C20,C31,A29,A30,A31,A32
238          DF3T=0
239          RETURN
240          END
241          DOUBLE PRECISION FUNCTION DF3V(ITER)
```

```
242              IMPLICIT REAL*8(A-H,O-Z)
243              COMMON /N2/A7,A8,A9,A10,A11,A21,A22,A23,A24,A25,A26,A27,A28
244              COMMON /N3/S,T,V,X,Y,Z,C1,C2,C3,C4,C20,C31,A29,A30,A31,A32
245              DF3V=X*A8
246              RETURN
247              END
248              DOUBLE PRECISION FUNCTION DF3X(ITER)
249              IMPLICIT REAL*8(A-H,O-Z)
250              COMMON /N2/A7,A8,A9,A10,A11,A21,A22,A23,A24,A25,A26,A27,A28
251              COMMON /N3/S,T,V,X,Y,Z,C1,C2,C3,C4,C20,C31,A29,A30,A31,A32
252              COMMON /N4/T2,T3,V2,V3,X2,X3,Y2,Y3,Z2,Z3,Z4
253              DF3X=1+V*A8+Y*A10+4*X*Y*A9+9*X2*S*A31+4*X*S*A32+S*A29
254              RETURN
255              END
256              DOUBLE PRECISION FUNCTION DF3Y(ITER)
257              IMPLICIT REAL*8(A-H,O-Z)
258              COMMON /N2/A7,A8,A9,A10,A11,A21,A22,A23,A24,A25,A26,A27,A28
259              COMMON /N3/S,T,V,X,Y,Z,C1,C2,C3,C4,C20,C31,A29,A30,A31,A32
260              COMMON /N4/T2,T3,V2,V3,X2,X3,Y2,Y3,Z2,Z3,Z4
261              DF3Y=X*A10+2*X2*A9
262              RETURN
263              END
264              DOUBLE PRECISION FUNCTION DF3Z(ITER)
265              IMPLICIT REAL*8(A-H,O-Z)
266              COMMON /N2/A7,A8,A9,A10,A11,A21,A22,A23,A24,A25,A26,A27,A28
267              COMMON /N3/S,T,V,X,Y,Z,C1,C2,C3,C4,C20,C31,A29,A30,A31,A32
268              DF3Z=0
269              RETURN
270              END
271              DOUBLE PRECISION FUNCTION DF4T(ITER)
272              IMPLICIT REAL*8(A-H,O-Z)
273              COMMON /N2/A7,A8,A9,A10,A11,A21,A22,A23,A24,A25,A26,A27,A28
274              COMMON /N3/S,T,V,X,Y,Z,C1,C2,C3,C4,C20,C31,A29,A30,A31,A32
275              COMMON /N4/T2,T3,V2,V3,X2,X3,Y2,Y3,Z2,Z3,Z4
276              DF4T=Y*A7+2*Y2*A27+3*Y3*A28
277              RETURN
278              END
279              DOUBLE PRECISION FUNCTION DF4V(ITER)
280              IMPLICIT REAL*8(A-H,O-Z)
281              COMMON /N2/A7,A8,A9,A10,A11,A21,A22,A23,A24,A25,A26,A27,A28
282              COMMON /N3/S,T,V,X,Y,Z,C1,C2,C3,C4,C20,C31,A29,A30,A31,A32
283              DF4V=0
284              RETURN
285              END
286              DOUBLE PRECISION FUNCTION DF4X(ITER)
287              IMPLICIT REAL*8(A-H,O-Z)
288              COMMON /N2/A7,A8,A9,A10,A11,A21,A22,A23,A24,A25,A26,A27,A28
289              COMMON /N3/S,T,V,X,Y,Z,C1,C2,C3,C4,C20,C31,A29,A30,A31,A32
290              DF4X=2*X*Y*A9+Y*A10
291              RETURN
292              END
293              DOUBLE PRECISION FUNCTION DF4Y(ITER)
294              IMPLICIT REAL*8(A-H,O-Z)
295              COMMON /N2/A7,A8,A9,A10,A11,A21,A22,A23,A24,A25,A26,A27,A28
296              COMMON /N3/S,T,V,X,Y,Z,C1,C2,C3,C4,C20,C31,A29,A30,A31,A32
297              COMMON /N4/T2,T3,V2,V3,X2,X3,Y2,Y3,Z2,Z3,Z4
298              DF4Y=1+X2*A9+X*A10+T*A7+4*T*Y*A27+9*T*Y2*A28
299              RETURN
300              END
301              DOUBLE PRECISION FUNCTION DF4Z(ITER)
```

```
302          IMPLICIT REAL*8(A-H,O-Z)
303          COMMON /N2/A7,A8,A9,A10,A11,A21,A22,A23,A24,A25,A26,A27,A28
304          COMMON /N3/S,T,V,X,Y,Z,C1,C2,C3,C4,C20,C31,A29,A30,A31,A32
305          DF4Z=0
306          RETURN
307          END
308          DOUBLE PRECISION FUNCTION DF5T(ITER)
309          IMPLICIT REAL*8(A-H,O-Z)
310          COMMON /N2/A7,A8,A9,A10,A11,A21,A22,A23,A24,A25,A26,A27,A28
311          COMMON /N3/S,T,V,X,Y,Z,C1,C2,C3,C4,C20,C31,A29,A30,A31,A32
312          COMMON /N4/T2,T3,V2,V3,X2,X3,Y2,Y3,Z2,Z3,Z4
313          DF5T=Z*A22+2*Z2*A23+3*Z3*A24+4*Z4*A25
314          RETURN
315          END
316          DOUBLE PRECISION FUNCTION DF5V(ITER)
317          IMPLICIT REAL*8(A-H,O-Z)
318          COMMON /N2/A7,A8,A9,A10,A11,A21,A22,A23,A24,A25,A26,A27,A28
319          COMMON /N3/S,T,V,X,Y,Z,C1,C2,C3,C4,C20,C31,A29,A30,A31,A32
320          DF5V=0
321          RETURN
322          END
323          DOUBLE PRECISION FUNCTION DF5X(ITER)
324          IMPLICIT REAL*8(A-H,O-Z)
325          COMMON /N2/A7,A8,A9,A10,A11,A21,A22,A23,A24,A25,A26,A27,A28
326          COMMON /N3/S,T,V,X,Y,Z,C1,C2,C3,C4,C20,C31,A29,A30,A31,A32
327          DF5X=0
328          RETURN
329          END
330          DOUBLE PRECISION FUNCTION DF5Y(ITER)
331          IMPLICIT REAL*8(A-H,O-Z)
332          COMMON /N2/A7,A8,A9,A10,A11,A21,A22,A23,A24,A25,A26,A27,A28
333          COMMON /N3/S,T,V,X,Y,Z,C1,C2,C3,C4,C20,C31,A29,A30,A31,A32
334          DF5Y=0
335          RETURN
336          END
337          DOUBLE PRECISION FUNCTION DF5Z(ITER)
338          IMPLICIT REAL*8(A-H,O-Z)
339          COMMON /N2/A7,A8,A9,A10,A11,A21,A22,A23,A24,A25,A26,A27,A28
340          COMMON /N3/S,T,V,X,Y,Z,C1,C2,C3,C4,C20,C31,A29,A30,A31,A32
341          COMMON /N4/T2,T3,V2,V3,X2,X3,Y2,Y3,Z2,Z3,Z4
342          DF5Z=1+T*A22+4*T*Z*A23+9*T*Z2*A24+16*T*Z3*A25
343          RETURN
344          END
345          DOUBLE PRECISION FUNCTION DF6S(ITER)
346          IMPLICIT REAL*8(A-H,O-Z)
347          COMMON /N2/A7,A8,A9,A10,A11,A21,A22,A23,A24,A25,A26,A27,A28
348          COMMON /N3/S,T,V,X,Y,Z,C1,C2,C3,C4,C20,C31,A29,A30,A31,A32
349          COMMON /N4/T2,T3,V2,V3,X2,X3,Y2,Y3,Z2,Z3,Z4
350          DF6S=X3*A31+X2*A32+X*A29+T*A30
351          RETURN
352          END
353          DOUBLE PRECISION FUNCTION DF6T(ITER)
354          IMPLICIT REAL*8(A-H,O-Z)
355          COMMON /N2/A7,A8,A9,A10,A11,A21,A22,A23,A24,A25,A26,A27,A28
356          COMMON /N3/S,T,V,X,Y,Z,C1,C2,C3,C4,C20,C31,A29,A30,A31,A32
357          COMMON /N4/T2,T3,V2,V3,X2,X3,Y2,Y3,Z2,Z3,Z4
358          DF6T=S*A30
359          RETURN
360          END
361          DOUBLE PRECISION FUNCTION DF6X(ITER)
```

```
362          IMPLICIT REAL*8(A-H,O-Z)
363          COMMON /N2/A7,A8,A9,A10,A11,A21,A22,A23,A24,A25,A26,A27,A28
364          COMMON /N3/S,T,V,X,Y,Z,C1,C2,C3,C4,C20,C31,A29,A30,A31,A32
365          COMMON /N4/T2,T3,V2,V3,X2,X3,Y2,Y3,Z2,Z3,Z4
366          DF6X=3*X2*S*A31+2*X*S*A32+S*A29
367          RETURN
368          END
369          IMPLICIT REAL*8(A-H,O-Z)
370          REAL*8 FX(15),XX(20),DT(60),N,M,CO(20,20),BB(20),D(20),
371         *IDEGRE
372          COMMON /N1/ FX,XX,DT,N,M,CO,BB,D,IDEGRE
373          COMMON /N2/A7,A8,A9,A10,A11,A21,A22,A23,A24,A25,A26,A27,A28
374          COMMON /N3/S,T,V,X,Y,Z,C1,C2,C3,C4,C20,C31,A29,A30,A31,A32
375          COMMON /N4/T2,T3,V2,V3,X2,X3,Y2,Y3,Z2,Z3,Z4
375.25       INTEGER DUMMY
376          REAL*8 MULT(50),MAX
377          DF6Y(DUMMY)=0.0D0
378          DF2S(DUMMY)=0.0D0
379          DF4S(DUMMY)=0.0D0
380          DF5S(DUMMY)=0.0D0
381          DF6V(DUMMY)=0.0D0
382          DF6Z(DUMMY)=0.0D0
382.25  11   REWIND5
383          READ(4,502,END=999) A7,A8,A9,A10,A11,A21,A22,A23,A24,A25,A26,A27,
384        #          A28,A29,A30,A31,A32
384.25       WRITE(6,610) A7,A8,A9,A10,A11,A21,A22,A23,A24,A25,A26,A27,
384.5      #          A28,A29,A30,A31,A32
384.6   610  FORMAT(' CONSTANTS A7...A32',/,(2D16.5))
385     502  FORMAT(12D20.10)
400     606  FORMAT ('1',T5,'C1',T10,'C2',T15,'C3',T20,'C4',T25,'C20',
401        X          T30,'FE',T35,'SO4',T40,' H',T45,'OX',T50,'CL')
402     1    READ(5,501,END=999) C1,C2,C3,C4,C20,C31,T,V,X,Y,Z ,S
402.25       BLANK=C1+C2+C3+C4+C20+C31
402.5        IF(BLANK.EQ.0)GOTO 11
403     501  FORMAT(12D20.10)
404          ITER=0
405     2    T2=T*T
406          T3=T2*T
407          V2=V*V
408          V3=V2*V
409          X2=X*X
410          X3=X2*X
411          Y2=Y*Y
412          Y3=Y2*Y
413          Z2=Z*Z
414          Z3=Z2*Z
415          Z4=Z2*Z2
416          BB(1)=-F1(ITER)
417          BB(2)=-F2(ITER)
418          BB(3)=-F3(ITER)
419          BB(4)=-F4(ITER)
420          BB(5)=-F5(ITER)
421          BB(6)=-F6(ITER)
422          CO(1,1)=DF1T(ITER)
423          CO(1,2)=DF1V(ITER)
424          CO(1,3)=DF1X(ITER)
425          CO(1,4)=DF1Y(ITER)
426          CO(1,5)=DF1Z(ITER)
427          CO(1,6)=DF1S(ITER)
428          CO(2,1)=DF2T(ITER)
```

```
429              CO(2,2)=DF2V(ITER)
430              CO(2,3)=DF2X(ITER)
431              CO(2,4)=DF2Y(ITER)
432              CO(2,5)=DF2Z(ITER)
433              CO(2,6)=DF2S(ITER)
434              CO(3,1)=DF3T(ITER)
435              CO(3,2)=DF3V(ITER)
436              CO(3,3)=DF3X(ITER)
437              CO(3,4)=DF3Y(ITER)
438              CO(3,5)=DF3Z(ITER)
439              CO(3,6)=DF3S(ITER)
440              CO(4,1)=DF4T(ITER)
441              CO(4,2)=DF4V(ITER)
442              CO(4,3)=DF4X(ITER)
443              CO(4,4)=DF4Y(ITER)
444              CO(4,5)=DF4Z(ITER)
445              CO(4,6)=DF4S(ITER)
446              CO(5,1)=DF5T(ITER)
447              CO(5,2)=DF5V(ITER)
448              CO(5,3)=DF5X(ITER)
449              CO(5,4)=DF5Y(ITER)
450              CO(5,5)=DF5Z(ITER)
451              CO(5,6)=DF5S(ITER)
452              CO(6,1)=DF6T(ITER)
453              CO(6,2)=DF6V(ITER)
454              CO(6,3)=DF6X(ITER)
455              CO(6,4)=DF6Y(ITER)
456              CO(6,5)=DF6Z(ITER)
457              CO(6,6)=DF6S(ITER)
458              WRITE(6,666)
459     666      FORMAT('0','              COEF. MATRIX ... R.H.S')
460              DO 3 I=1,6
461     3        WRITE(6,602) (CO(I,J),J=1,6),BB(I)
462              CALL SOLVE(4,IOK)
463              IF (IOK.EQ.0) GOTO 99
464              ITER=ITER+1
465              WRITE(6,602) (D(I),I=1,6),T,V,X,Y,Z,S
466              T=T+D(1)
467              V=V+D(2)
468              X=X+D(3)
469              Y=Y+D(4)
470              Z=Z+D(5)
471              S=S+D(6)
472              IF (ITER.GT.100) GOTO 99
473              IF ((DABS(D(1)).GT.1.0E-8).OR.(DABS(D(2)).GT.1.0E-8)
474          *    .OR. (DABS(D(3)).GT.1.0E-8).OR.(DABS(D(4)).GT.1.0E-8)
475          *    .OR. (DABS(D(5)).GT.1.0D-8).OR.(DABS(D(6)).GT.1.0E-8)) GOTO 2
476              FECL4=T*Z4*A25
477              FEOX2=T*Y2*A27
478              FEOX3=T*Y3*A28
479              FESO4=T*V*A11
480              HSO4=X*V*A8
481              FESO42=T*V*V*A21
482              FEOX=T*Y*A7
483              HOX=X*Y*A10
484              H2OX=X*X*Y*A9
485              FECL=T*Z*A22
486              FECL2=T*Z*Z*A23
487              FECL3=T*Z*Z*Z*A24
488              FEOH=T*A26/X
```

```
489             H3CIT=X3*S*A31
490             H2CIT=X2*S*A32
491             HCIT=X*S*A29
492             FECIT=T*S*A30
493             WRITE(6,607).
494     607     FORMAT('0',T4,'C1',T16,'C2',T28,'C3',T40,'C4',T52,'C20',T64,'T',
495           X       T76,'V',T88,'X',T100,'Y',T112,'Z')
496             WRITE(6,602)C1,C2,C3,C4,C20,T,V,X,Y,Z,S
497             WRITE(6,603)
498     603     FORMAT('0',T4,'FESO4',T16,'HSO4',T28,'FE(SO4)2',T40,'FEOX',T52,
499           X 'FECL',T64,'FECL2',T76,'FECL3',T88,'FEOH',T100,'H2OX',T112,'HOX')
500             WRITE(6,602) FESO4,HSO4,FESO42,FEOX,FECL
501           X           ,FECL2,FECL3,FEOH,H2OX,HOX
502             WRITE(6,605)
503     605     FORMAT('0',T4,'FE(CL)4',T16,'FE(OX)2',T28,'FE(OX)3',
504           X   T40,'FECIT',T52,'HCIT',T64,'H2CIT',T76,'H3CIT')
505             WRITE(6,602) FECL4,FEOX2,FEOX3,FECIT,HCIT,H2CIT,H3CIT
506     602     FORMAT(' ',12D12.5)
507             GOTO 1
508      99     WRITE(6,601)  T,V,X,Y,Z,S
509     601     FORMAT('0','****NO CONVERGENCE****(X,Y=)',6D20.10)
510             GOTO 1
511     999     STOP
512             END
END OF FILE
```